2001

DESIGN, SYNTHESIS AND ANTIMICROBIAL ACTIVITY OF NOVEL ANTIMICROBIAL PEPTIDES

Khaled Elsaid
University of Rhode Island

DESIGN, SYNTHESIS AND ANTIMICROBIAL ACTIVITY OF

NOVEL ANTIMICROBIAL PEPTIDES

BY

KHALED ELSAID

A THESIS SUBMITTED IN PARTIAL FULFILLMENT OF THE

REQUIREMENTS FOR THE DEGREE OF

MASTER OF SCIENCE

IN

BIOMEDICAL SCIENCES

UNIVERSITY OF RHODE ISLAND

2001

Library Rights Statement

In presenting this Thesis in partial fulfillment of the requirements for an advanced degree at the University of Rhode Island, I agree that the library shall make it freely available for inspection. I further agree that permission for copying, as provided for by the copyright law of the United States (Title 17, U. S. Code), of the Thesis for scholarly purposes be granted by the librarian. It is understood that any copying or publication of this thesis for financial gains shall not be allowed without my written permission.

I hereby (do/do not) grant permission to the University of Rhode Island Library to use my thesis for scholarly purposes.

Khaled Elbaid
Signature

_08 - 24 - 2001_
Date

MASTERS OF SCIENCE THESIS
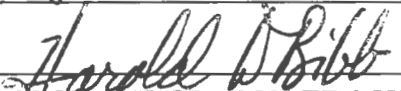
OF

KHALED ELSAID

APPROVED:

Thesis Committee:

Major Professor _____

_____

_____

DEAN OF THE GRADUATE SCHOOL

UNIVERSITY OF RHODE ISLAND

2001

ABSTRACT

In the past decade, a large number of naturally occuring thiazole and oxazole-containing peptides have been isolated from microbial and marine origins. These peptides exhibit important antimicrobial, antiviral, and anticancer activities. Solid phase synthesis of peptides provides the methods to prepare and investigate novel compounds for possible use as antibiotics. Three combinatorial peptide libraries, library **1**, an enantiomeric peptide library, library **2**, with guanidinium, thiazole and benzothiophene side chains and library **3**, designed from a template natural product, microcin B17, were tested against *Vibrio anguillarum* (wild type), *Escherichia coli* (ZK 4) and *Saccharomyces cerevisiae* in zone inhibition and cell culture growth inhibition assays. Library **2**, with guanidinium, thiazole and benzothiophene side chains exhibited significant antimicrobial activity towards *V. anguillarum* and *E. coli*, with greater activity than did the enantiomeric peptide library, library **1**, or the library based on microcin B17, library **3**. α-Helical antimicrobial peptides act by general permeabilization of bacterial membranes. Pleurocidin, a 25 amino acid peptide was extracted from the skin secretions of winter flounder. Pleurocidin is histidine rich, forms a well-defined amphipathic α-helix and exhibits no toxicity towards eukaryotic cells. Two novel *C*-terminally truncated pleurocidin amide peptides were synthesized by Solid Phase Peptide Synthesis (SPPS) and their identities were confirmed by Matrix Assisted Laser Desorption Ionization Mass Spectrometry (MALDI-TOF MS). The antimicrobial activities of the two *C*-terminally truncated peptides were

compared to pleurocidin amide against *E. coli* (ZK 4) and *V. anguillarum*. Methyl 2-*S*-(1`-Boc-2`-phenylethyl) thiazole-4-carboxylate can be used as a useful building block in combinatorial peptide libraries. A convenient synthesis of methyl 2-*S*- (1`-Boc-2`-phenylethyl) thiazole-4-carboxylate was developed. The synthetic scheme was based on the formation of the aldehyde from Boc-phenylalanine via reduction of *N*-methoxy-*N*-methylphenylalanine. Condensation of the resulting Boc-phenylalaninal with L-cysteine methyl ester yielded methyl 2-(1`-Boc-phenylethyl) thiazolidine-4-carboxylate in good yield. Subsequent oxidation by activated $MnO_2$ afforded methyl 2-(1`-Boc-2`-phenylethyl) thiazole-4-carboxylate but the yields were much lower. Topoisomerases are a class of enzymes that catalyzed topological interconversions of supercoiled DNA. Inhibition of topoisomerases I or II is a target for many anticancer drugs. DNA gyrase is a type II topoisomerase unique to bacteria, and inhibition of DNA gyrase is a target for selective antimicrobial agents. Sixteen compounds of tetrapeptide library **2** were screened for their topoisomerase I, and II inhibition. The inhibition assay depended on the differential migration of supercoiled DNA versus relaxed DNA. The results were inconclusive.

PREFACE

Many pathogenic micro-organisms are resistant to the existing antibiotics. The increasing resistance problem has prompted the search of new antimicrobial agents with novel mechanisms of action to which the pathogenic micro-organisms show little resistance. In the past decade, a large number of thiazole and oxazole containing natural products have been isolated from marine and insect origins that show important anticancer, antiviral and antimicrobial activities.

This thesis presents information on the design, synthesis and analysis of three combinatorial peptide libraries and a series of *C*-truncated pleurocidin amide peptides. The manuscript format was adopted for the thesis presentation according to the guidelines of the Graduate School of University of Rhode Island. The thesis is composed of three chapters, one appendix and a bibliography.

Chapter 1, "Antimicrobial activities of combinatorial peptide libraries", presents information on the antimicrobial activities of three combinatorial libraries with unnatural, thiazole and oxazole containing, amino acid building blocks. In this chapter, the three combinatorial libraries were tested against *Vibrio anguillarum* (wild type), *Escherichia coli* (ZK 4), a microcin-sensitive strain, and *Saccharomyces cerevisiae* (wild type) in both zone inhibition assays and cell culture growth inhibition assays.

Chapter 2, "Antimicrobial activities of pleurocidin amide and related peptides truncated at the *C*-terminus", presents information on the design, synthesis and

antimicrobial activities of a series of *C*-terminus truncated pleurocidin amide peptides.

Chapter 3, " Synthesis of novel thiazole-containing building blocks for combinatorial synthesis", describes the synthetic procedure employed to synthesize useful building blocks for combinatorial peptide libraries.

Appendix, " Topo I, II Inhibition of a tetrapeptide library", describes initial experiments towards characterization of topoisomerase I and topoisomerase II inhibition by a tetrapeptide library.

A total bibliography of all the articles referred to in the thesis is also presented.

TABLE OF CONTENTS

LIST OF TABLES

CHAPTER 2 ANTIMICROBIAL ACTIVITIES OF PLEUROCIDIN AMIDE AND RELATED PEPTIDES TRUNCATED AT THE *C*-TERMINUS

LIST OF FIGURES

CHAPTER 3 SYNTHESIS OF NOVEL THIAZOLE-CONTAINING AMINO ACID BUILDING BLOCKS FOR COMBINATORIAL PEPTIDE LIBRARIES

APPENDIX TOPO I, II INHIBITION OF A TETRAPEPTIDE LIBRARY

DESIGN, SYNTHESIS AND ANTIMICROBIAL ACTIVITY OF

NOVEL ANTIMICROBIAL PEPTIDES

BY

KHALED ELSAID

A THESIS SUBMITTED IN PARTIAL FULFILLMENT OF THE

REQUIREMENTS FOR THE DEGREE OF

MASTER OF SCIENCE

IN

BIOMEDICAL SCIENCES

UNIVERSITY OF RHODE ISLAND

2001

CHAPTER 1: ANTIMICROBIAL ACTIVITY OF COMBINATORIAL PEPTIDE LIBRARIES

ABSTRACT

In the past decade, a large number of naturally occuring thiazole and oxazole-containing peptides have been isolated from microbial and marine origins. These peptides exhibit important antimicrobial, antiviral, and anticancer activities. Heterocyclic rings alter peptide backbone connectivity and create new recognition surfaces for interaction with proteins, DNA and RNA. The thiazolidine and bisthiazole moieties are essential for the antimicrobial activities of bacitracin and bleomycin A_2 respectively.

Given the structural importance of thiazole and oxazole rings, three combinatorial peptide libraries with unnatural thiazole and oxazole-containing amino acid building blocks have been screened for their antimicrobial activities against the gram negative bacteria *Escherichia coli* (ZK 4), a microcin-sensitive strain, *Vibrio anguillarum* (wild type) and the yeast *Saccharomyces cerevisiae* (wild type). The Minimum Inhibitory Concentration (MIC) values were determined by a cell culture growth inhibition assay.

A library of tetrapeptides with guanidinium, thiazole, and benzothiophene side chains had higher potency (lower MIC values) against the candidate micro-organisms than did an enantiomeric library of thiazolylalanine building blocks or a library of designed analogs of a natural antimicrobial peptide, (microcin B17).

The increased positive charge and the presence of benzothiophene side chains, which have the ability to intercalate between DNA base pairs may have contributed to the enhanced antimicrobial activity.

Based on these results, it is recommended that future combinatorial peptide libraries should be designed to increase the number of positive charges and the number of building blocks with benzothiophene side chains.

1.1 INTRODUCTION

In the past decade, a large number of thiazole and oxazole-containing peptides have been isolated from microbial and marine origins. These peptides exhibit important antiviral, anticancer, antibacterial and antifungal activities[1]. GE 2270 A (Figure 1.1.1) has been isolated from the fermentation broth of a strain of the fungus *Planobispora rosea* and inhibits bacterial protein synthesis[2]. Lyngbyabellin A (Figure 1.1.2) is a cytotoxic hexapeptide from the marine cyanobacterium *Lyngbya majuscula*[3]. BE 10988 (Figure 1.1.3) has been isolated from the culture broth of a strain of actinomycetes and was shown to inhibit topoisomerase II[4]. Haligramides A and B (Figure 1.1.4) are cytotoxic peptides from the marine sponge *Haliclona nigra*[5]. Bacitracin (Figure 1.1.5) was isolated from the fermentation broth of *Bacillus* sp. and is currently used as a topical antibiotic[6]. Patellamide F (Figure 1.1.6) is a new cytotoxic cyclic peptide from the colonial ascidian *Lissoclinum patella*[7]. Microcins are a group of small molecular weight peptides secreted from enterobacteriaceae. Microcin B17 (Figure 1.1.7) is secreted by certain strains of *E. coli* and kills susceptible bacteria by inhibiting DNA gyrase[8].

2

1.1.1 GE 2270 A

1.1.2 Lyngbyabellin A

1.1.3 BE 10988

1.1.4 HaligramideA, $R_1 = R_2 = S\text{-Me}$
Haligramide B, $R_1 = S\text{-Me}$, $R_2 = S\text{-OMe}$
Waiakamide $R_1 = R_2 = SO\text{-Me}$

Leu-D-Glu-Ile-Lys-D-Orn-Ile

D-Phe

Asn-D-Asp-His

1.1.5 Bacitracin

3

1.1.6 Patellamide F, $R_1 =$

$R_2 = R_3 = H,$

$R_4 =$

1.1.7 Microcin B17
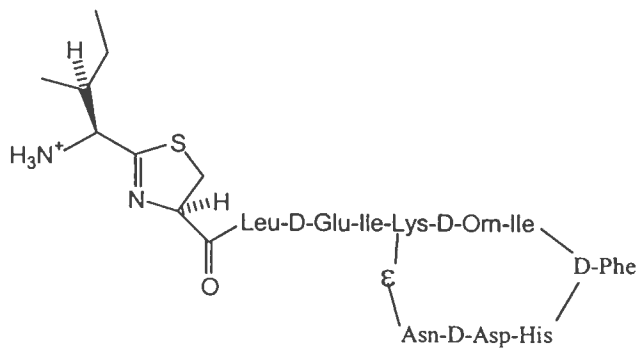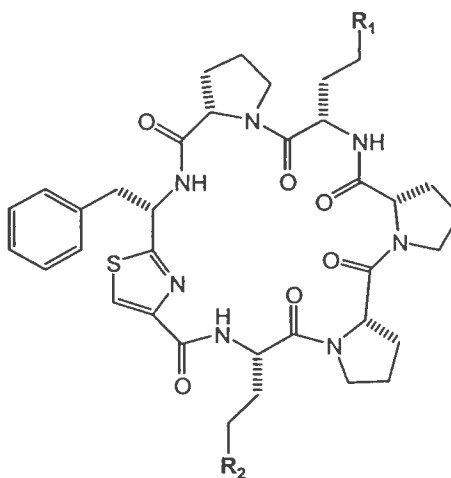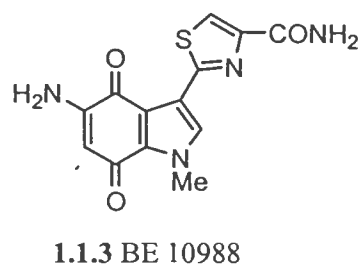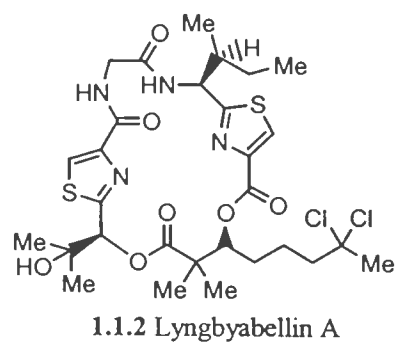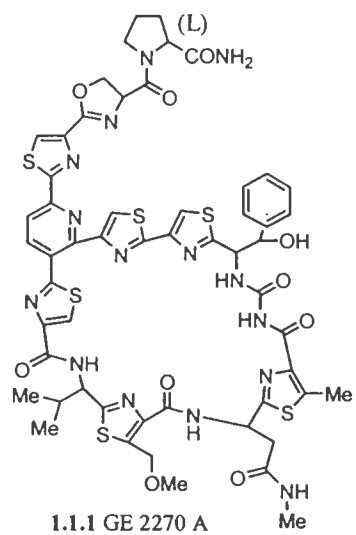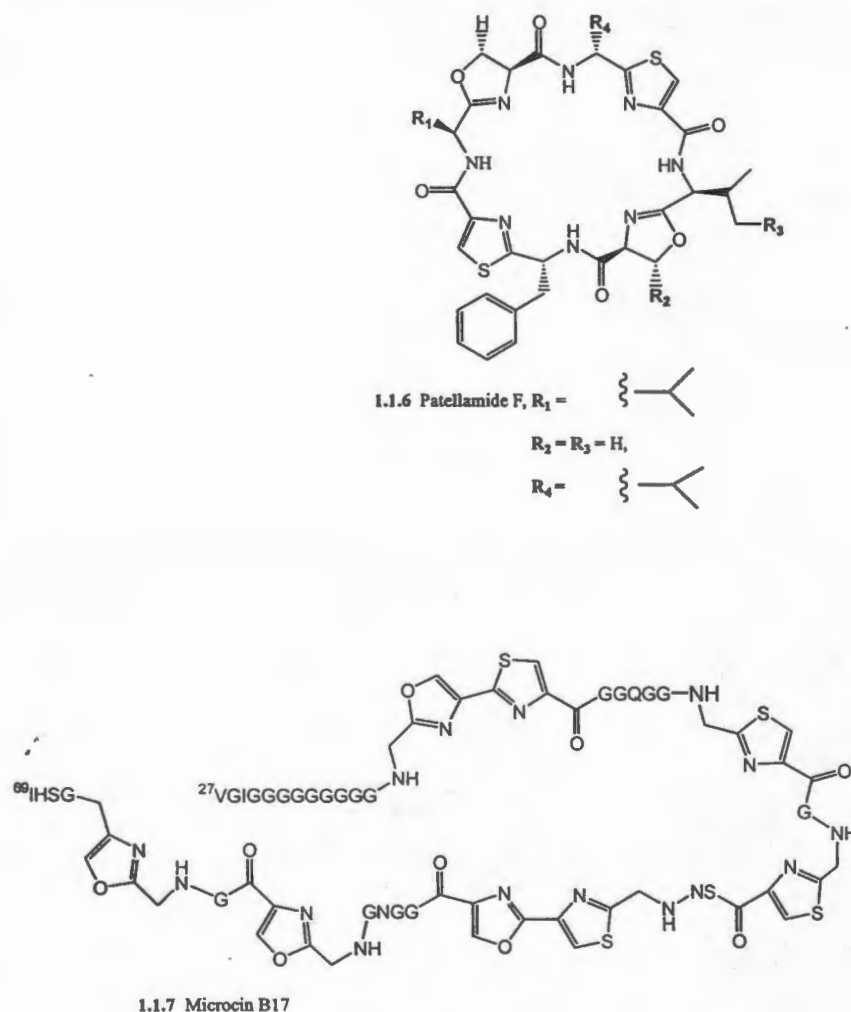
Figure 1.1 Structures of thiazole/oxazole containing natural products

A plausible mechanism for the formation of the heterocycles *in vivo* involves

the condensation of the side chains of threonine, serine and cysteine onto the

preceding carbonyl group to form oxazoline and thiazoline moieties, that can

either undergo a two-electron oxidation to yield the heteroaromatic oxazoles

and thiazoles, or a two-electron reduction to yield oxazolidines and

thiazolidines (Figure 1.2)[9].

4

-X aa-Ser- (X=O)
-X aa-Cys-(X=S)

Tetrahedral Intermediate

- H$_2$O

Oxazole (X=O)
, Thiazole (X=S)

- 2 e

+ 2 e

Oxazoline (X=O)
Thiazoline (X=S)

Oxazolidine (X=O)
Thiazolidine (X=S)
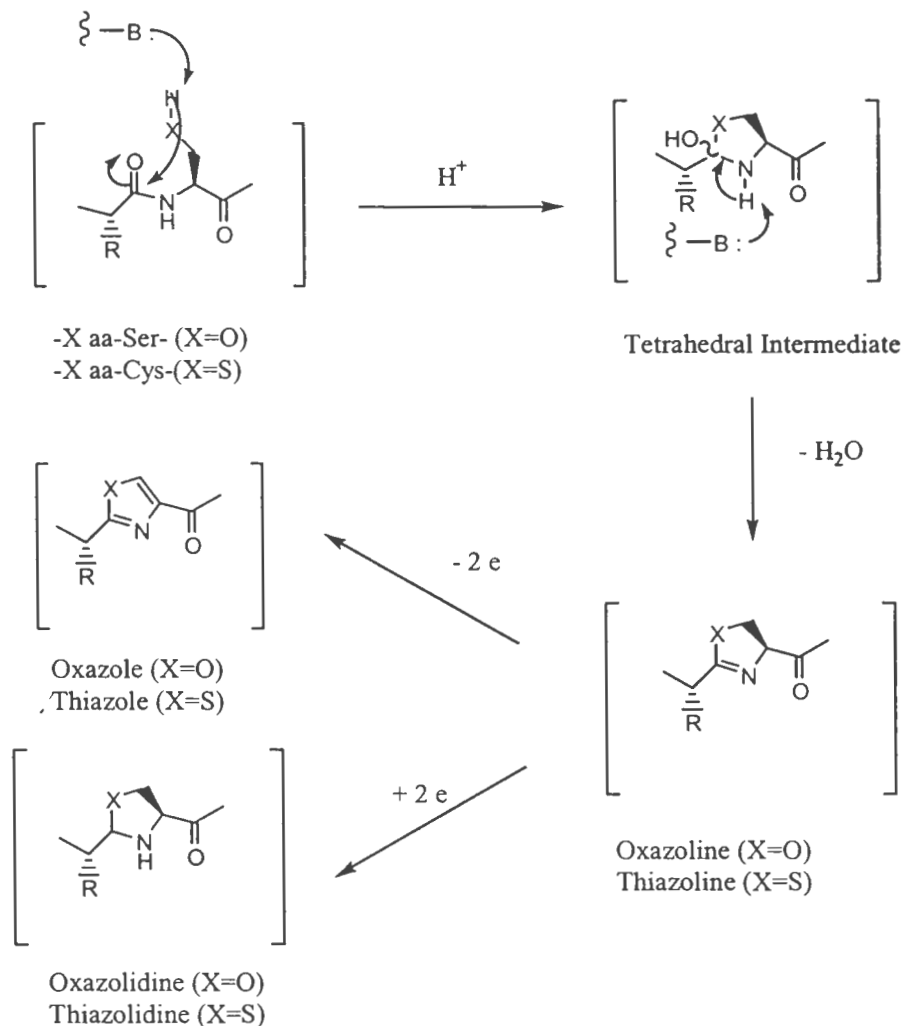
Figure 1.2 Proposed mechanism of heterocycle formation in natural products[9]

Patterns of enzymatic heterocyclization have emerged in the past few years,

and at least two types of enzyme systems are known. One type is exemplified

by bacitracin synthetase, a non ribosomal peptide synthetase that assembles the

growing product chain as an acyl-enzyme complex covalenty linked to the

enzyme during initiation, elongation and termination[10].

Another example is the post-translational modification of microcin B17 (Figure 1.3)[11].

[1] MELKASEFGVVLSVDALKLSRQSPLGVGIGGGGGGGGGGGSCGGQGG
[47] GCGGCSNGCSGGNGGSGGSGSHI[69]

PreproMicrocin B17 (Mcb A)

Microcin Synthetase (McbBCD, ATP)

Mcb A$_{1-38}$

ProMicrocin B17

Proteolysis of the first 26 amino acids

Mcb A$_{27-38}$
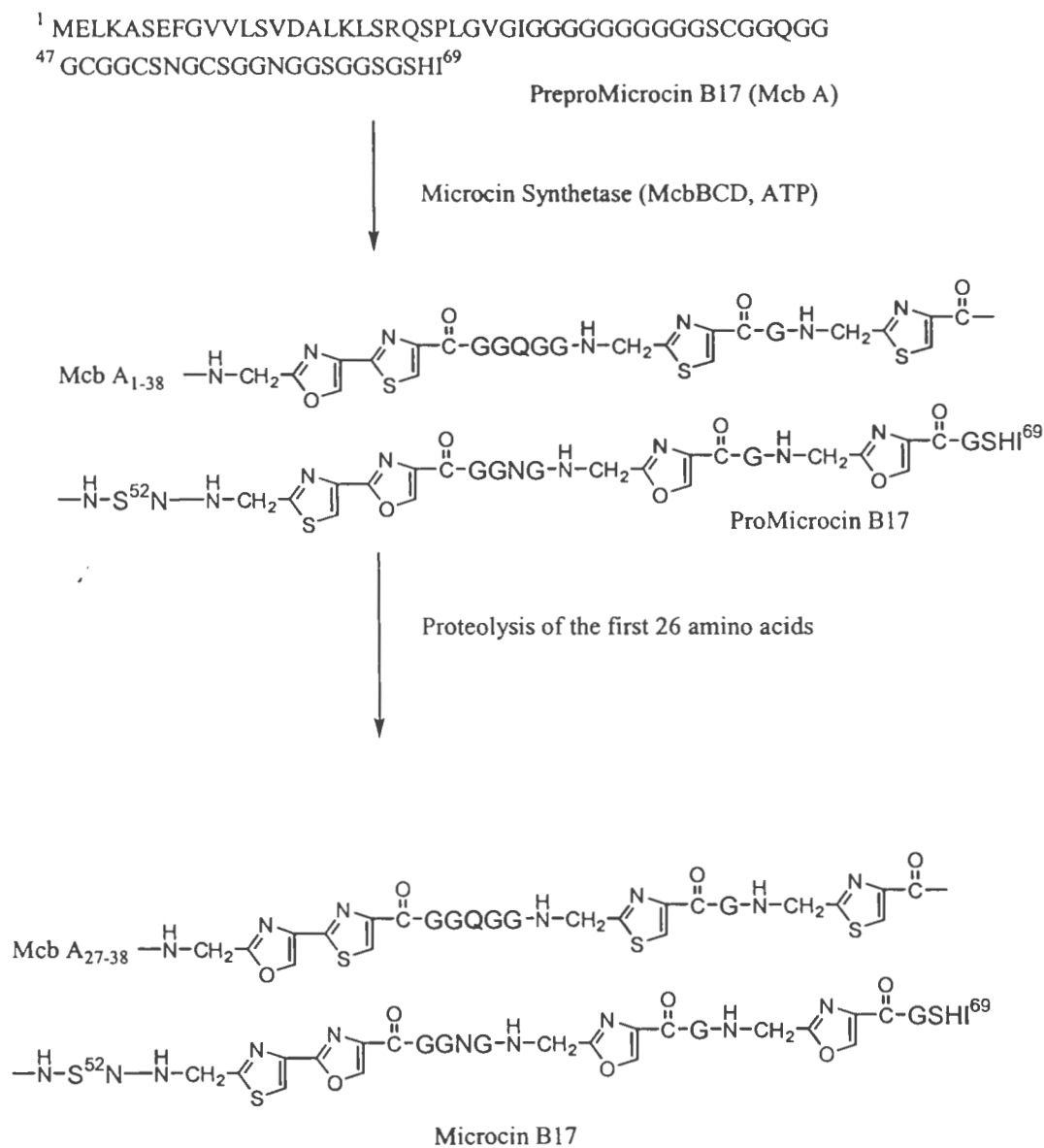
Microcin B17

Figure 1.3 Biosynthesis of Microcin B17[11]

Seven genes *mcb A-G*, clustered in an operon are necessary and sufficient for microcin production. The 69 residue Mcb A polypeptide (also known as PreproMicrocin B17) is a substrate for the enzyme microcin synthetase

composed of Mcb B, C and D subunits which introduces the eight heterocycles and converts Mcb A to inactive promicrocin B17[12]. Subsequent proteolytic cleavage of the first 26 amino acids yields mature microcin B17[13]. Mcb E, and F act as an ATP-dependant export pump that secretes active microcin B17 into the medium[14]. Microcin B17 is taken up by both producer and recipient *E. coli* cells with the help of membrane proteins.

Producer cells express *mcb G* and gain protection against microcin effects, recipient cells lack *mcb G* and accumulate DNA double strand breaks that lead to cell death[15].

Physiological effects of microcin B17 include the inhibition of semiconservative DNA replication. Inhibition of DNA replication induces the SOS response, which results in massive DNA degradation[16]. The molecular target for microcin B17 is DNA gyrase[16].

DNA gyrase is a type II topoisomerase. DNA gyrase is specific to prokaryotes, which makes it an attractive site for the selective activity of antibiotics[17]. DNA gyrase controls the level of DNA supercoiling, catalizes double strand breaks in an ATP-dependant reaction, relaxes supercoiled DNA and re-ligates the cut strands[18]. *E. coli* DNA gyrase is an A_2B_2 tetramer. Gyr A is responsible for DNA cleavage and religation, Gyr B is responsible for the ATPase activity[19]. Other known DNA gyrase inhibitors include coumarins like coumermycin A_1 and novobiocin that compete with ATP for binding to the enzyme, and fluoroquinolones like ciprofloxacin[20] that binds the DNA-enzyme complex.

The mechanism by which microcin B17 inhibits DNA gyrase is similar to that of ciprofloxacin. It is hypothesized that microcin B17 traps the covalent DNA-enzyme complex, slows down the enzyme and causes dissociation of the enzyme from the DNA, leaving the DNA double strands permanently cut[21]. It remains to be shown that the bisheterocycle moieties in microcin B17 intercalate between DNA base pairs which can effectively localize the compound and explains how it inhibits DNA gyrase.

Heterocyclic rings alter peptide backbone connectivity and create new recognition surfaces for interaction with proteins, DNA and RNA.

The thiazoline functionality is essential to the antibiotic activity of bacitracin. Bacitracin inhibits the incorporation of peptidoglycan strands into bacterial cell walls. The thiazoline ring of bacitracin forms a divalent-metal ion-bridged complex with C_{55} – isoprenyl pyrophosphate, preventing C_{55} – isoprenyl pyrophosphate from ferrying disaccharide pentapeptides to their sites of attachment on the cell wall[22].

The bisthiazole moiety in Bleomycin A_2 intercalates between stacked DNA base pairs leading to an increased local concentration of the drug, leading ultimately to double strand cleavage of DNA, which accounts for its anticancer activity[23].

The synthetic combinatorial library (SCL) is a powerful tool for drug discovery. The combinatorial drug discovery process comprises the simultaneous generation of a large number of compounds by the systematic connection of a set of building blocks to form a library and screening of these compounds with their targets to identify novel compounds with enhanced

8

activity[24]. Solid phase peptide synthesis (SPPS) has allowed the synthesis of a large number of peptides simultaneously attached to a polymeric bead. Each bead contains only one peptide species. Combinatorial peptide library technology has been previously employed in designing inhibitors of chemotrypsin[25], and to identify substrates that bind tyrosine kinase [26]. Given the structural importance of thiazole and oxazole heterocycles, synthetic combinatorial libraries with unnatural amino acid building blocks containing thiazole and oxazole heterocycles in the backbone of the peptide or on the side chains can be designed and their antimicrobial activities can be investigated. Library 1 is an enantiomeric tetrapeptide library made of two building blocks, L-3- (4-thiazolyl) alanine and D-3- (4-thiazolyl) alanine[27].

Boc-L-3-(4-thiazolyl) alanine (**L**).   Boc-**D**-3-(4-thiazolyl) alanine (**D**).
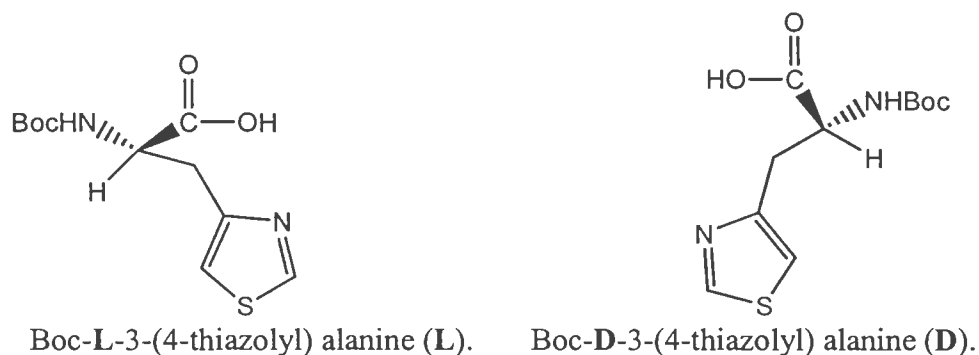
Figure 1.4 The building blocks used to synthesize library 1[27].

The sequences of compounds in library 1 are shown in table 1.1.

Compound	Sequence	Compound	Sequence
L_1 1	DDDD-NH$_2$	L_1 9	DLLL-NH$_2$
L_1 2	DDDL-NH$_2$	L_1 10	DLDL-NH$_2$
L_1 3	LDDL-NH$_2$	L_1 11	LLDL-NH$_2$
L_1 4	LDDD-NH$_2$	L_1 12	LLLL-NH$_2$
L_1 5	DDLL-NH$_2$	L_1 13	DLDD-NH$_2$
L_1 6	DDLD-NH$_2$	L_1 14	DLLD-NH$_2$
L_1 7	LDLL-NH$_2$	L_1 15	LLLD-NH$_2$
L_1 8	LDLD-NH$_2$	L_1 16	LLDD-NH$_2$

Table 1.1: Library **1**, (MW=634.11) from building blocks shown in Figure 1.4.

Library **2** is a tetrapeptide library of 16 compounds. Library **2** design included

a greater number of amino acid building blocks with heterocyclic side chains,

such as imidazole (H) and benzothiophene (S). Arginine (R) was introduced to

increase the overall positive charge on the tetrapeptides[28].

Increasing the positive charge on the tetrapeptides may increase their transport

across negatively charged bacterial membranes as well as increasing their

binding affinities to DNA backbones.

The sequences of the designed peptides comprising combinatorial library **2** are

shown in Figure 1.5.
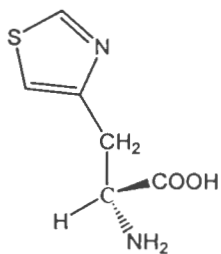
D-3-(4-thiazolyl) alanine (**D**)   L-arginine (**R**)   L-3-(3-benzothienyl) alanine (**S**)
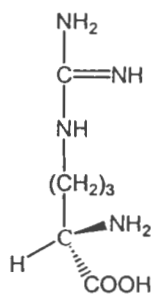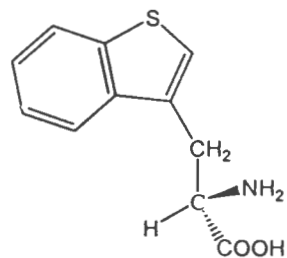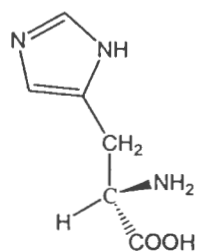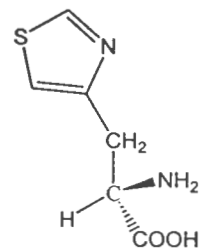
L-histidine (**H**)   L-3-(4-thiazolyl) alanine (**L**)

Figure 1.5 The structures of the building blocks of library **2**

Compound	Sequence	M. W., g. /mol.	Compound	Sequence	M. W., g./mol.
L_2 1	RSSS-NH$_2$	783.5	L_2 9	SSSR-NH$_2$	783.5
L_2 2	RLSS-NH$_2$	734.4	L_2 10	SLSR-NH$_2$	734.4
L_2 3	RDSS-NH$_2$	734.4	L_2 11	SDSR-NH$_2$	734.4
L_2 4	RHSS-NH$_2$	717.6	L_2 12	SHSR-NH$_2$	717.6
L_2 5	RSSH-NH$_2$	717.6	L_2 13	SSHR-NH$_2$	717.6
L_2 6	RLSH-NH$_2$	668.5	L_2 14	SLHR-NH$_2$	668.5
L_2 7	RDSH-NH$_2$	668.5	L_2 15	SDHR-NH$_2$	668.5
L_2 8	RHSH-NH$_2$	651.7	L_2 16	SHHR-NH$_2$	651.7

Table 1.2 Library 2[(28)], tetrapeptide amides from building blocks shown in Figure 1.5.

Library **3** was designed to assess the importance of thiazole and oxazole

moieties in the overall antimicrobial activity of microcin B17 (figure 1.1.7).
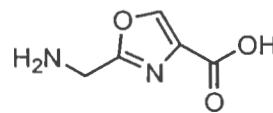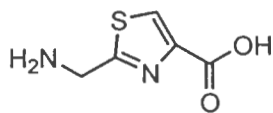
2-Aminomethyl-thiazole-4-carboxylic acid (**A**) 2-Aminomethyl-oxazole-4-carboxylic acid (**B**)
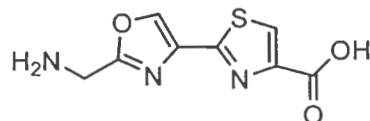
2-(2`-Aminomethyl-oxazole-4`-yl)-thiazole-4-carboxylic acid (**C**)

Glycine (**G**)

Figure 1.6 The structures of the building blocks of library **3**.

Compound	Sequence	M.W., g. / mol.
L₃ 1	Ac-AGA-NH-(CH₂)₃-NH2	454.2
L₃ 2	Ac-BGA-NH-(CH₂)₃-NH2	438.2
L₃ 3	Ac-CGA-NH-(CH₂)₃-NH2	521.5
L₃ 4	Ac-AGB-NH-(CH₂)₃-NH2	438.2
L₃ 5	Ac-BGB-NH-(CH₂)₃-NH2	422.2
L₃ 6	Ac-CGB-NH-(CH₂)₃-NH2	505.2
L₃ 7	Ac-AGC-NH-(CH₂)₃-NH2	521.5
L₃ 8	Ac-BGC-NH-(CH₂)₃-NH2	505.2
L₃ 9	Ac-CGC-NH-(CH₂)₃-NH2	588.4
L₃ 10	Ac-AA-NH-(CH₂)₃-NH2	397.3
L₃ 11	Ac-BA-NH-(CH₂)₃-NH2	381.3
L₃ 12	Ac-AB-NH-(CH₂)₃-NH2	381.3
L₃ 13	Ac-BB-NH-(CH₂)₃-NH2	364.9
L₃ 14	Ac-AAA-NH-(CH₂)₃-NH2	537.1
L₃ 15	Ac-BBB-NH-(CH₂)₃-NH2	489.2
L₃ 16	Ac-CGGQGGAG-NH₂	820.3

Table 1.3 Library 3[29] from building blocks shown in Figure 1.6.
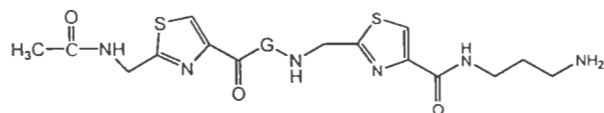
L₃ 1
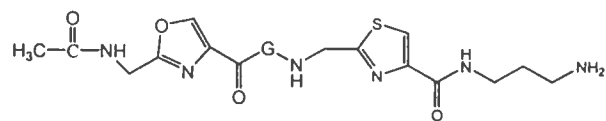
L₃ 2

L₃ 3

L₃ 4

L₃ 5

L₃ 6

L₃ 7

14
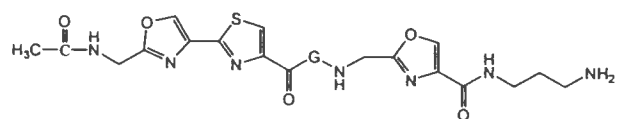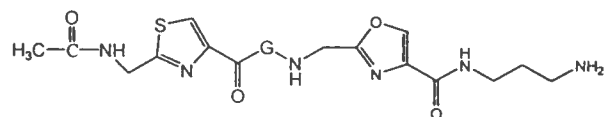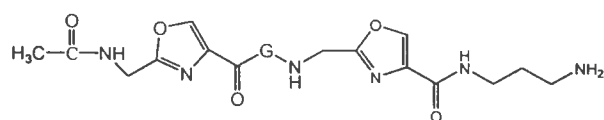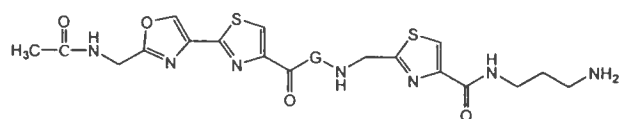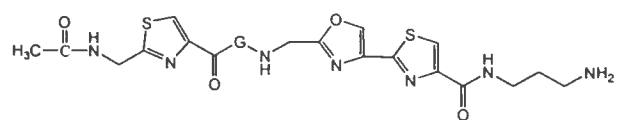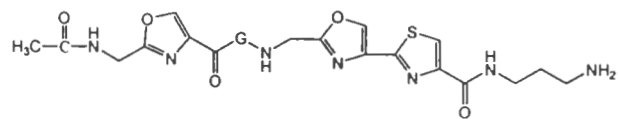
L₃ 8
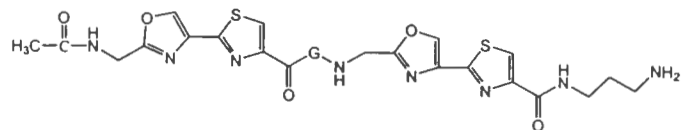
L₃ 9
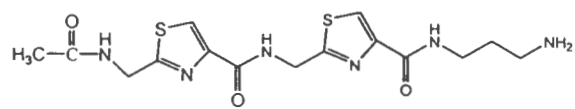
L₃ 10

L₃ 11

L₃ 12

L₃ 13

15
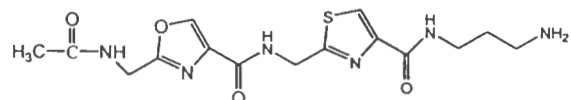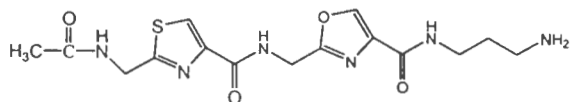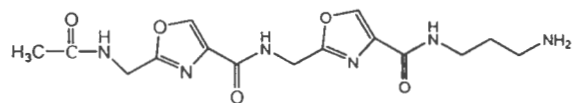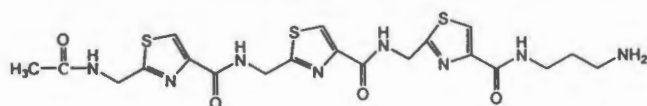
L₃ 14
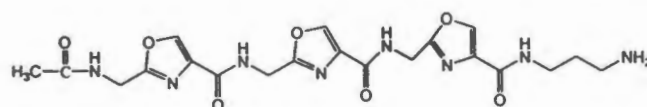
L₃ 15
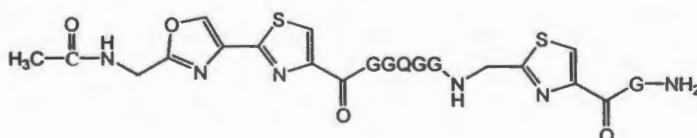
L₃ 16

Figure 1.7 Structures of Compounds in Library **3**[(29)].

Library **3** was designed based on microcin B17 (Figure 1.1.7).

Given that the thiazole, oxazole and bisheterocycle moieties may be essential

to the antibacterial activities of microcin B17, these moieties were

systematically connected in a combinatorial library (library **3**).

Compounds L₃ 1-9 have a central glycine residue that separates the two

heterocyclic moieties, which confers flexibility on the molecules.

Compounds L₃ 10-13 have two heterocycles directly attached to each other

giving it a certain degree of rigidity which is even higher in compounds L₃ 14

and L₃ 15 with three heterocycles directly attached to each others.

Compound L₃ 16 is a microcin B17 fragment.

Three combinatorial libraries with thiazole and oxazole-containing amino acids

that had been designed and synthesized were tested for cytotoxicity against the fish pathogen, *Vibrio anguillarum*, the enterobacterium *Escherichia coli* and the yeast *Saccharomyces cerevisiae* in cell culture growth inhibition assays and in zone inhibition assays.

Zone inhibition assay is a classical method to screen antimicrobial agents. In zone inhibition assays, only the lethal activity of the antimicrobial compounds can be assessed after incubating the antimicrobial compounds with growing cultures of micro-organisms on agar plates for a period of 12-24 hours.

In cell culture growth inhibition assays on the other hand, both lethal and inhibitory effects of antimicrobial compounds can be determined.

It has been reported that synthetic analogs of gramicidin S antibacterial activities were highly dependent on the type of the assay used with growth inhibition assays showing greater activity against gram-negative bacteria than agar-based assays[30]. Factors such as variation in the diffusion rates of the compounds in the peptide libraries under screening may lead to different reported MIC values than cell culture growth inhibition assays.

In this chapter, both zone inhibition assays and growth inhibition assays were used to screen the peptide libraries compounds but growth inhibition assay data was used to determine the MIC values.

The selection of candidate micro-organisms followed that *V. anguillarum* causes vibriosis, a fish disease that causes severe economic losses. *E. coli* is an opportunistic enteric pathogen which causes enteric diseases in immunely

17

compromised humans, *E. coli* (ZK4) is a genetically engineered species that is microcin-sensitive which makes it a good selection to screen compounds in library **3** and compare their activities against microcin B17. *S. cerevisiae* is a representative example of an eukaryotic micro-organism.

Species selectivity of the antimicrobial activities of the combinatorial libraries against prokaryotic pathogens (*V. anguillarum* and *E. coli*) and eukaryotic pathogens (*S. cerevisiae*) were also investigated.

1.2 EXPERIMENTAL

Equipment

Analytical HPLC experiments were performed on a Waters HPLC system which consisted of a gradient controller, two 501 pumps and a 486 tunable UV / VIS absorbance detector set at 220 nm and a Vydac 218TP C 18 10 micron (250 x 4.6 mm I. D.) protein and peptide column.

Scanning of the growth inhibition plates was done on a Dynex MRX, (Dynex Technologies Inc, VA).

1.2.1 Zone Inhibition Assay

Zone inhibition assays were done on *E. coli* (ZK4) and *V. anguillarum*.

E. coli (ZK4):

E. coli (ZK4) was streaked from a frozen sample (-70°C) on a Luria Bertani (LB 10) medium and incubated at 37°C overnight. A string of individually growing colonies was collected with a sterile loop and put into 5 ml of 1 x LB 10 in a sterile centrifuge tube.

The solution was shaken at 37°C for 3 hours. The optical density (OD) was measured at 650 nm and the dilution factor to give a bacterial concentration of 2×10^3 colony-forming unit (cfu) / ml was calculated using the equation that 1 OD at 650 nm is equal to 2.5×10^8 cfu / ml.

The bacterial suspension was inoculated into 0.1 x LB 10, 1 % agarose medium and poured into a petri dish. Peptide solution (5 µl) was added to the wells in the agar and incubated for 3 hours at 37°C. Full-strength LB 10, 1 % agarose medium was added on top of the previous layer and the plate was

incubated at 37°C overnight and the diameters of the observed zones of inhibition were measured.

V. anguillarum:

V. anguillarum was streaked from a frozen sample (-70°C) on a Luria Bertani (LB 20) medium and incubated at 28°C overnight. A string of individually growing colonies was collected with a sterile loop and put into 5 ml of 1 x LB 20 in a sterile centrifuge tube.

The solution was shaken at 28 °C for 3 hours. The optical density (OD) was measured at 650 nm and the dilution factor to give a bacterial concentration of 2×10^3 colony-forming unit (cfu) / ml was calculated using the equation that 1 OD at 650 nm is equal to 2.5×10^8 cfu / ml. The bacterial suspension was inoculated into 0.1 x LB 10, 1 % agarose medium and poured into a petri dish. Peptide solution (5 µl) was added to the wells in the agar and incubated for 3 hours at 28 °C. Full-strength LB 20, 1 % agarose medium was added on top of the previous layer and the plate was incubated at 28°C overnight and the diameters of the observed zones of inhibition were measured.

1.2.2 Cell Culture Growth Inhibition Assay

Cell culture growth inhibition assays were done on *E. coli* (ZK4), *V. anguillarum* and *S. cerevisiae*.

E. coli (ZK4):

E. coli (ZK4) was streaked from a frozen sample (-70°C) on a LB 10 plate and incubated at 37°C overnight. A string of individually growing colonies was

collected with a sterile loop and put into 5 ml of 1 x LB 10 in a sterile centrifuge tube.

The solution was shaken at 37°C for 3 hours. The bacterial suspension was diluted with 0.1 x LB 10 to an OD of 0.001 AU / ml at 650 nm.

Diluted bacterial suspension was incubated with the peptide solutions (30 µl each) in the wells of a sterile 96 well plate for 3 hours at 37°C.

The controls included blank controls (60 µl 0.1 x LB 10, no peptide and bacteria were added), positive growth controls (30 µl 0.1 x LB 10, 30 µl bacterial suspension), positive killing controls (30 µl of 0.5 M NaOH, 30 µl bacterial suspension).

Full strength LB 10 medium (100 µl) was then added to each well and the absorbance was measures at 570 nm at different time intervals.

V. anguillarum:

V. anguillarum was streaked from a frozen sample (-70°C) on a LB 20 plate and incubated at 28°C overnight. A string of individually growing colonies was collected with a sterile loop and put into 5 ml of 1 x LB 20 in a sterile centrifuge tube. The solution was shaken at 28°C for 3 hours.

The bacterial suspension was diluted with 0.1 x LB 20 to an OD of 0.001 AU / ml at 650 nm. Diluted bacterial suspension was incubated with the peptide solutions (30 µl each) in the wells of a sterile 96 well plate for 3 hours at 28°C.

The controls included blank controls (60 µl 0.1 x LB 20, no peptide and bacteria were added), positive growth controls (30 µl 0.1 x LB 20, 30 µl

21

bacterial suspension), positive killing controls (30 μl of 0.5 M NaOH, 30 μl bacterial suspension). Full strength LB 20 medium (100 μl) was then added to each well and the absorbance was measures at 570 nm at different time intervals.

S. cerevisiae:

S. cerevisiae was streaked from a frozen sample (-70°C) on a YPD, 1 % agarose plates and incubated at 30°C overnight. A string of individually growing colonies was collected with a sterile loop and put into 5 ml of 1 x YPD broth in a sterile centrifuge tube.

The solution was shaken at 30°C for 3 hours. The yeast suspension was diluted with 0.1 x YPD broth to an OD of 0.001 AU / ml at 650 nm. Diluted yeast suspension was incubated with the peptide solutions (30 μl each) in the wells of a sterile 96 well plate for 3 hours at 30 °C.

The controls included blank controls (60 μl 0.1 x YPD, no peptide and yeast added), positive growth controls (30 μl 0.1 x YPD , 30 μl yeast suspension), positive killing controls (30 μl of 0.5 M NaOH, 30 μl yeast suspension).

Full strength YPD broth (100 μl) was then added to each well and the absorbance was measured at 570 nm at different time intervals.

1.2.3 HPLC Analysis

HPLC analysis of peptide libraries was used to compare the hydrophobicities of the compounds in the libraries and to prepare serial dilutions of the compounds for antimicrobial testing.

Peptide libraries **1, 2** and **3** were analyzed by RP-HPLC on a Vydac 218TP C 18, 5 μ column (250 x 4.6 mm i. d., 300 Å).

Conditions: Linear gradient from 5% to 60% CH_3CN over 40 minutes; solvent A consists of 5 % CH_3CN aqueous solution, 0.1 % trifluoroacetic acid; solvent B consists of 95 % CH_3CN, 0.1 % trifluoroacetic acid, 1.37 % CH_3CN / min; flow rate 1 ml / min; UV detection at 220 nm.

The absorbance of the peptide peak at 220 nm represents the amount of peptide in a known injected volume of peptide solution and was used to calculate peptide concentrations.

1.2.4 Media Preparation:

Yeast extract, tryptone peptone (pancreatic digest of casein), YPD broth and YPD Bacto agar were from Difco, sodium chloride (enzyme grade) was from Fisher. Distilled water was obtained from Milli-Q Plus PF system (Millipore).

LB 10

Yeast extract   5 g.

Tryptone peptone   10 g.

Sodium chloride   10 g.

Add distilled water to 1 liter and autoclave at 120-124°C for 15 min.

LB 20

Yeast extract   5 g.

Tryptone peptone   10 g.

Sodium chloride   20 g.

Add distilled water to 1 liter and autoclave at 120-124°C for 15 min.

YPD broth

Formula per liter

Bacto yeast extract   10 g.

Bacto peptone   20 g.

Bacto dextrose   20 g.

50 grams of YPD broth was dissolved in 1 liter distilled water and sterilized at 120-124°C for 15 min.

YPD Bacto agar

Formula per liter

Bacto yeast extract   10 g.

 Bacto peptone   20 g.

Bacto dextrose   20 g.

Bacto agar   15 g.

50 grams of YPD Bacto agar was dissolved in 1 liter distilled water and sterilized at 120-124°C for 15 min.

1.3 RESULTS AND DISCUSSION

1.3.1 HPLC Analysis of Peptide Libraries

Studies have shown a direct correlation between peptide hydrophobicities and the % CH_3CN required to elute them from a reverse phase column[31].

The more hydrophobic peptides eluted at higher CH_3CN percentage.

Peptides in library **2** are arranged in order of decreasing retention times in Table 1.4.

The number of L-3-(3-benzothienyl) alanine (S) residues was correlated with the hydrophobicity of the compounds in library **2**.

Compounds # **1** and # **9**, Table 1.4, each contains 3 (S) residues and were the most hydrophobic compounds in the library followed by compounds # **2-5** and **10-13** with 2 (S), and then # **6-8** and # **14-16** with 1 (S) residue.

The presence of 2 histidine and 1 arginine residues makes compound # **8** and compound # **16** the least hydrophobic compounds in the library.

Peptides in libraries **1** and **3** had overall lower retention times than did compounds in library **2**.

The % CH_3CN required to elute compounds in libraries **1** and **3** ranged between 20-25 %.

The lower % CH_3CN correlated with the less hydrophobic nature of the building blocks used in libraries **1** and **3** compared to the more hydrophobic L-3-(3-benzothienyl) alanine (S) residues used in the design of library **2**.

Compound	Sequence	* Average retention time (min)	% CH$_3$CN at retention time.	ε_{220} extinction coefficient (L mole^{-1} cm^{-1})
L$_2$ 1	RSSS-NH$_2$	31.8	49.6	44.03
L$_2$ 9	SSSR-NH$_2$	29.7	46.6	46.24
L$_2$ 3	RDSS-NH$_2$	29.4	46.3	33.50
L$_2$ 11	SDSR-NH$_2$	27.7	43.9	36.95
L$_2$ 2	RLSS-NH$_2$	27.4	43.4	33.50
L$_2$ 10	SLSR-NH$_2$	25.0	39.4	35.039
L$_2$ 4	RHSS-NH$_2$	24.6	38.7	14.04
L$_2$ 5	RSSH-NH$_2$	23.4	37.2	41.57
L$_2$ 12	SHSR-NH$_2$	22.5	36.0	39.02
L$_2$ 13	SSHR-NH$_2$	22.4	35.8	50.84
L$_2$ 7	RDSH-NH$_2$	20.3	32.8	18.45
L$_2$ 15	SDHR-NH$_2$	19.8	32.2	22.97
L$_2$ 6	RLSH-NH$_2$	17.6	29.2	17.46
L$_2$ 14	SLHR-NH$_2$	16.4	27.5	19.92
L$_2$ 16	SHHR-NH$_2$	14.7	25.1	25.34
L$_2$ 8	RHSH-NH$_2$	12.0	21.5	23.31

Table 1.4 Compounds of library **2** arranged in order of decreasing retention times.
* An average of 2 runs.

1.3.2 Zone Inhibition Assay

Compounds in library **2** were tested against *E. coli* ZK4 and *V. anguillarum* in a zone inhibition assay. Antimicrobial activity was tested using serial dilutions of the peptides, and the diameters of the zones of inhibition were measured after overnight incubation. As expected, the diameters of the zones of inhibition decreased with decreasing peptide concentrations. Tables 1.5.1, 1.5.2, 1.6.1 and 1.6.2 list the library **2** peptide concentrations and the measured zones of inhibition of *E. coli* ZK4 and *V. anguillarum* respectively. Sodium hydroxide and microcin B17 were included in the zone inhibition assay as positive controls.

The MIC* is considered to be the minimum amount of peptide that gives a zone of inhibition.

For compounds in library **2**, we also employed growth assays that were more sensitive than zone assays (section 1.3.3). The peptide concentrations tested in the zone inhibition assays were above the MIC values of peptides in library **2** determined using the growth assay technique.

The growth inhibition assays monitor the growth curves of bacteria after a 3 hour incubation of the bacteria with the peptides. This approach aims to elucidate the mechanism by which these peptides exert their inhibitory effects on the bacteria.

In a zone inhibition assay, the diameter of the clearing zone of inhibition corresponds to the bactericidal effects of the compounds tested.

In a growth inhibition assay, the inhibition of bacterial growth is

monitored over a long period of time and the difference between bactericidal and bacteristatic effects can be observed.

Library 1 contained enantiomeric and diastereomeric compounds that did not show any variation in their antimicrobial activities. They all had identical MIC* values of 4.5 μmoles, higher than MIC values of library 2 compounds.

Library 2 tetrapeptide amides, (Tables 1.5.1, 1.5.2, 1.6.1 and 1.6.2), showed a higher antibacterial activities against *E. coli* (ZK4) and *V. anguillarum* than did library 1 compounds.

The concentration ranges that were tested in the zone inhibition assay were above the MIC values of the compounds in library 2. The activities of the library 2 compounds were comparable against *E. coli* and *V. anguillarum*. Cell culture growth inhibition assays were used to report MIC values of library 2 tetrapeptide amides against *E. coli*, *V. anguillarum* and *S. cerevisiae* (section 1.3.3).

Library 3 compounds, at concentrations in the μmolar range and lower, were not able to produce measurable zones of inhibition against either *E. coli* ZK4 or *V. anguillarum* under the assay conditions.

*MIC in zone inhibition assays denotes the peptide amount (μmoles) in the wells of the agar plates, and in cell culture growth inhibition assays, MIC denotes the peptide concentration (μmolar) incubated with the micro-organism cultures in the 96 well plate.

Compound	M.W., g. / mol.	Sequence	Peptide (μmoles)	Peptide (mg)	Measured zone of inhibition (mm)*.	MIC (μmoles).
L_2 1	783.5	RSSS-NH$_2$	28.1	22.02	6	
			14.05	11.01	4	
			2.81	2.20	4	<2.81
L_2 2	734.4	RLSS-NH$_2$	6.19	4.54	8	
			3.09	2.27	7	
			0.62	0.45	6	<0.62
L_2 3	734.4	RDSS-NH$_2$	6.19	7.40	12	
			3.09	3.70	9	
			0.62	0.74	3	<0.62
L_2 4	717.6	RHSS-NH$_2$	9.70	6.96	10	
			4.85	3.48	8	
			0.97	0.70	4	<0.97
L_2 5	717.6	RSSH-NH$_2$	28.90	20.74	10	
			14.45	10.37	8	
			2.89	2.07	4	<2.89
L_2 6	668.5	RLSH-NH$_2$	13.06	9.00	4	
			6.53	4.50	0	6.53
			1.30	0.90	0	
L_2 7	668.5	RDSH-NH$_2$	13.79	9.21	10	
			6.89	4.60	10	
			1.37	0.92	6	<1.37
L_2 8	651.7	RHSH-NH$_2$	17.88	11.65	16	
			8.94	5.83	10	
			1.78	1.17	8	<1.78

Table 1.5.1 Measured zones of inhibition of peptides L_2 1-L_2 8 on *E. coli* ZK4 12 hours after incubation.

* The well diameter was subtracted from the measured zone of inhibition

Compound	M.W. g. / mol.	Sequence	Peptide (μmoles)	Measured zone of inhibition (mm)*.	Peptide (mg)	MIC (μmoles)
L_2 9	783.5	SSSR-NH_2	29.50	10	23.11	
			14.75	6	11.56	
			2.95	6	2.31	<2.95
L_2 10	734.4	SLSR-NH_2	23.84	10	17.51	
			11.92	7	8.76	
			2.38	4	1.75	<2.38
L_2 11	734.4	SDSR-NH_2	25.15	6	18.50	
			12.58	4	9.25	
			2.52	4	1.85	<2.52
L_2 12	717.6	SHSR-NH_2	27.18	12	19.5	
			13.59	10	9.75	
			2.72	6	1.95	<2.72
L_2 13	717.6	SSHR-NH_2	35.42	8	25.41	
			17.71	8	12.71	
			3.54	6	2.54	<3.54
L_2 14	668.5	SLHR-NH_2	14.89	8	10.00	
			7.45	NO	5.00	7.45
			1.49	NO	1.00	
L_2 15	668.5	SDHR-NH_2	17.18	8	11.50	
			8.59	6	5.75	<8.59
L_2 16	651.7	SHHR-NH_2	19.44	10	12.70	
			9.72	10	6.35	<9.72

Table 1.5.2 Measured zones of inhibition of peptides L_2 9-L_2 16 on *E. coli* ZK4 12 hours after incubation.

* The well diameter was subtracted from the measured zone of inhibition.

Compound	M.W. g. / mol.	Sequence	Peptide (μmoles)	Measured zone of inhibition (mm)*.	Peptide (mg)	MIC (μmoles)
L_2 9	783.5	SSSR-NH$_2$	29.50 14.75 2.95	10 6 6	23.11 11.56 2.31	 <2.95
L_2 10	734.4	SLSR-NH$_2$	23.84 11.92 2.38	10 7 4	17.51 8.76 1.75	 <2.38
L_2 11	734.4	SDSR-NH$_2$	25.15 12.58 2.52	6 4 4	18.50 9.25 1.85	 <2.52
L_2 12	717.6	SHSR-NH$_2$	27.18 13.59 2.72	12 10 6	19.5 9.75 1.95	 <2.72
L_2 13	717.6	SSHR-NH$_2$	35.42 17.71 3.54	8 8 6	25.41 12.71 2.54	 <3.54
L_2 14	668.5	SLHR-NH$_2$	14.89 7.45 1.49	8 NO NO	10.00 5.00 1.00	 7.45
L_2 15	668.5	SDHR-NH$_2$	17.18 8.59	8 6	11.50 5.75	 <8.59
L_2 16	651.7	SHHR-NH$_2$	19.44 9.72	10 10	12.70 6.35	 <9.72

Table 1.5.2 Measured zones of inhibition of peptides L_2 9-L_2 16 on *E. coli* ZK4 12 hours after incubation.

* The well diameter was subtracted from the measured zone of inhibition.

Compound	M.W. g. / mol.	Sequence	Peptide (μmoles)	Peptide (mg)	Measured zone of inhibition (mm)*.	MIC (μmoles)
L_2 1	783.5	RSSS-NH$_2$	28.10	22.02	10	
			14.05	11.01	8	
			2.81	2.20	3	<2.81
L_2 2	734.4	RLSS-NH$_2$	6.19	4.54	6	
			3.09	2.27	3	
			0.62	0.45	0	0.62
L_2 3	734.4	RDSS-NH$_2$	6.19	4.54	13	
			3.09	2.27	8	
			0.62	0.45	6	<0.62
L_2 4	717.6	RHSS-NH$_2$	9.70	7.00	10	
			4.85	3.50	6	
			0.97	0.70	4	<0.97
L_2 5	717.6	RSSH-NH$_2$	28.90	20.74	10	
			14.45	10.37	6	
			2.89	2.07	4	<2.89
L_2 6	668.5	RLSH-NH$_2$	13.06	8.73	10	
			6.53	4.37	5	
			1.30	0.87	0	1.30
L_2 7	668.5	RDSH-NH$_2$	13.79	9.22	8	
			6.89	4.61	6	
			1.37	0.92	3	<1.37
L_2 8	651.7	RHSH-NH$_2$	17.88	11.65	10	
			8.94	5.83	5	
			1.78	1.17	1	<1.78

Table 1.6.1 Measured zones of inhibition of peptides L_2 1-L_2 8 on *V. anguillarum* 12 hours after incubation.

* The well diameter was subtracted from the measured zone of inhibition.

	M.W. g. / mol.	Sequence	Peptide (μmoles)	Measured zone of inhibition (mm)*.	Peptide (mg)	MIC (μmoles)
L_2 9	783.5	SSSR-NH$_2$	29.50	8	23.11	
			14.75	5	11.56	
			2.95	2	2.31	<2.95
L_2 10	734.4	SLSR-NH$_2$	23.84	7	17.51	
			11.92	3	8.76	
			2.38	2	1.75	<2.38
L_2 11	734.4	SDSR-NH$_2$	25.15	6	18.50	
			12.58	2	9.25	
			2.52	0	1.85	2.52
L_2 12	717.6	SHSR-NH$_2$	27.18	8	19.50	
			13.59	5	9.75	
			2.72	0	1.95	2.72
L_2 13	717.6	SSHR-NH$_2$	35.42	8	25.14	
			17.71	6	12.57	
			3.54	2	2.51	<3.54
L_2 14	668.5	SLHR-NH$_2$	14.89	7	9.95	
			7.45	3	4.97	
			1.49	0	1.00	1.49
L_2 15	668.5	SDHR-NH$_2$	17.18	8	11.48	
			8.59	6	5.74	
			1.72	0	1.15	1.72
L_2 16	651.7	SHHR-NH$_2$	19.44	8	12.67	
			9.72	3	6.34	
			1.94	0	1.27	1.94

Table 1.6.2 Measured zones of inhibition of peptides L_2 9-L_2 16 on *V. anguillarum* 12 hours after incubation.

* The well diameter was subtracted from the measured zone of inhibition.

1.3.3 Cell Culture Growth Inhibition Assay

The growth inhibition assay is a kinetic assay. Logarithmically growing cultures of *E. coli*, *V. anguillarum* and *S. cerevisiae* were diluted into nutrient-poor medium and pre-incubated with the peptides for 3 hours in 96-well plates, cultures were then diluted with nutrient-rich media and the bacterial growth was monitored by measuring the optical density at 570 nm.

Controls in the assay included a freely growing bacterial suspension (positive control), and uninoculated medium (blank). To control for variability in the assay, the experiments were repeated on different days, and in each assay every peptide concentration was run in triplicate.

Time points between 6 and 8 hours (9 and 11 hours post-exposure) were selected to measure the MICs of the peptides.

For each peptide concentration, the average of the optical density in three wells was used to calculate the average optical density in the wells at each time point. A plot of the peptide concentration versus the % growth relative to the positive control was used to determine the MIC values.

Table 1.7 lists the results from library **2** peptides in order of decreasing activity against *E. coli* ZK4. Table 1.8 lists the results from library **2** peptides in order of decreasing activity against *V. anguillarum*. Table 1.9 lists the results from library **2** peptides in order of decreasing activity against *S. cerevisiae*.

The growth inhibition MIC values of peptides in library **2** against gram negative bacteria, *E. coli* and *V. anguillarum* were comparable to each other but the activity against a fungus , *S. cerevisiae* showed a different pattern.

Peptides, L_2 **1** and L_2 **9** both with three L-3-(3-benzothienyl)alanine (S)

residues, had a ten fold lower MIC values than peptides L_2 **14**, L_2 **15** and L_2 **16**

with one (S) residue (Tables 1.7 and 1.8).

Compound	M. W., g. / mol.	Sequence	MIC, μM.
L_2 1	783.5	RSSS-NH$_2$	0.26
L_2 9	783.5	SSSR-NH$_2$	0.26
L_2 2	734.4	RLSS-NH$_2$	0.39
L_2 3	734.4	RDSS-NH$_2$	0.39
L_2 11	734.4	SDSR-NH$_2$	0.42
L_2 13	717.6	SSHR-NH$_2$	0.59
L_2 12	717.6	SHSR-NH$_2$	0.70
L_2 10	734.4	SLSR-NH$_2$	0.70
L_2 8	651.7	RHSH-NH$_2$	1.30
L_2 5	717.6	RSSH-NH$_2$	1.33
L_2 6	668.5	RLSH-NH$_2$	1.64
L_2 4	717.6	RHSS-NH$_2$	1.90
L_2 7	668.5	RDSH-NH$_2$	2.00
L_2 16	651.7	SHHR-NH$_2$	2.30
L_2 15	668.5	SDHR-NH$_2$	2.50
L_2 14	668.5	SLHR-NH$_2$	2.90

Table 1.7 Antimicrobial activity of library **2** peptides against *E. coli* ZK4 arranged in order of increasing MIC.

Compound	M. W., g. / mol.	Sequence	MIC, μM
L$_2$ 1	783.5	RSSS-NH$_2$	0.16
L$_2$ 9	783.5	SSSR-NH$_2$	0.17
L$_2$ 4	717.6	RHSS-NH$_2$	0.65
L$_2$ 12	717.6	SHSR-NH$_2$	0.69
L$_2$ 11	734.4	SDSR-NH$_2$	0.70
L$_2$ 10	734.4	SLSR-NH$_2$	0.74
L$_2$ 16	651.7	SHHR-NH$_2$	1.18
L$_2$ 15	668.5	SDHR-NH$_2$	1.30
L$_2$ 14	668.5	SLHR-NH$_2$	1.40
L$_2$ 6	668.5	RLSH-NH$_2$	1.60
L$_2$ 5	717.6	RSSH-NH$_2$	0.22
L$_2$ 2	734.4	RLSS-NH$_2$	0.27
L$_2$ 3	734.4	RDSS-NH$_2$	0.27
L$_2$ 8	651.7	RHSH-NH$_2$	0.41
L$_2$ 13	717.6	SSHR-NH$_2$	0.51
L$_2$ 7	668.5	RDSH-NH$_2$	0.52

Table 1.8 Antimicrobial activity of library **2** peptides against *V. anguillarum* arranged in order of increasing MIC

Compound	M. W., gram / mol.	Sequence	MIC, μM.
L_2 4	717.6	RHSS-NH$_2$	1.10
L_2 1	783.5	RSSS-NH$_2$	2.79
L_2 13	717.6	SSHR-NH$_2$	3.22
L_2 5	717.6	RSSH-NH$_2$	3.31
L_2 9	783.5	SSSR-NH$_2$	3.63
L_2 11	734.4	SDSR-NH$_2$	4.34
L_2 2	734.4	RLSS-NH$_2$	4.40
L_2 3	734.4	RDSS-NH$_2$	4.73
L_2 12	717.6	SHSR-NH$_2$	5.04
L_2 10	734.4	SLSR-NH$_2$	5.34
L_2 6	668.5	RLSH-NH$_2$	8.90
L_2 7	668.5	RDSH-NH$_2$	9.32
L_2 16	651.7	SHHR-NH$_2$	10.52
L_2 14	668.5	SLHR-NH$_2$	10.80
L_2 15	668.5	SDHR-NH$_2$	11.25
L_2 8	651.7	RHSH-NH$_2$	17.15

Table 1.9 Antimicrobial activity of library **2** peptides against *S. cerevisiae* in order of decreasing activity

Antibacterial activity also correlated with hydrophobicity, since the more hydrophobic peptides(Table 1.4) had lower MIC values. These patterns were not observed in the activity against *S. cerevisiae*.

Increasing the number of benzothienylalanine residues did not correlate with a decrease in the MIC values. The MIC values of peptides in library **2** were generally ten folds higher against *S. cerevisiae* (Table 1.9) than against either *E. coli* or *V. anguillarum* (Tables 1.7 and 1.8).

The activity of peptides in library **2** against *E. coli* did not change by changing the position of arginine residue between the *N* and the *C* terminus for compounds L_2 **1**, $(RSSS-NH_2)$, and L_2 **9**, $(SSSR-NH_2)$.

The interchange between L-3-(4-thiazolyl)alanine, (**L**), and D-3-(4-thiazolyl)alanine, (**D**), at position two did not affect the activity of peptides in library **2** since peptide pairs L_2 **2** and L_2 **3**, L_2 **14** and L_2 **15** had the same MIC values against *E. coli* while peptide pairs L_2 **10** and L_2 **11**, L_2 **6** and L_2 **7** had less than two fold differences in their MIC values against *E. coli*.

This pattern is also observed in the activity of peptides in library **2** against *V. anguillarum*. This pattern is lost in the activity of peptides in library **2** against *S. cerevisiae*.

A second set of experiments were aimed at further characterization of the interactions of compound in library **2** with *V. anguillarum*. For this, we chose to test the most active compounds in library **2** L_2 **1**, L_2 **2**, L_2 **5** and L_2 **9**.

The MIC values were compared at 9 hours and 19 hours after incubating the peptide

solutions with growing cultures of *V. anguillarum* (Table 1.10).

Compound	M. W., g. / mol.	Sequence	9 hours MIC, μM	19 hours MIC, μM
L_2 1	783.5	RSSS-NH$_2$	0.34 ± 0.02	0.69 ± 0.01
L_2 9	783.5	SSSR-NH$_2$	0.11 ± 0.03	0.22 ± 0.03
L_2 5	717.6	RSSH-NH$_2$	0.16 ± 0.02	0.32 ± 0.02
L_2 2	734.4	RLSS-NH$_2$	0.54 ± 0.01	1.08 ± 0.01

Table 1.10 Growth inhibition leading to calculated MIC values of library **2**

compounds at 9 hours and 19 hours against *V. anguillarum*.

The observed decrease in bacterial growth at 9 hours may be due to a

bacteriostatic effect, where the peptides inhibit the growth of bacteria but the

bacteria may recover.

At 19 hours, the inhibition of growth of bacteria is more likely to be due to a

bactericidal effect. The MIC values at 19 hours were two fold higher than

those at 9 hours.

Peptides in library **1** did not show variations in their antimicrobial activities

against *E. coli* ZK4 and *V. anguillarum*. The MIC values were consistently

around 6.3 μM.

Although members in library **1** were shown to bind DNA with different

binding affinities[32], this had no measurable effect on their activities against *E.*

coli ZK4 and *V. anguillarum*.

Library **3** peptides did not cause inhibition of the growth of either *E. coli* or *V. anguillarum* in the μmolar concentration range tested. Although the compounds in library **3** were designed analogs of a template natural antimicrobial peptide, microcin B17, and incorporated certain elements of activity that are unique to the natural compound, this lack of potency compared with its naturally-occuring micrtemplate may be due to the larger size of microcin B17 and additional intervening amino acids that may play a role in providing an optimum spacing between the heterocyclic–containing amino acid moieties.

1.4 CONCLUSIONS AND FUTURE DIRECTIONS

Library **2** was the most active library among the three libraries tested.
The features that make library **2** more effective may be the presence of arginine residues and / or the benzothiophene moiety.
It has been shown that poly-arginine peptides can help transport larger peptides across electrically charged membranes[33]. Bacterial membranes have a negative membrane potential as opposed to the electrically neutral eukaryotic membranes due to the nature and distribution of fatty acids in the lipid bilayer.
The potency of library **2** peptides may be due to improved transport across the bacterial membranes as opposed to the less charged peptides in the other libraries.
Benzothienylalanine residues have unnatural benzothiophene groups in their

side chains, which are aromatic planar and have the potential to intercalate

between DNA base pairs. Intercalation can cause cytotoxicity

due to topoisomerase inhibition. Arginine residues may also enhance

localization of the peptide on the DNA by electrostatic attraction to the

negatively charged phosphate backbone of DNA.

In order to further investigate the mechanism of action of library **2**

peptides, the peptides were assayed for topoisomerase inhibition (*Appendix A*).

Further directions include designing additional peptide libraries incorporating

more arginine residues and / or incorporating novel amino acid residues with

side chains that can intercalate between DNA base pairs.

CHAPTER 2 ANTIMICROBIAL ACTIVITIES OF PLEUROCIDIN AMIDE AND RELATED PEPTIDES TRUNCATED AT THE *C*-TERMINUS

ABSTRACT

Antimicrobial peptides (AMPs) are found in insects, fish and mammals where they play an integral role in the host defense mechanism against pathogenic micro-organisms. Many AMPs act via general permeabilization of the microbial membranes. So-called amphipathic α-helical peptides are an abundant and widespread class of AMPs. However, such short peptides are generally unstructured in solution, yet due to their cationic nature they are electrostatically attracted to negatively charged lipids and form α-helices in the microbial membrane. Two extensively-studied AMPs were isolated from insects. Cecropin A was isolated from the giant silk moth (*Hylophora cecropia)* while mellitin was isolated from bee venom (*Apis mellifera)* and unfortunately had a strong hemolytic toxicity.

In order to maximize the antimicrobial activity while minimizing undesirable properties, such as hemolytic activity, several strategies have been used to develop novel AMPs. Amino acid residues can be deleted or substituted at either the *N*-terminus or the *C*-terminus. Hybrid formation of AMPs from different sources has been used to design cecropin – mellitin hybrids having increased antimicrobial activity and lower hemolytic toxicity.

Pleurocidin is a 25-amino acid peptide from the skin secretions of the winter flounder (*Pleuronectes americanus)*. Pleurocidin could potentially form a

single well-defined amphipathic α-helix and exhibits no hemolytic activity. Previous SAR studies using pleurocidin have indicated that changing the *C*-terminal carboxylic acid group to a *C*-terminal amide increases the potency (decreased the MIC value by 4 fold) against *Vibrio anguillarum*.

Given the small size of pleurocidin compared to other naturally-occuring AMPs, its lack of hemolytic activity, and its potential ability to form an amphipathic α-helix, we chose to further investigate the SAR of pleurocidin amide.

In this chapter, we describe the synthesis of two novel *C*-terminally truncated peptide amides derived from pleurocidin, pleurocidin amide, and CP-29, a cecropin-melittin hybrid. The antimicrobial activities of these peptides were explored against *Vibrio anguillarum* (wild type), a marine bacterium that causes vibriosis in fish, and *Escherichia coli* (ZK4), a microcin sensitive strain of *E. coli*.

2.1 INTRODUCTION

Problem   Antibiotics are therapeutic agents, interfering with functions that are essential to bacterial growth or survival. Antibiotic resistance has become a major problem in the past decade[34]. Bacteria can resist antibiotics as a result of chromosomal mutation or inductive expression of a latent chromosomal gene or by exchange of genetic material through transformation (the exchange of DNA), transduction (bacteriophage), or conjugation by plasmids[35]. *Streptococcus pneumonia*, *Streptococcus pyogenes* and

Cecropins were the first AMPs to be characterized[40]. Cecropins are induced in the hemolymph of the pupae of the giant silk moth *Hylophora cecropia* following the injection of live bacteria[40]. Cecropin A (Figure 2.1.1) is a 37 amino acid peptide amide with a basic *N*-terminal sequence and a hydrophobic *C*-terminal region [41]. Mellitins (Figure 2.1.3) were isolated from bee venom and have a broad-spectrum antimicrobial activity, but are also unfortunately hemolytic[42]. Mellitins contain two helical regions, a basic *C*-terminal region and an *N*-terminal hydrophobic region that are separated by a flexible hinge region[42]. Pleurocidin (Figure 2.1.5) is a 25-amino acid peptide from the skin secretions of the winter flounder[43]. Pleurocidin is histidine rich, forms a single well-defined amphipathic helix and kills both gram-positive and gram-negative bacteria[43]. Pardaxins are excitatory toxins composed of 33 amino acids and have been purified from the red sea Moses sole *Pardachirus marmoratus* and also from the western pacific *Pardachirus pavoninus*[44] (Figure 2.1.6). Pardaxins` effects have been attributed to its ability to form channels in cell membranes, thus interfering with ionic transport[44]. Magainin I (Figure 2.1.7) has been purified from frog skin secretions and was shown to exhibit wide spectrum activity against gram positive and gram negative bacteria[45].

Figure 2.1 Amino Acid Sequence and Edmundson Helical Wheels Projections[54] of Antimicrobial Peptides

Solid circles indicate hydrophobic amino acid residues, open circles indicate hydrophilic amino acid residues.

2.1.1 Cecropin A[40]

H-KWKLFKKIEKVGQNIRDGIIKAGPAVAVVGQATQIAK-NH₂
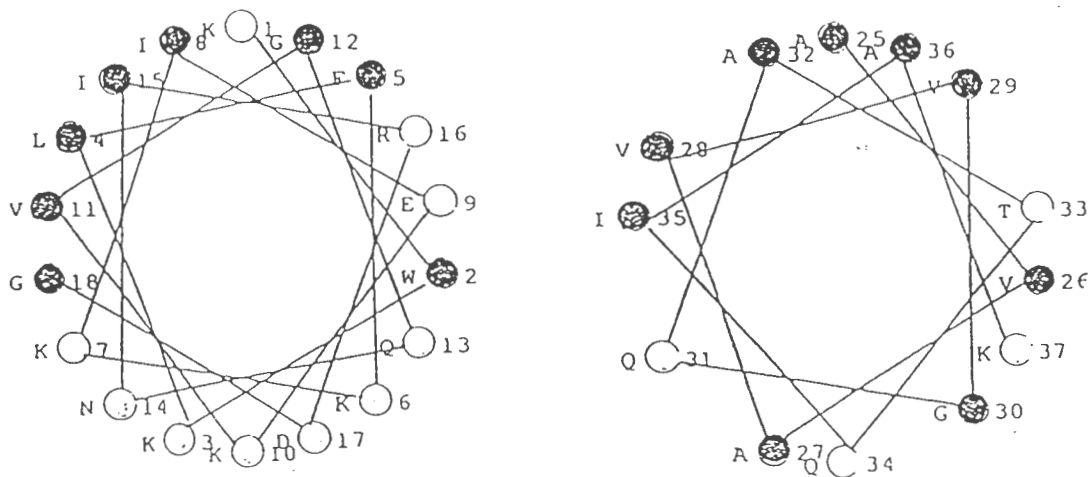
2.1.2 *N*-Terminus truncated and modified cecropin A[50]

H-WKLFKKILKVL-NH₂

2.1.3 Mellitin[42]

H-GIGAVLKVLTTGLPALISWIKRKRQQ-NH$_2$

2.1.4 MCFA, mellitin C-terminus with redistributed basic residues[51]

H-GLKKLISWIKRAAQQG-NH$_2$

2.1.5 Pleurocidin[(43)]

H-GWGSFFKKAAHVGKHVGKAALTHYL-COOH

2.1.6 Paradaxin[(44)]

H-GFFALIPKIISSPLFKTLLSAVGSALSSGEQE-COOH

2.1.7 Magainin I[(45)]

H-GIGKFLHSAKKFGKAFVGEIMKS-COOH
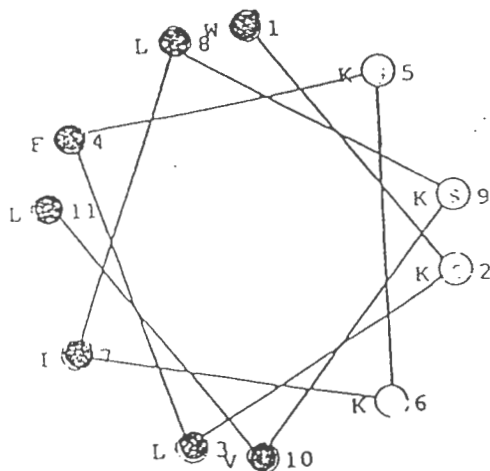
2.1.8 CEME[49], Hybrid of the first 8 amino acids of cecropin A and the first 18 amino acids of mellitin

H-KWKLFKKIGIGAVLKVLTTGLPALIS-NH$_2$
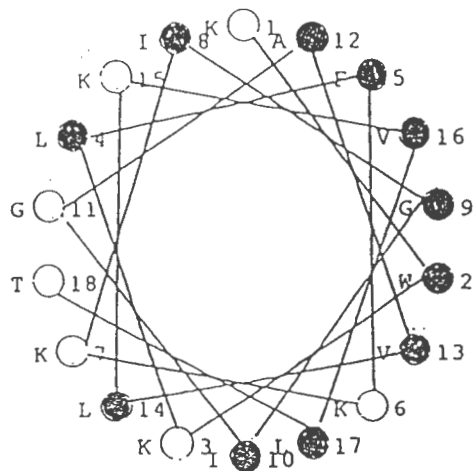
2.1.9 CP-29 [52]

H-KWKSFIKKLTTAVKKVLTTGLPALIS-NH$_2$
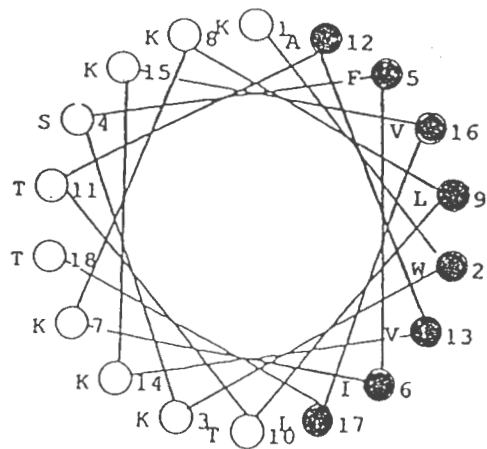
Peptide synthesis   Solid phase peptide synthesis (SPPS) was invented by R.B. Merrifield in 1963 to overcome the many problems of solution phase peptide synthesis[46]. The desired sequence is assembled on an insoluble polymer support and subsequently cleaved off the polymer at the conclusion of the synthesis. Much research has been done since then to improve the type of polymer support, linkers, protecting groups, and the overall synthetic strategy. To avoid base-catalyzed racemization of amino acid residues during synthesis of the peptide chains, the peptide chains are synthesized from the *C*-terminus to the *N*-terminus using *N*-protected amino acids. Coupling reagents such as DCC and HBTU have been shown to catalyze formation of amide bonds without racemization. At the end of the synthesis, a cleavage reagent such as hydrogen fluoride (HF) is typically utilized to simultaneously liberate the product peptide from the resin and remove the protecting groups. The HF is then completely removed under vacuum so that the crude deprotected peptide can be separated from the resin by dissolving it in aqueous solution, and lyophilizing it for further purification. A general scheme for solid-phase peptide synthesis is illustrated in Figure 2.2. In general, SPPS consists of attachment of the first amino acid via a linker onto the resin support, cycles of deprotection and coupling to assemble the amino acid residues in the correct order on the polymer support, and selective cleavage of the peptide from the resin and removal of the protecting groups.

R^1, R^2 = Side chain groups, B$_2$, B$_3$, B$_4$, B$_5$ = side chain protecting groups
B$_1$= *N*-terminus protecting group.
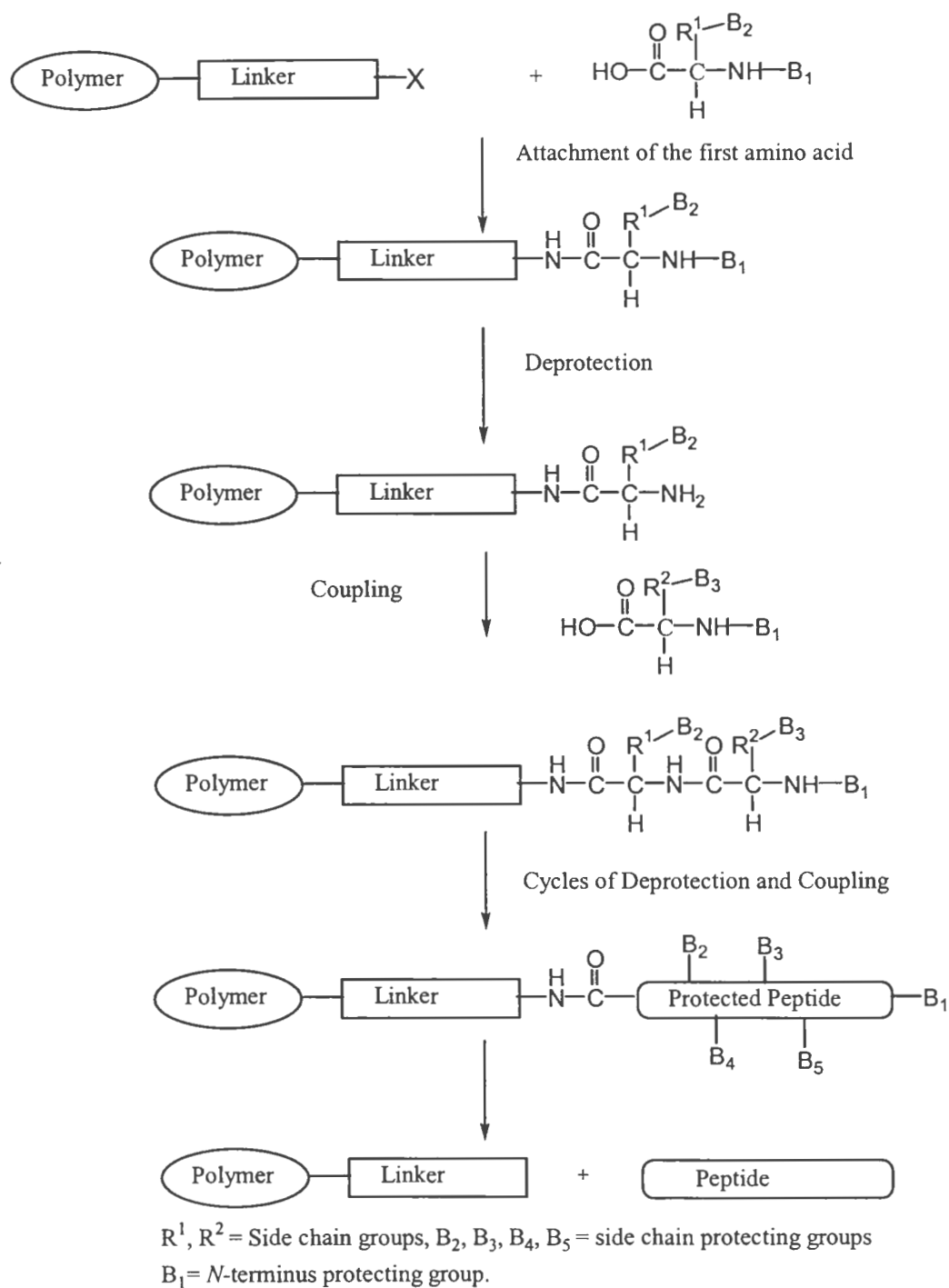
Figure 2.2 Schematic Representation of Solid Phase Peptide

Synthesis

The selection of the correct combination of an α-amino protecting group, a

linker, and the side chain protecting groups is very important for the success of

the synthetic scheme. The deprotecting agent used during stepwise synthesis

should selectively remove the α-amino protecting groups without affecting

side chain protecting groups. In our synthesis, the amino acids had t-Boc (t-

butyloxycarbonyl) (Figure 2.3) as the α-amino protecting group, and 50 %

trifluoroacetic acid/CH_2Cl_2 was used as the deprotecting agent. The linker

used in our experiment was p-methylbenzhydrylamine, and the resin was

polystyrene with 1 % divinylbenzene cross-linker (MBHA , 1% DVB). In

general, the insoluble polymer support for peptide synthesis is prepared via co-

polymerization of polystyrene and 1% DVB for optimum swelling and

mechanical stability. The peptide-resin linkage in a MBHA resin is p-

methylbenzhydrylamine (Figure 2.3.2), such that cleavage by hydrofluoric acid

yields a C-terminal amide. Peptide C-terminal amides are desirable since

amidation of the C-terminal carboxylic acid increases the net positive charge

on the peptide, and offers extra hydrogen bonding sites for stabilizing the α-

helix.
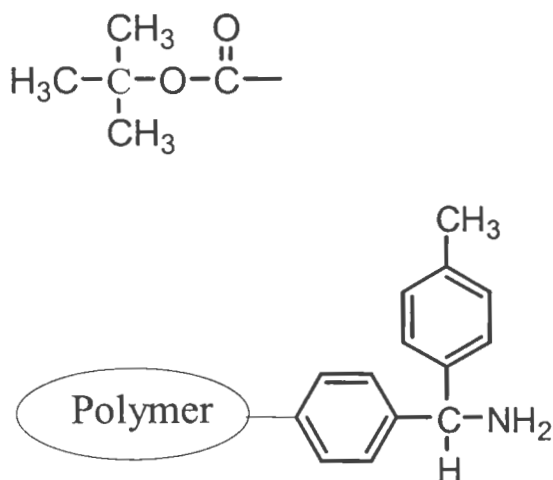
2.3.1. *t*-Butyloxycarbonyl (Boc) group.   2.3.2. *p*-Methylbenzhydrylamine (MBHA) linker.

Figure 2.3. Structures of α- amino protecting group and resin-peptide linkage in SPPS.

Prior SAR studies   Solid phase peptide synthesis (SPPS) has been effectively utilized to synthesize cecropin A[47] and other AMPs with increased yields and effective purification of the active peptides from the reaction mixture. The overall potency and spectrum of activity of AMPs are influenced by the charge, the hydrophobicity, the degree of amphipathicity and the % α-helical content. Naturally occurring α-helical peptides vary in their cationicity and hydrophobicity. They have been found to have net positive charges varying from zero to $^{+}16$ at physiologic pH, however most of the peptides fall into the intermediate range ($^{+}4$ to $^{+}6$). Several studies have indicated that in peptides below that range, an increase in the positive charge of the peptides increased the overall antibacterial activity. Increasing the charge on peptides

within the optimum range has a minimal effect on the antimicrobial activity.

Excessive charge can have a dramatic effect on the activity of the AMPs. It

was shown that synthetic analogs of magainins with increased positive charge

led to smaller, less stable, and shorter--lived pores, with faster translocation of

the peptides through the membranes, leading to a lower antibacterial

activity[48]. The percentage of hydrophobic residues may vary among naturally

occurring antibacterial peptides but is generally found to be between 40%-

60%. Amphipathicity, the pattern of charged/hydrophobic residues in a

peptide, may be harder to define than charge or hydrophobicity, however most

natural AMPs have a moderate to high amphipathicity. Structure Activity

Relationship (SAR) analysis of the naturally occurring α-helical peptides aims

at identifying the maximum possible antimicrobial activity accompanied by the

minimum toxicity towards the host. One approach to SAR analysis is through

sequence modifications by deleting, adding or substituting amino acids from

either the N-terminus, or C-terminus. Helical wheel diagrams and structural

studies indicate the presence of a hinge in cecropin A between two α-helical

segments at residue #23[49]. Several studies have shown that it is possible to

considerably reduce the size of the α-helical AMPs, while retaining their

antimicrobial activity, thus simplifying their synthesis. A shortened version of

cecropin A based on the N-terminal region (Figure 2.1.2) showed promising

antimicrobial activity[50]. The peptide MCFA, designed based on the 15 amino

acid residues from the C-terminus of mellitin, contained an extra glycine

residue at the C terminus and had an interchange of pro[14] with lys, ala[15] with

lys, lys^{23} with ala and arg^{24} with ala, (Figure 2.1.4). MCFA exhibited comparable antimicrobial activity to the parent compound but had a 100-fold lower hemolytic activity than mellitin[51]. Another design approach was through the formation of hybrids between different naturally occurring AMPs. Cecropin-Mellitin (CEME) was a hybrid of the first 8 amino acids of cecropin A and the first 18 amino acids of mellitin (Figure 2.1.8), and exhibited a better antimicrobial activity than either cecropin or mellitin alone, with no hemolytic effect[49]. Further modifications in the amino acid sequence of CEME yielded CP-29 (Figure2.1.9)[52]. These modifications included interchange of leu^4 with ser, lys^6 with ile, ile^8 with lys, gly^9 with leu, ile^{10} with thr, gly^{11} with thr, and leu^{14} with lys. CP-29 yielded a higher amphipathic α-helix content than CEME and gave a higher activity against gram-negative bacteria[52].

Peptide design   Pleurocidin is an extremely promising AMP first isolated in 1997. Pleurocidin is shorter (25 amino acid residues) than other natural AMPs (e.g.: cecropin A has 37 amino acid residues), forms a well-defined amphipathic α-helix and exhibits antimicrobial activity with no hemolytic activity. In this work, CP-29 and pleurocidin amide were both synthesized using solid-phase methods, and served as positive controls in the antimicrobial assays.

Pleurocidin amide
$H-GWGSFFKKAAHVGKHVGKAALTHYL-NH_2$

CP-29[52]
$H-KWKSFIKKLTTAVKKVLTTGLPALIS-NH_2$

54

In this chapter, we describe the further investigation into the SAR of pleurocidin through design and synthesis of two new *C*-terminally-truncated peptide amides. Pleurocidin was chosen as a good lead compound for the design of novel AMPs due to its potent MIC against *Vibrio anguillarum* (0.76 uM), absence of hemolytic toxicity, short length, and ability to form an amphipathic α-helix. The goal was to achieve improved antimicrobial activity while simplifying the synthesis by shortening the length of the peptide. Previous SAR studies on pleurocidin showed that addition of a lysine residue to the *N*-terminus of pleurocidin did not enhance its antimicrobial activity against *Vibrio anguillarum*, but that formation of a *C*-terminal amide yielded an 8-fold increase in the activity of pleurocidin against *Vibrio anguillarum* [53]. SAR studies of AMPs that act through formation of pores through the bacterial membranes has shown that a minimum number of 15 amino acid residues is needed for the peptide to span the lipid bilayer of the bacterial membrane[51]. The first designed peptide **A,** an 18 amino acid-long peptide amide starting from the *N*-terminus of pleurocidin should therefore be long enough to span the membrane. A comparison of Edmundson[54] helical wheels and hydrophobicity plots (Kyte-Doolittle[55]) of pleurocidin indicated that peptide A could potentially form an amphipathic α-helix, and the *C*-terminal amide should improve the stability of the helix.

Peptide 1: $H-GWGSFFKKAAHVGKHVGK-NH_2$

Upon comparing the sequence of pleurocidin to other AMPs with highly homologous sequences (e.g.: dermaceptin and ceratotoxins), the residues 19-21 appear to be highly conserved, so a longer peptide **B** was designed to include them. The second designed peptide **B,** is a 21 amino acid-long peptide amide starting from the *N*-terminus of pleurocidin:

Peptide 2:   H-GWGSFFKKAAHVGKHVGKAAL-NH$_2$

To evaluate the effectiveness of the design, the antimicrobial activities of all four synthetic peptides were evaluated using *Vibrio anguillarum* (wild type) and *Escherichia coli* (ZK4).

2.2 Experimental

Chemicals:

Dimethylformamide (DMF), trifluoroacetic acid (TFA), dichloromethane (DCM), glacial acetic acid and N-methylpyrrolidinone (NMP) were purchased from Fisher. N, N`-diisopropyl ethylamine (DIEA), p-cresol and thiocresol were purchased from Fluka. Anhydrous hydrogen fluoride (HF) was purchased from Matheson. MBHA resin was purchased from Advanced ChemTech. HBTU reagent was purchased from Peptides International. Protected amino acids were purchased from Bachem Inc or Peptides International.

Apparatus:

Solid phase peptide synthesis was performed on a CS036 automated peptide synthesizer from CS Bio Co. Analytical HPLC experiments were performed on a Waters HPLC system which consisted of a model 680 gradient controller, two 501 pumps, a 486 tunable UV/VIS detector, a Rheodyne injector, and a Vydac 218TP C_{18} protein and peptide column (10 um, 250 x 4.6 mm I.D.). Data was collected and analyzed using a model 1020 personal integrator and PE Nelson software (Perkin-Elmer Corp., USA). Preparative HPLC was performed using a miniPump® metering pump (thermo separation products, Riviera Beach, FL, USA) on a Vydac C_{18}, (Nest Group, Southboro, MA, USA, 15 x 1.2 cm). HF cleavage of the peptide was performed on a Model 2A HF apparatus (Immuno-Dynamics, La Jolla, CA, USA). Matrix-Assisted Laser

Desorption Time-of-Flight Mass spectrometry (MALDI-TOF MS) was performed at Harvard Microchemistry (Boston, MA, USA) on a PE Biosystems Voyager System 4074 (α-cyano-4-hydroxycinnamic acid matrix, 700-5000 Da). Amino Acid Analysis (AAA) was performed on an Applied Biosystems 420 instrument at Harvard Microchemistry (Boston, MA, USA) using PTC amino acid derivatives normalized to alanine and phenylalanine.

2.2.1 Synthesis

MBHA resin, (1 g., sub 1.1 mmoles/g., 1% DVB) was swollen overnight in 20 ml DMF in an inverting type shaker. DMF was drained the next day, and the resin was washed with DCM (2 x 20 ml). The synthetic program used in the synthesis of peptide **1**, peptide **2**, **pleurocidin amide** and **CP-29** is shown in table 2.1.

Step #	Description
1	Shake the resin with DCM, 15 ml for 5 min.
2	Drain, shake the resin with 50 % TFA/DCM, 15 ml for 2 min.
3	Drain, shake the resin with 50 % TFA/DCM, 15 ml for 28 min.
4	Drain, wash the resin with DCM, 10 ml.
5	Drain, wash the resin with 20 %DIEA/DCM, (2 x 10 ml).
6	Drain, wash the resin with NMP (3 x 10 ml)
7	Drain, add solution of 1 mmole of protected amino acid in 5 ml DMF.
8	Add 1 eq (1 mmole HBTU, 0.375 g.) dissolved in 5 ml DMF.

9	Add 5 ml with 20 %DIEA/DCM.
10	Shake the reaction vessel for 30 min.
11	Drain, wash with NMP (2 x 10 ml)
12	Drain, wash with DCM (2 x 20 ml)
13	Ninhydrin Test

Table 2.1 Synthetic cycle used in the SPPS.

Test for complete reaction: Ninhydrin Test[46]:

The quantitative ninhydrin test was used to detect free amine groups at the *N*-terminus of growing peptide chains on the resin. Free amine groups react with the ninhydrin reagent to give a blue-purple color (Rhuemann's purple) after heating at 100°C for 10 min. After a complete reaction cycle, the protected peptide-resin compound should have no free amine groups and give no blue color in the ninhydrin test if the coupling reaction went to completion. The ninhydrin test was carried out using two solutions: solution A and solution B. Solution A is prepared by mixing a solution of 40 g phenol in 10 ml absolute ethanol (warmed until the phenol is completely dissolved) and a solution of 2 ml of 65% (W/V) potassium cyanide (KCN) in water and then diluting the mixture to 100 ml with pyridine. Solution B is prepared by dissolving 2.5 g. ninhydrin (0.28 M) in 50 ml absolute ethanol and is stored in the dark under nitrogen or argon. A clean dry glass pipette was used to transfer a small sample of the resin (~1 mg) into a test tube (14 x 100 mm). Four drops of solution A, followed by two drops of solution B were added to the resin

sample. The test tube was heated for 10 min. at 100°C. Absence of a blue-purple color indicated a successful synthetic cycle (> 99.9 % coupling). Tables 2.2, 2.3, 2.4 and 2.5 list the types of protected amino acids used for each peptide synthesis, and the number of amino acid coupling reactions required for each amino acid to achieve a complete reaction. In multiple couplings, (usually from the second coupling onward), 0.4 mmoles of the amino acid was used instead of 1 mmole to prevent waste.

Sequence	Protected Amino Acid	Coupling Reagent Used	# of couplings
K	1- Boc-Lys (Cl-Z)	HBTU	4
G	2- Boc-Gly	HBTU	4
V	3- Boc-Val	HBTU	4
H	4- Boc His, Dnp.	HBTU	3
K	5- Boc-Lys (Cl-Z)	HBTU	3
G	6- Boc-Gly	HBTU	3
V	7- Boc-Val	HBTU	3
H	8- Boc-His, Dnp.	HBTU	2
A	9- Boc-Ala	HBTU	2
A	10- Boc-Ala	HBTU	2
K	11- Boc-Lys (Cl-Z)	HBTU	2
K	12- Boc-Lys (Cl-Z)	HBTU	2

F	**13**- Boc-phe	HBTU	2
F	**14**- Boc-phe	HBTU	2
S	**15**- Boc-Ser (*O*-Benzyl)	HBTU	2
G	**16**- Boc-Gly	HBTU	2
W	**17**- Boc-Trp	HBTU	2
G	**18**- Boc-Gly	HBTU	2

Table 2. 2 Peptide **1** synthesis: Protected amino acid building blocks used, number of couplings needed to achieve a negative ninhydrin test.

Sequence	Protected Amino Acid	Coupling Reagent Used	# of couplings
L	**1**- Boc-Leu	HBTU	5
A	**2**- Boc-Ala	HBTU	5
A	**3**- Boc-Ala	HBTU	4
K	**4**- Boc-Lys (Cl-Z)	HBTU	4
G	**5**- Boc-Gly	HBTU	4
V	**6**- Boc-Val	HBTU	4
H	**7**- Boc-His, Dnp	HBTU	4
K	**8**- Boc-Lys	HBTU	3

	(Cl-Z)		
G	9- Boc-Gly	HBTU	3
V	10- Boc-Val	HBTU	3
H	11- Boc-His, Dnp	HBTU	3
A	12- Boc-Ala	HBTU	3
A	13- Boc-Ala	HBTU	2
K	14- Boc-Lys (Cl-Z)	HBTU	2
K	15- Boc-Lys (Cl-Z)	HBTU	2
F	16- Boc-Phe	HBTU	2
F	17- Boc-Phe	HBTU	2
S	18- Boc-Ser (O-Benzyl)	HBTU	2
G	19- Boc-Gly	HBTU	2
W	20- Boc-Trp	HBTU	2
G	21- Boc-Gly	HBTU	2

Table 2. 3 Peptide 2 synthesis: Protected amino acid building blocks used, number of couplings needed to achieve a negative ninhydrin test.

Sequence	Protected Amino Acid	Coupling Reagent Used	# of couplings
L	1- Boc-Leu	HBTU	4
Y	2- Boc-Tyr	HBTU	4
H	3- Boc-His-Dnp	HBTU	4
T	4- Boc-Thr (*O*-Benzyl)	HBTU	3
L	5- Boc-Leu	HBTU	4
A	6- Boc-Ala	HBTU	3
A	7- Boc-Ala	HBTU	3
K	8- Boc-Lys (Cl-Z)	HBTU	3
G	9- Boc-Gly	HBTU	3
V	10- Boc-Val	HBTU	3
H	11- Boc-His, Dnp	HBTU	2
K	12- Boc-Lys (Cl-Z)	HBTU	2
G	13- Boc-Gly	HBTU	2
V	14- Boc-Val	HBTU	2
H	15- His, Dnp, Boc	HBTU	2
A	16- Boc-Ala	HBTU	2

A	17- Boc-Ala	HBTU	2
K	18- Boc-Lys (Cl-Z)	HBTU	1
K	19- Boc-Lys (Cl-Z)	HBTU	1
F	20- Boc-Phe	HBTU	1
F	21- Boc-Phe	HBTU	1
S	22- Boc-Ser (*O*-Benzyl)	HBTU	1
G	23- Boc-Gly	HBTU	1
W	24- Boc-Trp	HBTU	1
G	25- Boc-Gly	HBTU	1

Table 2.4 Pluerocidin amide synthesis: Protected amino acid building blocks, number of couplings needed to achieve a negative ninhydrin test.

Sequence	Protected Amino Acid	Coupling Reagent Used	# of couplings
S	1- Boc-Ser (*O*-Benzyl)	HBTU	4
I	2- Boc-Ile	HBTU	4
L	3- Boc-Leu	HBTU	4
A	4- Boc-Ala	HBTU	3
P	5- Boc-Pro	HBTU	4
L	6- Boc-Leu	HBTU	3
G	7- Boc-Gly	HBTU	2
T	8- Boc-Thr (*O*-Benzyl)	HBTU	2
T	9- Boc-Thr (*O*-Benzyl)	HBTU	2
L	10- Boc-Leu	HBTU	2
V	11- Boc-Val	HBTU	2
K	12- Boc-Lys (Cl-Z)	HBTU	2

K	13- Boc-Lys (Cl-Z)	HBTU	2
V	14- Boc-Val	HBTU	2
A	15- Boc-Ala	HBTU	2
T	16- Boc-Thr(O-Benzyl	HBTU	2
T	17- Boc-Thr-O-Benzyl	HBTU	2
L	18- Boc-Leu	HBTU	2
K	19- Boc-Lys (Cl-Z)	HBTU	2
K	20- Boc-Lys (Cl-Z)	HBTU	2
I	21- Boc-Ile	HBTU	2
F	22- Boc-phe	HBTU	2
S	23- Boc-Ser	HBTU	2
K	24- Boc-Lys (Cl-Z)	HBTU	2
W	25- Boc-Trp	HBTU	2
K	26- Boc-Lys (Cl-Z)	HBTU	2

Table 2.5: CP-29 synthesis: Protected amino acid building blocks used, number of couplings needed to achieve a negative ninhydrin test.

2.2.3 Deprotection and Cleavage from the Resin Support :

After the last synthetic cycle was complete, the protected peptide-resin was washed with DCM (2 x 20ml), transferred to a clean manual peptide synthesis reaction vessel and dried under vacuum overnight. The dried resin was weighed and the yield of the crude protected peptide was calculated. Peptide **1**, wt. of the peptide-resin = 2.65 g., crude protected yield = 48%. Peptide **2**, wt. of the peptide-resin = 2.71 g., crude protected yield = 46.6%. **Pleurocidin amide**, wt. of the peptide-resin = 2.95 g., crude protected yield = 44.4%. **CP-29**, wt. of the peptide-resin = 3.2 g., crude protected yield = 48%.

Dinitrophenol (Dnp) Removal: Dnp was used as the protecting group for the imidazole side chains of the histidine residues of peptide **A**, peptide **B** and **pleurocidin amide**. The Boc-protected peptide-resin in the reaction vessel was shaken with a mixture of thiophenol and DMF (4.5 ml, 5 ml) for 6 hours at room temperature to remove the Dnp groups. The resin was washed successively with DMF (4 x 20 ml), DCM (4 x 20 ml) until there was no yellow color in the drained liquid. *t*- butyloxycarbonyl (Boc) group Removal: Following the removal of Dnp, the pepide-resin was subsequently treated with 10 ml of 50 % TFA/DCM for 30 min., then the resin was washed with DIEA (2 x 20 ml), and *i*-propanol (2 x 10 ml). The peptide-resin was then transferred to the HF reaction vessels (PFA Teflon) and dried overnight under vacuum.

2.2.4 HF Cleavage:

The HF treatment was done in an HF apparatus, and simultaneously accomplished the cleavage of the peptide from the resin, the removal of the *O*-benzyl protecting group on serine, and the removal of Cl-Z protecting group on lysine. *p*-cresol (0.5 ml), *p*-thiocresol (0.5 ml) scavengers were added to the dry resin and 9 ml of anhydrous HF was condensed in the vessel at $-50^{\circ}C$ in a bath of *i*-propanol and $CO_{2(s)}$. The vessel was then warmed to $4^{\circ}C$ and the mixture was stirred for 1 hour on ice. The HF was subsequently evaporated away with the aid of nitrogen (the HF was trapped with KOH) and then with water aspirator.

2.2.5 Peptide Purification:

Following HF treatment, peptide-resins were typically washed with 5 ml ether to remove most of the scavengers and protecting groups, and then extracted first with 10 ml of 10 % acetic acid (fraction A) and subsequently with 10 ml of glacial acetic acid (fraction B). The combined peptide extracts A and B were lyophilized and then re-dissolved in a minimum volume of 10 % acetic acid for gel filtration chromatography. The concentrated peptide extract was loaded on a Sephadex® G-25 column (31 cm x 3 cm). The crude peptide was eluted with 10 % acetic acid, flow rate 1.5 ml/min., UV-detection at 254 nm. Fractions (3 ml each) were collected and the initial fractions representing excluded material were pooled and lyophilized (Peak A in Figure 2.4). The crude peptide was then dissolved in deionized water and was analyzed by
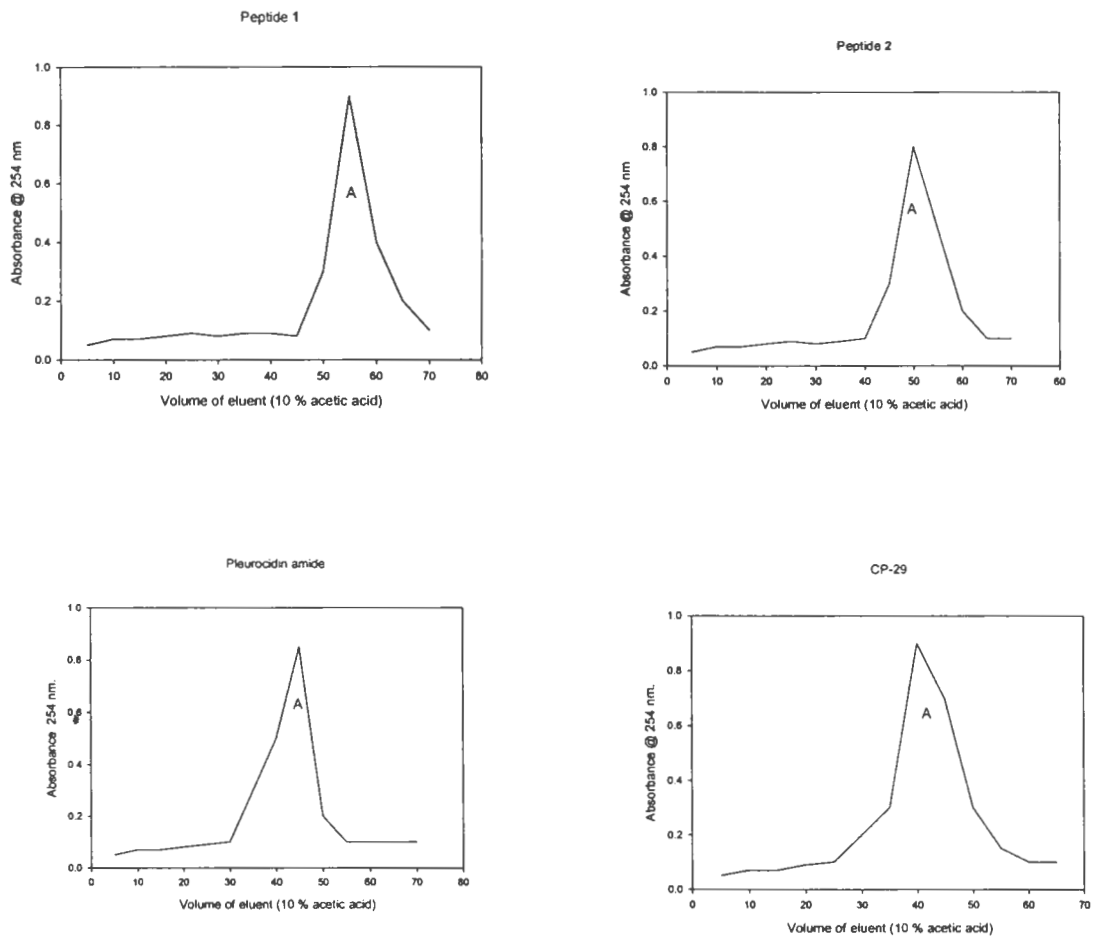
Figure 2.4 Peptide **1**, peptide **2**, pleurocidin amide and CP-29 elution profiles from

Sephadex®G-25 gel filtration chromatography.

Volume of eluent (ml.) and absorbance (AU).

hydrophobic gradient HPLC on a Vydac 218TP C_{18} column (10 um, 250 x 4.6 mm I. D). Solvent A: 5 % CH_3CN / H_2O, 0.1 % TFA; solvent B: 85 % CH_3CN / H_2O, 0.1 % TFA; linear gradient from 5%-85% CH_3CN; 2.0 % CH_3CN / min., 1 ml / min., absorbance measured at 220 nm. The crude peptides were then purified using preparative isocratic HPLC and analyzed using MALDI-TOF mass spectrometry.

Peptide 1: The analytical gradient HPLC chromatogram of crude peptide 1 is shown in Figure 2.5. The most intense peak (designated by an arrow in Figure 2.4) eluted at 35% CH_3CN, and was selected to be purified by preparative HPLC. Figure 2.6.1 shows the isocratic HPLC chromatogram of crude peptide 1 at 25%. Preparative HPLC was run by first preparing a concentrated solution of the crude peptide in 10% acetic acid (20 mg/mL), and then injecting 3 mL aliquots onto the preparative column, eluted isocratically at a flow rate of 9 mL/min. in 25% CH_3CN/H_2O, 0.1% TFA. 3 mL fractions were collected and evaporated using a speed-vac centrifuge to first remove the acetonitrile and TFA. Fractions corresponding to peaks **I** and **II**, were then pooled and lyophilized to obtain fluffy solids. Purified peak **II**, expected to be the desired peptide, was further analyzed by MALDI-TOF MS. Purified peptide weight: 350 mg, overall yield = 18%.

Peptide 2: The analytical HPLC chromatogram of crude peptide **2** is shown in Figure 2.7. The peak designated by an arrow (37% CH_3CN) was selected to be purified by preparative HPLC. Preparative HPLC was performed at 27 % CH_3CN, 0.1 % TFA (Figure 2.8.1). Fractions corresponding to Peak **IV** in the

chromatogram shown in figure 2.8.1 were evaporated to remove acetonitrile, pooled, and lyophilized. Figure 2.8.2 shows purified peptide **2**. Purified peptide **2** was further analyzed by MALDI-MS. Purified peptide weight: 400 mg, overall yield = 20 %.

Pleurocidin: The analytical HPLC chromatogram of crude **pleurocidin amide** is shown in Figure 2.9. The peak designated by an arrow (44% CH_3CN) was selected to be purified by preparative HPLC. Preparative HPLC was performed at 28 % CH_3CN / H_2O, 0.1 % TFA (Figure 2.10.1). Peak **II** in the chromatogram shown in Figure 2.10.1 was collected and analyzed by analytical HPLC (Figure 2.9.2) and by MALDI-MS. Purified peptide weight = 700 mg, overall yield = 25 %.

CP-29: The analytical HPLC chromatogram of **CP-29** is shown in Figure 2.11. The peak designated by an arrow (67% CH_3CN) was selected to be purified by preparative HPLC (Figure 2.12.1). Peak **III** in the chromatogram shown in Figure 2.12.1 was collected and analyzed by analytical HPLC (Figure 2.12.2) and by MALDI-MS. Purified peptide weight = 600 mg., overall yield = 20 %.

2.2.6 Antimicrobial assays: Assays were carried out by Tarquin Dorrington in Professor Marta Gomez-Chiarri's laboratory at URI similarly to those described in chapter 1.
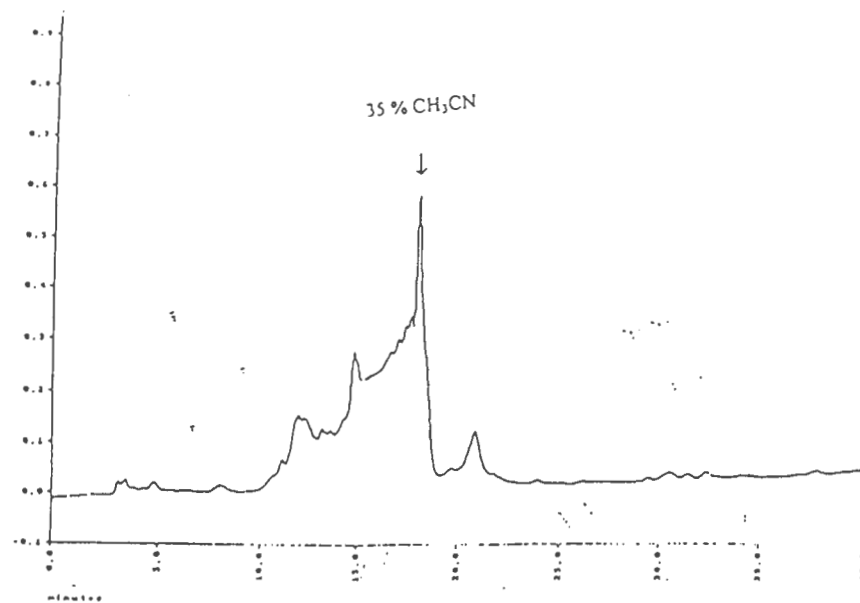
35 % CH₃CN

Figure 2.5 HPLC Analysis of Crude Peptide 1, arrow points to peak of interest.
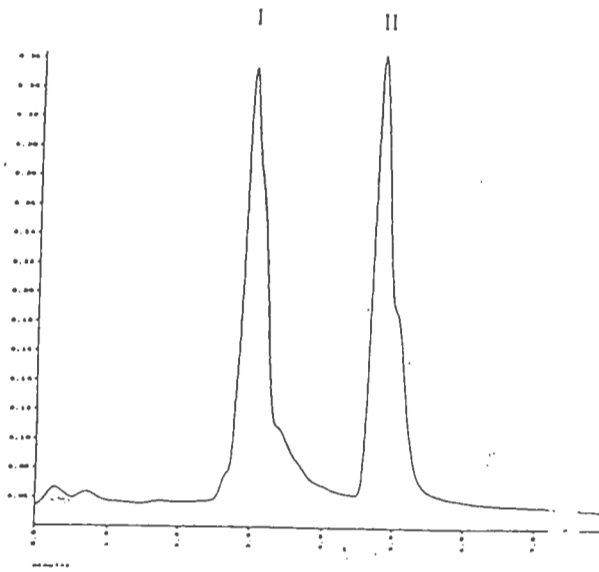
2.6.1 Isocratic HPLC Analysis of Crude Peptide 1,
   prior to preparative HPLC
   Conditions: Vydac C18, 25 % CH$_3$CN / H$_2$O, 0.1 % TFA
   I-   Less hydrophobic peptides
   II-   Most hydrophobic peptides
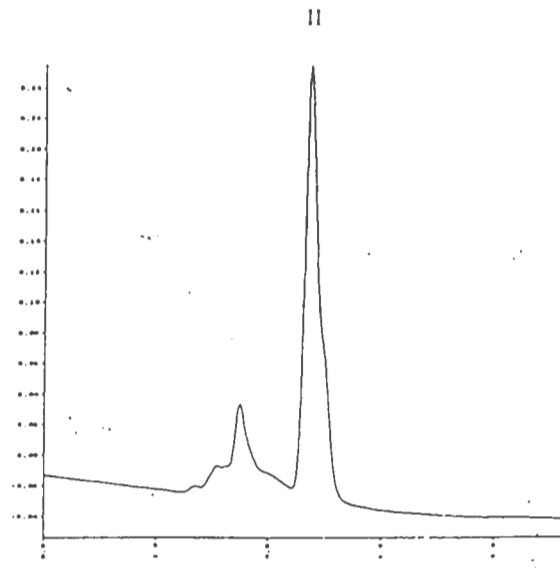
2.6.2 Isocratic HPLC Analysis of purified
   peptide 1, after preparative HPLC
   Conditions: Vydac C18, 25 % CH$_3$CN / H$_2$O, 0.1 %
   TFA.

Figure 2.6 Preparative HPLC Analysis of Crude Peptide 1.
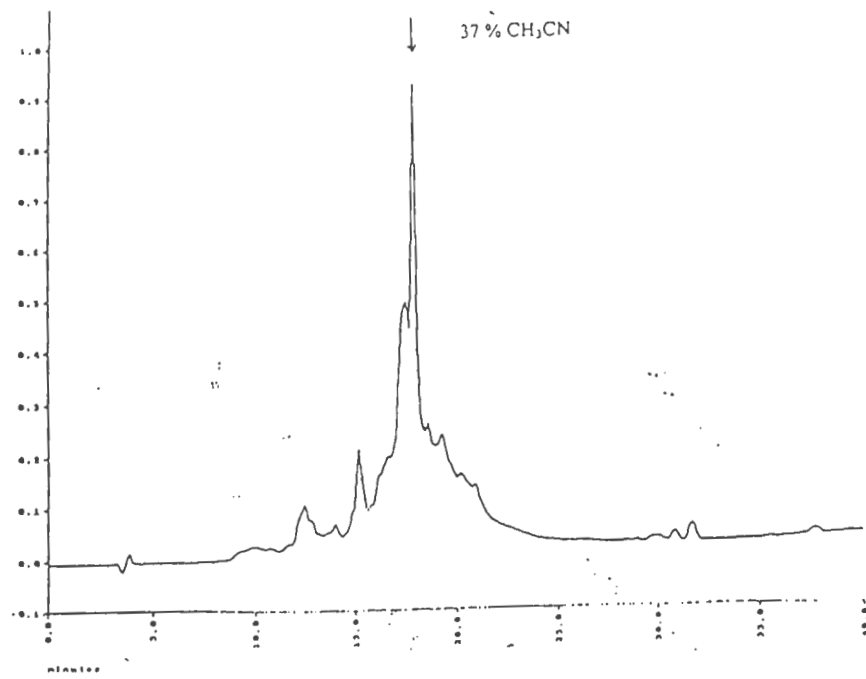
37 % CH₃CN

Figure 2.7 HPLC Analysis of Crude Peptide **2**, arrow points to peak of interest.
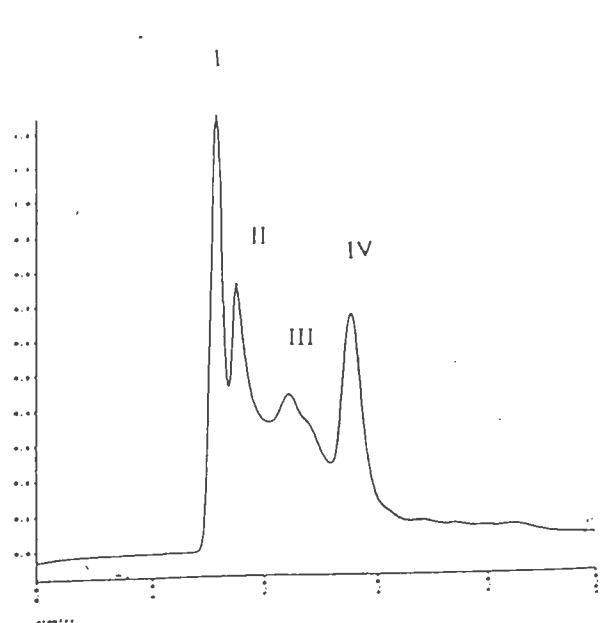
2.8.1 Isocratic HPLC Analysis of Crude Peptide 2,
prior to preparative HPLC
Conditions: Vydac C18, 27 % CH₃CN / H₂O, 0.1 % TFA
IV- Peak of interest.
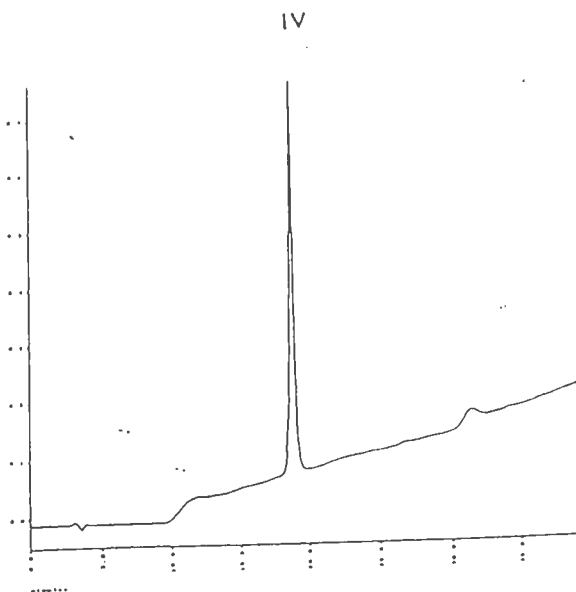
2.8.2 Purified peptide 2, after preparative HPLC
Conditions: Vydac C18, 5-85 % CH₃CN over 40 min.

Figure 2.8 Preparative HPLC Analysis of Crude Peptide 2.

44 % CH₃CN
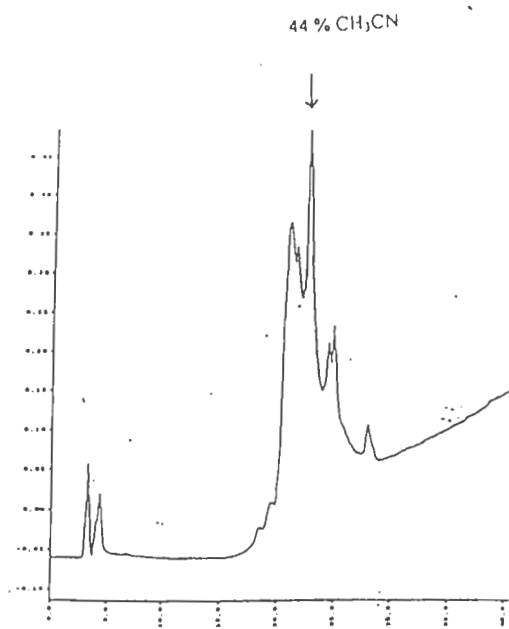
Figure 2.9 HPLC Analysis of Crude **Pleurocidin amide**, arrow points to peak of interest.
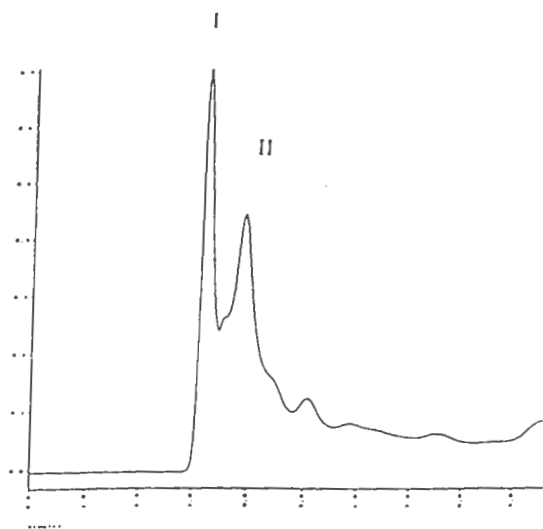
2.10.1 Isocratic HPLC Analysis of Crude Pleurocidin amide, prior to preparative HPLC
Conditions: Vydac C18, 28 % CH_3CN / H_2O, 0.1 % TFA
I-   Less hydrohphobic peptides
II-   Most hydrophobic peptides

2.10.2 Purified Pleurocidin amide, after preparative HPLC
Conditions: Vydac C18, 28 % CH_3CN / H_2O, 0.1 % TFA.

Figure 2.10 Preparative HPLC Analysis of Crude **Pleurocidin amide**

2.12.1 Isocratic HPLC Analysis of Crude CP-29,
  prior to preparative HPLC
Conditions: Vydac C18, 62 % CH₃CN / H₂O, 0.1 % TFA
III- Peak of interest.

2.12.2 Purified CP-29, after preparative HPLC
  Conditions: Vydac C18, 5-85 % CH₃CN over 40 min.
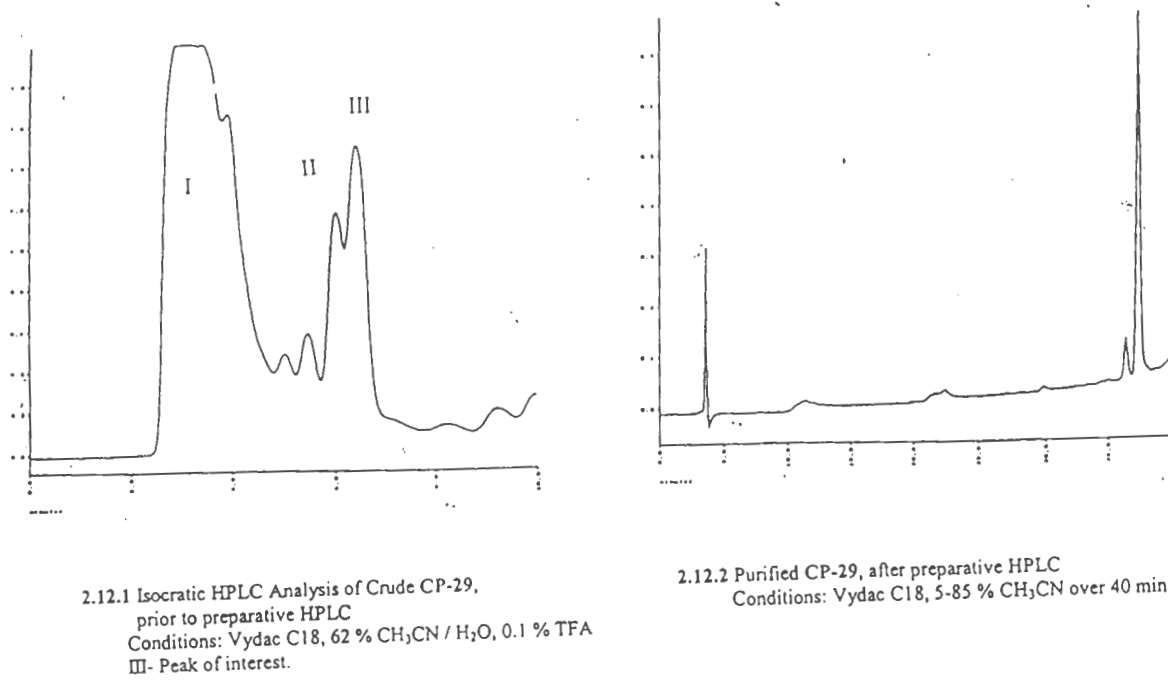
Figure 2.12 Preparative HPLC Analysis of Crude CP-29

2.3 RESULTS AND DISCUSSION

Peptide Synthesis   Four solid-phase syntheses of peptide amides ranging from 18-26 amino acids were completed without premature termination in 2-3 days each. Judging by increases in the weight of the resins, the yields of protected peptides ranged from 44.4% for **pleurocidin amide**, 46.6% for peptide **2** to 48% for peptides **1** and **CP-29**. Following HF deprotection, cleavage from the resin, and gel filtration chromatography to remove scavengers and protecting groups, the crude product mixtures were characterized using analytical gradient HPLC. It is clear that the same synthetic protocol can lead to variable success in obtaining the desired peptide. The solid-phase method yielded more than one peptide species in some crude product mixtures and this was indicated by the multiple peaks observed in the analytical gradient HPLC chromatograms that were obtained following gel filtration. Peptide **2** (Figure 2.7) gave the cleanest chromatogram for a crude product, and therefore it seems that this synthesis went most smoothly. Peptide **1** (Figure 2.5) also showed one predominant product, although the overall chromatogram was not as clean. Analytical HPLC chromatograms of crude product mixtures from the syntheses of **pleurocidin amide** (Figure 2.9) and **CP-29** (Figure 2.11) contained a significant number of additional peaks, some products having similar retention times to the largest peak, and therefore presenting possible purification problems.

Peptide **1** was extracted from the resin following HF cleavage using 10% acetic acid, applied to a gel filtration column and the first peak that eluted from

the column (Sephadex® G-25 column, exclusion ~5,000 Da) was collected and lyophilized to give a yellow solid. In case the peptide was not sufficiently soluble in 10% acetic acid, the same resin was then re-extracted with glacial acetic acid, the extract applied to the same gel filtration column and the first peak was collected and lyophilized to give a white solid. Both excluded peaks were then combined and injected onto the HPLC for analysis of the crude product (Figure 2.5). By experimenting with isocratic conditions on the analytical column, the separation shown in figure 2.6.1 was achieved using 25 % acetonitrile. The crude peptide in **peak II** was then isolated using a preparative HPLC column eluted using 25 % acetonitrile. Individual fractions were re-injected on the analytical HPLC column before pooling those fractions containing **peak II**. The purity of the final product was calculated to be 84% based on HPLC, because some of **peak I** was still present.

Peptide **2** was processed in the same manner to achieve >99% purity as shown in figures 2.8.1 and 2.8.2. Peptide **2** eluted at 37 % CH_3CN in the gradient run from 5-85 % CH_3CN and was then purified using 27 % CH_3CN.

Pleurocidin amide was purified to >99% purity using 28 % CH_3CN (figure 2.10.2), and eluted at 44 % CH_3CN in the gradient run (figure 2.9).

CP-29 was purified to 90% from the crude product of the CP-29 synthesis, peak **IV** eluted at 67 % CH_3CN in the gradient run, and was purified at 62 % CH_3CN (figures 2.11 and 2.12).

2.3.1 MALDI-MS

Matrix-assisted laser desorption ionization (MALDI) time of flight (TOF) mass

spectrometry is a relatively new mass spectrometry technique. It has rapidly

evolved as a valuable tool for the detection and characterization of

biopolymers such as peptides, proteins, oligonucleotides and oligosaccharides.

The use of laser beams to induce ionization without matrix assistance was

more or less restricted to small biomolecules (below 1000 Da) bearing

aromatic residues. The basic rational to employ matrices for MALDI-TOF MS

was to assist in the ion formation of large biomolecules. The matrix candidate

should be water soluble, not too volatile and chemically not aggressive. α-

Cyano-4-hydroxycinnamic acid has been used successfully as a matrix for

MALDI. One of the most important conditions for the matrix to work well is

an intimate mixing of the analyte and the matrix. Optimal molar ratios range

from 1:1000 to 1: 10,000 (analyte to matrix) so that the analyte molecules are

singularized and fully surrounded by the matrix molecules. The absence of

fragmentation peaks in MALDI-TOF MS suggests the high ion stability of

$[M+H]^+$ under the experimental conditions.

The identity of the peptides synthesized was determined by MALDI-TOF MS

in the following manner. First, the predicted monoisotopic masses and M+H

ions of the synthetic peptides were calculated using Peptide companion®

software from CoshiSoft/Peptide search (Tucson, AZ). The monoisotopic

molecular weight is the weight for the peptide formula containing exclusively

^{12}C, ^{1}H, ^{14}N, and ^{16}O isotopes. The relative abundance of ^{12}C is 98.90%, mass

12 exactly and ^{13}C is 1.10%, mass 13.00336. The relative abundance of ^{1}H is

99.985%, mass 1.00783 and ^{2}H is 0.015%, mass 2.01410. The abundance of

^{14}N is 99.63%, mass 14.00310 and ^{15}N is 0.37%, mass 15.00001. The

abundance of ^{16}O is 99.76%, mass 15.99490 and ^{18}O is 0.2%, mass 17.99900.

Therefore, mass spectra are expected to show multiple peaks provided the

resolution is adequate, with relative intensities depending upon the molecular

formula. Table 2.6 lists the calculated monoisotopic molecular weights and

corresponding expected M+H values for peptide 1, peptide 2, **pleurocidin**

amide and **CP-29**.

Peptide	MW* (AMU)	Abundance of MW			
		M	M+1	M+2	M+3
Peptide 1	1939.07	46.1 %	47.3%	6.32%	0.21%
Peptide 2	2194.23	39.4%	51.0%	7.5%	2.0%
Pleurocidin Amide	2708.48	35.4%	55.6%	8.6%	0.2%
CP-29	2869.79	33.3%	54.87%	8.7%	3.0%

Table 2.6 Calculated monoisotopic* molecular weights, and relative isotopic

abundances for Peptide 1, Peptide 2, **Pleurocidin amide** and **CP-29**.

Matrix-assisted laser desorption time-of-flight mass spectrometry (MALDI-

TOF MS) was then performed on HPLC purified samples of peptide 1, peptide

2, **CP-29**, and **pleurocidin amide**. The mass spectrometry results for

pleurocidin amide, peptide 1, peptide 2, and **CP-29** are tabulated in Table 2.7.

MALDI-TOF Results	Measured m/z	Assignments M ± x	MW* + H
Pleurocidin amide	2731.5736	+22.0936	
	2710?	+1	
	2709.61	0	2709.48
	2688.583	-21.0713	
	2561.1896	-148.2912	
	1396.8377	-1312.6423	
Peptide A	1816.1853	+23.0274	
	1793.1579	0	1793.00
(Peptide 1 - Phe)	1736.1237	-56.9209	
	1707.1456	-86.0123	
	1665.0406	-128.1173	
Peptide 2	2465.2273	+270.9973	
	2218.0110	+22.8715	
	2198.1294	+3	
	2197.1294	+2	
	2196.1347	+1	
	2195.1586	0	2195.23
	2094.039	-101.1906	
	2067.9396	-127.2904	
	1296.6936	-898.536	
Peptide B	6105.33	+3305.5812	
	5504.31	+2704.5631	
(CP-29 - Ala)	2921.14	+121.3935	
	2902.58	+102.8324	
	2884.71	+84.9530	
	2850.04	+50.2921	
	2797.41	-2.3400	2799.75
	2726.85	-72.9200	
	2695.47	-104.2810	
	2384.96	-414.7912	

*Calculated monoisotopic molecular weight, calculated using Peptide companion ® software from CoshiSoft / Peptide search (Tucson, AZ).

Table 2.7 MALDI-TOF results for purified synthetic peptides **Pleurocidin amide**, Peptide **A**, Peptide **2**, and Peptide **B** corresponding to sequences for **pleurocidin amide**, peptide **1**(-Phe), peptide **2**, and **CP-29(-Ala)**.

The identities of purified synthetic peptide **2**, peak **IV**, and synthetic

pleurocidin amide, peak **II** were both confirmed by MALDI-TOF MS to have

the expected molecular weights (Table 2.7). For synthetic peptide **2** (Table

2.7) the peak at 2196.1347 corresponds to the calculated mass of the M+1+H

isotopic ion, and the peak at 2218.0110 corresponds to the calculated mass of

the M+1+Na which should be the largest intensity peaks around the molecular

ion according to the calculations in table 2.6 (M = 39.4% and M+1 = 51.0%

isotopic abundance). The peak at m/z 2067.9396 is likely a fragment

containing the first 20 amino acids (calc. M+H= 2067.45) to due cleavage of

the C-terminal Leu-NH$_2$. The peak at 2094.0394 is likely a valine deletion

peptide and the one at 2067.9396 is likely a lysine deletion peptide. The peaks

at 2465 and 1296 could not be assigned to any likely intact peptide and may be

fragments or incompletely deprotected peptides. The mass spectrum of

pleurocidin amide was pretty clean, with the base peak at the molecular ion at

2709.6065 (calc. M+H = 2709.48). There was a small peak at 2561.1896

corresponding to the phenylalanine deletion peptide and 1396.8377

corresponding to the fragment pleurocidin (13-25) amide.

The actual mass of peptide **A** was less than the expected mass for peptide **1**,

indicating that the major product of the synthesis was likely a deletion peptide.

The difference between the found mass (1793.15) and the expected mass

(1940.07) could indicate the loss of a phenylalanine residue giving a deletion

peptide with a calculated mass of (1793.00) for the M+H ion which is in close

agreement with the measured m/z (1793.15). No other amino acid deletion

could give the observed mass. Since the only two phenylalanine residues are fortunately located adjacent to one another in the sequence of peptide **1**, the synthetic product could be unambiguously identified as a 17 amino-acid peptide having the sequence:

Peptide **A** (Peptide **1**-des-[5 or 6]Phe)

H-GWGSFKKAAHVGKHVGK-NH$_2$

Peptide **B**, peak **III** also had less than the expected mass of **CP-29**. An alanine residue was probably deleted in the synthesis of **CP-29** although the calculated mass still differs from the measured one by two mass units (Table 2.8).

		Monoisotopic Mass	M+H
CP - 29 ′	**Calculated** *	2869.79	2870.79
	Found	2796.41	2797.41
CP-29 –Ala*		2798.6	2799.6

Table 2.8 Monoisotopic Masses and M+H of CP-29 and Peptide **B** (**CP-29** – **Ala**?). Calculated, the masses were calculated using Peptide companion $^®$ software from CoshiSoft / Peptide search (Tucson, AZ). The sequence of **CP-29** contains two non-adjacent alanine residues, however the loss of either one of alanine residues should not affect the formation of an amphipathic α-helix. The two possible sequences are shown below.

CP-29 (-Ala)   H-KWKSFIKKLTTVKKVLTTGLPALIS-NH$_2$

H-KWKSFIKKLTTAVKKVLTTGLPLIS-NH$_2$

2.3.2 Peptide Quantification For Antimicrobial Assays:

Amino acid analysis

Weighing peptides accurately is a problem due to the presence of moisture and

uncetainties about counter ions and salts. To accurately report MIC values of the synthesized AMPs, we used amino acid analysis (AAA) of peptide **2** to calculate the extinction coefficients of peptide solutions. AAA was performed following acid hydrolysis of peptide **2.**

PITC-AA	Ser	Gly	His	Ala	Val	Leu	Phe	Lys
Peak area / Ave. (Ala+Phe) (calc)	0.76 (1)	4.20 (4)	2.10 (2)	4.00 (4)	1.50 (2)	0.98 (1)	1.95 (2)	3.33 (4)

Table 2.9 Amino acid analysis (AAA) of acid hydrolysate of purified peptide **2**

Monitoring integrity of synthetic peptides

HPLC analysis was used to determine the purity and concentration of each peptide solution used in the antimicrobial assays. The extinction coefficient (ϵ_{220}) of peptide **2** was calculated from the AAA data using Beer's law $A=\epsilon*b*c$. A solution of peptide **2** (100 µl) was acid hydrolyzed using 12 N HCl. 25 µl was subsequently derivatized using PITC method. The residue was brought up in 40 µl distilled water and 6 µl was injected in the HPLC system for quantification. The amount of peptide **2** (8450 picomoles) was normalized to phenylalanine and alanine. HPLC analysis of the intact peptide solution of the same concentration showed an absorbance of 0.0065 AU / µl in the peptide peak indicating that peptide **2** has ϵ_{220} 0.3466 L*µmole^{-1} * cm^{-1}. Since absorbance (A) at 220 nm is primarily due to the amide bonds in the

backbone of the peptide, the number of amide bonds is proportional to the intensity of absorbance at 220 nm. Therefore the ε_{220} for any similar peptide can be determined by adjusting for the number of amide bonds. The data from AAA of peptide **2** was used to calculate an appropriate ε_{220} and quantify peptide **A**, **pleurocidin amide** and peptide **B** using absorbance at 220 nm.

	Peptide A	Peptide 2	**Pleurocidin amide**	Peptide B
Number of amide bonds	17	21	25	25
ε_{220}	0.2805	0.3466	0.4126	0.4126

Table 2.10 Calculated extinction coefficients for synthetic peptides using the results obtained from AAA of an acid hydrolysate of peptide **2** and analytical HPLC results on the same solution.

2.3.3 Antimicrobial activities of synthetic peptides:

The synthetic peptide solutions were diluted and tested for their antibacterial activities against *Vibrio anguillarum* (wild type) and *Escherichia coli* (ZK4) in cell culture growth inhibition assays. The bactericidal activities of the synthetic peptides were explored by co-incubating peptide solutions, in serial concentrations, with the bacteria for a period of 48 hours. Table 2.11 lists the minimum inhibitory concentrations (MICs) and minimum bactericidal

concentrations (MBCs) in micromoles/L of the synthetic peptides against *V. anguillarum* and *E. coli*. Since *V. anguillarum* is a marine bacterium, the effect of salt on antimicrobial activity was also assessed.

	V. anguillarum				*E. coli*	
	MIC	MIC (1.5 %NaCl	MBC	MBC (1.5 % NaCl)	MIC	MBC
Peptide **A**	12.50	50	> 100	> 200	200	> 200
Peptide **2**	12.50	25	100	200	100	200
Pleurocidin amide	6.25	50	25	50	25	100
Tachyplesin	12.50	25	25	25	25	25
Peptide **B**	> 100	> 100	> 100	> 200	> 200	> 200

Table 2.11 MICs and MBCs of synthetic peptides against *V. anguillarum* and *E. coli* (μM). *MBC denotes Minimum Bactericidal Concentration, defined as the minimum peptide concentration where bacterial growth was not observed at 21 or 23 hours.

MIC is the concentration where the growth of the bacteria is 50% of control at 21 or 24 hours. MBC is the concentration where there is no bacterial growth after 21 or 23 hours. *V. anguillarum* cells were incubated at 22°C at an initial cell count (10^5) cfu / ml for 21 hours. *E. coli* (ZK 4) cells were incubated at 37°C at an initial cell count (10^5) cfu / ml for 23 hours. Bacterial cells were co-incubated with the peptides in 96-well plates at the indicated temperatures and times so that the effect of the peptide on the bacterial growth could be

assessed. Each peptide was assayed in duplicate at eleven different concentrations. In addition, tachyplesin, an antimicrobial peptide that acts via a different mechanism than pleurocidin was used as a control peptide. Bacterial growth was monitored by absorbance at 650 nm.

Conclusions

Studies have shown that when gradients of increasing CH_3CN are used to elute peptides adsorbed on a C_{18} column, the more hydrophobic peptides elute at a higher percentage of $CH_3CN^{[31]}$. Hydrophilic contaminants from the synthesis and HF cleavage should elute first, followed by the peptide products in order of increasing hydrophobicity. The largest peak, indicated by an arrow on each chromatogram, was selected for further characterization. In the case of pleurocidin, when the hydrophobicity of the peptide was evaluated using the Hopp-Woods algorithm, the *C*-terminal region was markedly more hydrophobic. Thus it was expected that peptide **1** would elute at a lower % CH_3CN than peptide **2**, and this was the case.

Assuming that in each synthetic step, the reaction went to completion, the strongest intensity peak should correspond to the full length peptide, while other peaks likely represent failure sequences (deletion or terminated sequences), that are shorter than the desired product. Since each coupling reaction was monitored during the synthesis using the ninhydrin test, and the next amino acid was not added until the ninhydrin test was negative, this assumption seemed justified. Since the synthesis proceeded from the *C*-terminus of the peptide, any failure sequences would contain the same pattern

of amino acids but would be shorter, and thus should elute before the desired full-length peptide. Incompletely deprotected peptides would be expected to be more hydrophobic, and thus elute later than the desired product. In the case of both peptide **A** and peptide **2**, the largest peak was also the last significant peak to elute from the column, and was expected to be the full-length peptide. As confirmed by the MALDI-TOF results, this strategy worked well in the case of peptide **2**, where peak **IV** in figure 2.8.1 had the correct molecular weight and amino acid analysis. In the case of peptide **A**, which turned out to be a deletion peptide, missing a phenylalanine residue at position 5, the desired product, peptide **1**, would be expected to elute later than the failure sequence which was purified and characterized. The mass spectrometry results showed that during the solid-phase synthesis of pleurocidin amide and it's analogs, there was a difficult coupling of one of the adjacent phenylalanines, which merits further study. The problem with the synthesis of **CP-29** was more obscure, and could be due to some problem with the peptide synthesizer or the HF cleavage process.

In our experiments, peptide **B** was not active against either *V. anguillarum* or *E. coli*. The literature reported value of the MIC for pleurocidin amide against *V. anguillarum* is 0.74 μM[53]. Our value was 6.25 uM and we determined the MBC to be 50 uM.

CHAPTER 3: Synthesis of Novel Thiazole-Containing Amino Acid Building Blocks For Combinatorial Peptide Libraries.

ABSTRACT

Many thiazole and oxazole-containing natural products exert biological activities e.g.: anticancer, antiviral, antibacterial and antifungal activities. Thiazole and oxazole rings may be important pharmacophores in these compounds. One traditional approach to thiazole synthesis is through Hantzsch synthesis, a one hundred year old method. The Hantzsch approach requires prior preparation of thioamides, which involves several steps. The thioamides easily revert to nitriles upon heating. Despite the difficulty of preparing the starting materials, the Hantzsch cyclocondensation itself proceeds smoothly in high yields.

In this chapter, we discuss the synthesis of a novel thiazole-containing amino acid building block: Methyl 2-S-(1`-Boc-2`-phenylethyl) thiazole-4-carboxylate.

Our synthesis involved the formation of Boc-phenylalanine-N-methoxy-N-methylamine. Subsequent reduction by LiALH$_4$ yielded Boc-phenylalaninal. Condensation of Boc-phenylalaninal with L-cysteine methyl ester yielded Methyl 2-(1`-Boc-phenylethyl) thiazolidine-4-carboxylate, which was further oxidized by activated MnO$_2$ in benzene to yield Methyl 2-(1`- Boc-2`-phenylethyl) thiazole-4-carboxylate.

3.1 INTRODUCTION

Many thiazole and oxazole-containing natural products exert important

biological activities e.g.: anticancer, antiviral, antibacterial and antifungal

activities. Thiazole and oxazole rings may be important pharmacophores in

these compounds[1].

In this chapter, we describe the synthesis of a novel thiazole-containing amino

acid building block: Methyl 2-S-(1`-Boc-2`-phenylethyl) thiazole-4-

carboxylate (1).

One approach to the synthesis of thiazole rings is through Hantzsch synthesis

(eq 3.1), a one hundred year old method that, despite its antiquity, is still

used.

eq (3.1)
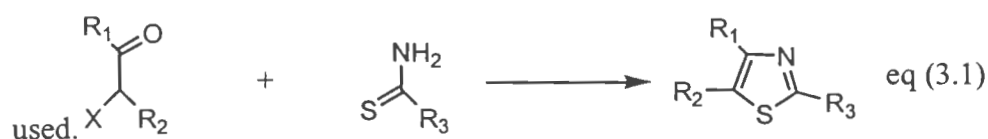
The mechanism of Hantzsch synthesis involves initial nucleophilic attack by

sulfur followed by cyclocondensation[56]. The Hantzsch approach requires

prior preparation of thioamides, which involves several steps. The thioamides

easily revert to nitriles upon heating. Despite the difficulty of preparing the

starting materials, the hantzsch cyclocondensation itself proceeds smoothly in
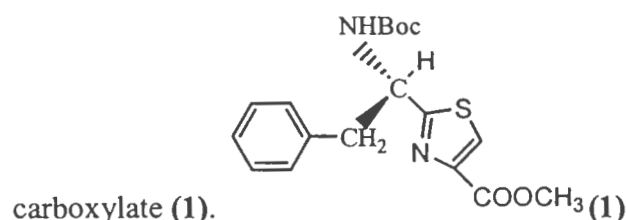
high yields. Another approach to thiazole rings involves the condensation of

C-terminal aldehydes (2) prepared from the corresponding amino acids (5,

R=amino acid side chain.) with L-cysteine methyl ester to form a thiazolidine

93

$(3)^{[57]}$. Thiazolidines can be dehydrogenated by active manganese dioxide in the presence of pyridine in benzene to yield the Boc-thiazole amino acids (4). L-amino acids are not expected to undergo racemization when they are converted to aldehydes and then condensed with L-cysteine methyl ester$^{[57]}$. The cyclocondensation is not stereospecific, and is expected to give a mixture of diastereomeric thiazolidines.
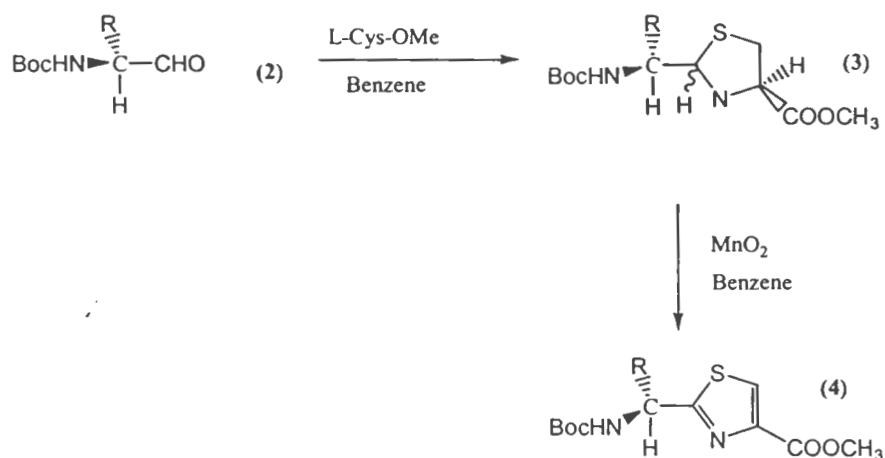
The precursor aldehydes (2) of protected amino acids can be prepared via two different approaches.

1) Oxidation of the C-terminal alcohols (6) of protected amino acids $(5)^{[58]}$.
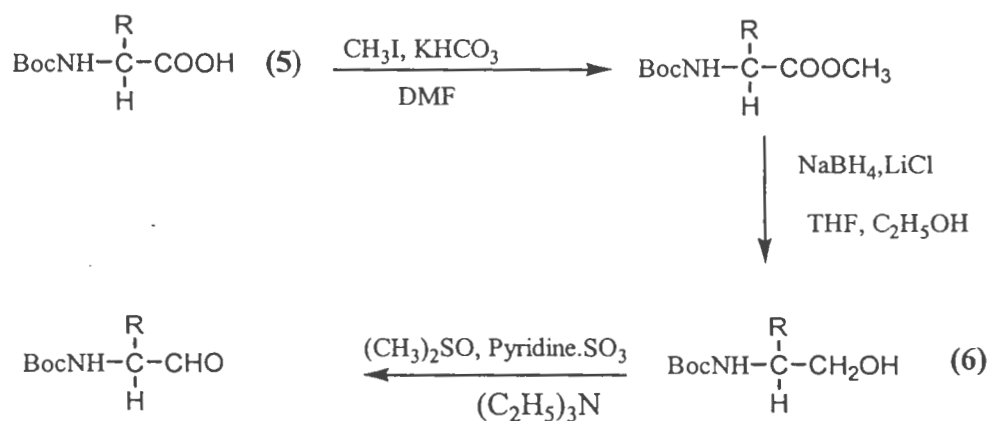
2) Direct reduction of the protected amino acids via the corresponding Weinreb

N-methoxy-*N*-methylamine amides (**7**)[59].
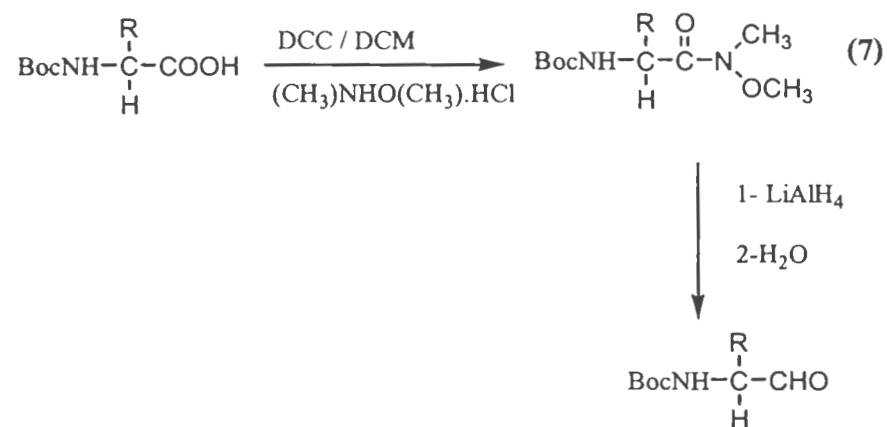
Our synthesis of compound (**1**) is illustrated in Figure (3.1).
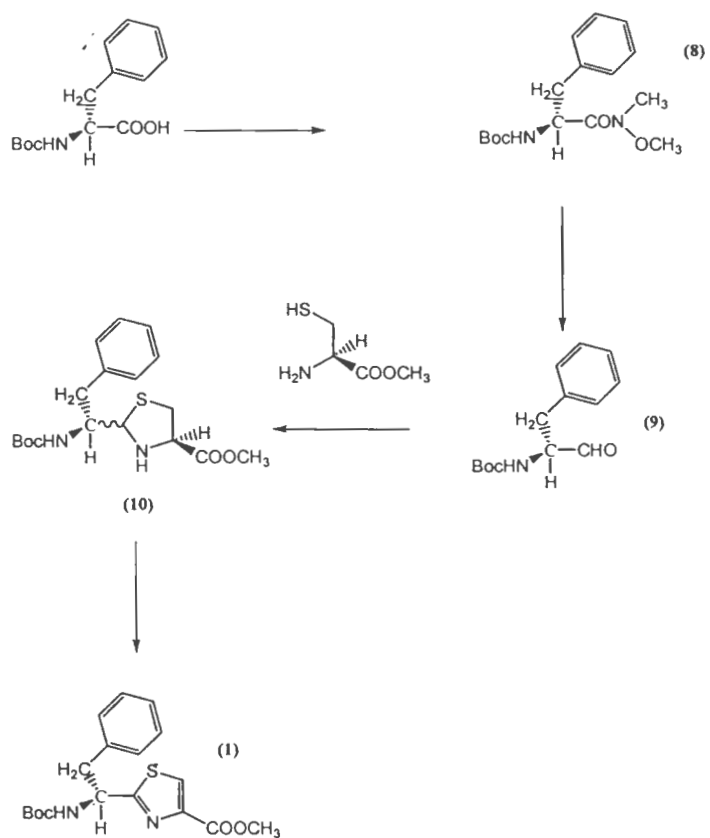
Figure 3.1 Synthetic Scheme of Methyl 2-*S*-(1`-Boc-phenylethyl)thiazole-4-carboxylate.

3.2 EXPERIMENTAL

Chemicals:

Lithium aluminum hydride (LAH), *N*, *O*-dimethylhydroxylamine hydrochloride, L-cystine methyl ester hydrochloride were purchased from Aldrich. *N*, *N*`-dicyclohexylcarbodiimide (DCC), manganese (IV) oxide (activated), *N*, *N*-diisopropylethylamine (DIEA) were purchased from Fluka. Diethyl ether and trifluoroacetic acid were purchased from Fisher. Dichloromethane was purchased from Burdick & Jackson. Boc-L-phenylalanine was purchased from Novabiochem. Silica gel 60 for column chromatography (70-230 mesh), (surface area 500 m^2/g., pore volume 0.75 cm^3/g.) and silica gel TLC plates F 254 were purchased from E. Merck. TLC developing system: hexane-ethyl acetate, TLC plates were visualized under UV (254 nm); then the plate was exposed to I$_2$ vapors in a jar for 5 min.

Apparatus:

The ^{1}H NMR spectra (90 MHZ) were obtained on a modified EM-390 Varian spectrometer (EFT-90-30, Anasazi Instruments Inc., Indianapolis, IN), and data was processed with the NUTS program (Win 95 version, Acorn NMR Inc., Fermont, CA).

Chemical shifts (δ) are given in ppm from tetramethylsilane (TMS). Abbreviations for peak description are s = singlet, d = doublet, t = triplet, q = quartet, m =multiplet.

Synthesis of methyl 2-(1`-Boc-phenylethyl) thiazole-4-carboxylate (1).

Boc-phenylalanine-*N*-methoxy-*N*-methylamine (8)

To a well stirred solution of Boc-L-Phenylalanine (7 g, 0.03 mole) and *N, N*-dicyclohexylcarbodiimide (DCC) (6.18g., 0.03 mole) in 100 ml dichloromehtane (DCM), was added *N,N*-diisopropyl-N-ethylamine (DIEA) (5.22 ml, 0.03 mole). After 5 min., a solution of *O, N*-dimethylhydroxylamine HCl (3.4 g, 0.03 mole) in 100 ml of DCM was added to the above stirred solution. The reaction was monitored by TLC (silica gel, hexane : ethyl acetate 1:1) R_f: starting material 0.45, product 0.34. After 30 min., the solution was filtered through a filter paper (Whatman no 1) to remove dicyclohexylurea (side product of the coupling reaction) and 100 ml of DCM was added to the filterate. The DCM layer was washed with 1 N HCl (4 x 250 ml), then saturated aqueous Na_2CO_3 solution (2 x 250 ml) and finally with saturated NaCl solution (250 ml). The organic layer was dried over 3 g. of $MgSO_4$ overnight, filtered and concentrated under reduced pressure. The oily yellow residue was purified using silica gel column (20 cm x 0.5 cm), eluted with hexane: ethyl acetate (1:1); fractions of 1 ml were collected and the appropriate fractions were pooled and evaporated under reduced pressure to yield a white solid (7.13 g., 0.022 mole).

Yield: 75%,

¹H NMR (CDCl₃, 90 MHZ).

Figure 3.2.δ ppm:7.25 (s, 5H), 5.38 (d,1.3 H), 5.00 (d, 0.9 H), 3.66 (s, 3 H), 3.16 (s, 3 H), 3.00 (m, 2.3 H), 1.39 (s, 8.8 H).

Boc-phenylalaninal (9)

Boc-L-Phenylalanine-*N*-methoxy-*N*-methylamine (7.3 g., 0.023 mole) in 200 ml anhydrous diethyl ether was stirred at room temperature for 15 min. under argon. Solid LiAlH₄ was added in excess, more than 10 equivalents. After 30 min., HCl (5%) was added gradually to the solution and stirred for 5 min. at room temperature. Organic solvents in the reaction mixture were removed under reduced pressure. The aqueous residue was extracted with DCM (4 x 200 ml). The combined DCM extracts were washed with 1 N HCl (2 x 100 ml), then with saturated Na₂CO₃ (2 x 100 ml), and finally with saturated aqueous NaCl (100 ml) and dried over 2 g. of MgSO₄ overnight and filtered. Evaporation under reduced pressure yielded a yellow oil (4.2 g., 0.017 mole).

TLC Analysis: (silica gel, hexane : ethyl acetate 1:1) R_f starting material 0.34, product 0.54.

Yield: 74%,

¹H NMR (CDCl₃, 90 MHZ).

Figure 3.3.δ ppm:9.05 (s, 0.92 H), 7.28 (s, 5 H), 5.30 (m, 0.76 H), 3.1 (d, 1.62 H), 1.4 (s, 9.05 H).

Methyl 2-(1`-Boc-phenylethyl) thiazolidine-4-carboxylate (10)

Boc-phenylalaninal (2g., 0.008 mole) was dissolved in 100 ml DCM. A solution of L-cysteine methyl ester * (1.1 g., 0.008 mole) in DCM was added dropwise and the Mixture was stirred for 3 hours at room temperature. The DCM layer was evaporated under reduced pressure, and the residue was redissolved in 200 ml benzene, stirred for 30 min., then evaporated under reduced pressure. This process was repeated three times. After the final evaporation, TLC analysis (silica gel, hexane: ethyl acetate 1: 1) showed several spots, (R_f 0.45, 0.44, 0.1, 0) and the starting material was gone. The spots at 0.45, 0.44 are the two stereoisomers of the thiazolidine with one spot of higher intensity. The crude products were isolated using a silica gel column (22 cm x 0.7 cm), eluted with ethyl acetate : hexane (1:1). Appropriate fractions were collected, pooled and evaporated to remove the solvent to yield a pale yellow solid (2g., 0.005 moles).

Yield: 63%, ^{1}H NMR (CDCl$_3$, 90 MHZ), Figure 3.4. δ ppm:7.28 (s, 5 H), 3.90 (s, 2.9 H), 3.3 (d, 0.9 H), 3.1 (d, 1.62 H), 1.4 (s, 8.7 H).

*Note: The L-cysteine methyl ester solution was prepared by dissolving (3.4 g., 0.01 moles) of (H-Cys-OMe)$_2$ 2HCl and 2-mercaptoethanol (2.3 g., 0.03 moles) in 50 ml distilled water, and stirring at room temperature for 20 min. Solid NaHCO$_3$, (0.84 g., 0.01 moles) was added and the reduced product extracted with DCM (2 x 100 ml), and evaporated under reduced pressure to yield an oily liquid.

Methyl 2-(1`- Boc-2`-phenylethyl) thiazole-4-carboxylate (1)

To a well stirred solution of methyl 2-(1`- Boc-2`-phenylethyl) thiazolidine-4-carboxylate in 100 ml benzene, 10 ml pyridine, MnO_2 (purchased as activated MnO_2 from the manufacturer) was added in excess, more than 10 equivalents and the solution was refluxed at $70^{\circ}C$ for 12 hours. TLC analysis of the reaction (silica gel, hexane : ethyl acetate,1 : 1) showed one new spot at R_f 0.47 and the starting materials disappeared. The solution was filtered through a filter paper, Whatman no 1, and the organic solvent was evaporated under reduced pressure. White crystals of **1** were obtained by recrystallization from ethyl acetate and hexane. The synthetic scheme suffered a drastic decrease in yield in this step. In an attempt to improve the yields, MnO_2 was sometimes suspended in benzene and the benzene was distilled off to remove any traces of moisture, however the yields of this reaction did not improve. ($\sim$ 5-10 %).

^{1}H NMR (CDCl$_3$, 90 MHZ).

Figure 3.5.δppm: 8.1 (s, 0.9 H), 7.28 (s, 5 H), 3.90 (s, 2.9 H), 3.2 (d, 1.62 H), 1.4 (s, 8.7 H).

3.3 RESULTS AND DISCUSSION

The synthetic strategy reported in this chapter is a general method that can be used to prepare heterocyclic amino acids. Replacing Boc-phenylalanine with other Boc-amino acids, it can be used to synthesize additional thiazole-containing amino acid building blocks for combinatorial library synthesis. The preparation of aldehydes via N- methoxy-N-methylamides is increasing in popularity due to the ease of preparation of amides and the selective reduction to form amino acid aldehyes[60]. In the formation of the Weinreb amides, DCC is a classic coupling reagent used to form amides without racemization and the reaction finished within 10 min., the precipitation of dicyclohexylurea pushed the reaction forward.For the reduction of N- methoxy-N-methylamides to yield the amino acid aldehydes, the mechanism is thought to proceed through initial formation of a stable complex that is then hydrolyzed to give the aldehyde[59].
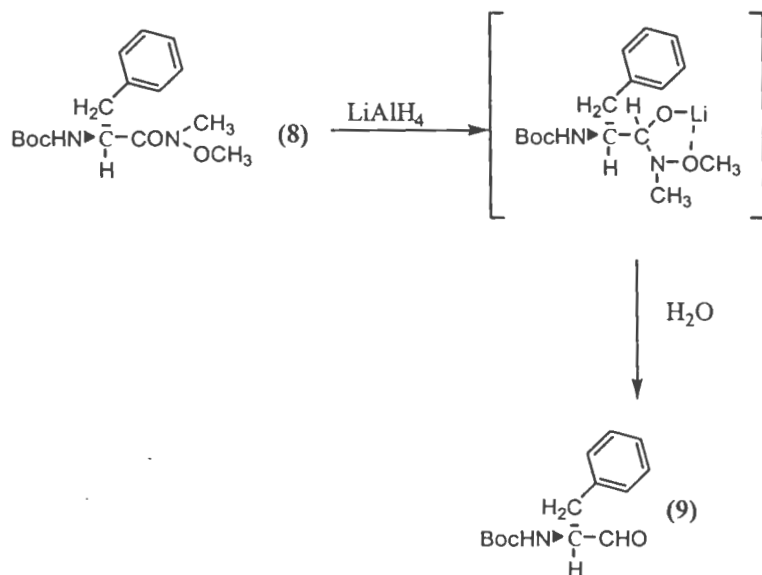
Peak List

Peak Number	δppm	Relative Intensity
1	1.39	8.8
2	3.16	3.0
3	3.66	3.0
4	7.25	5.0
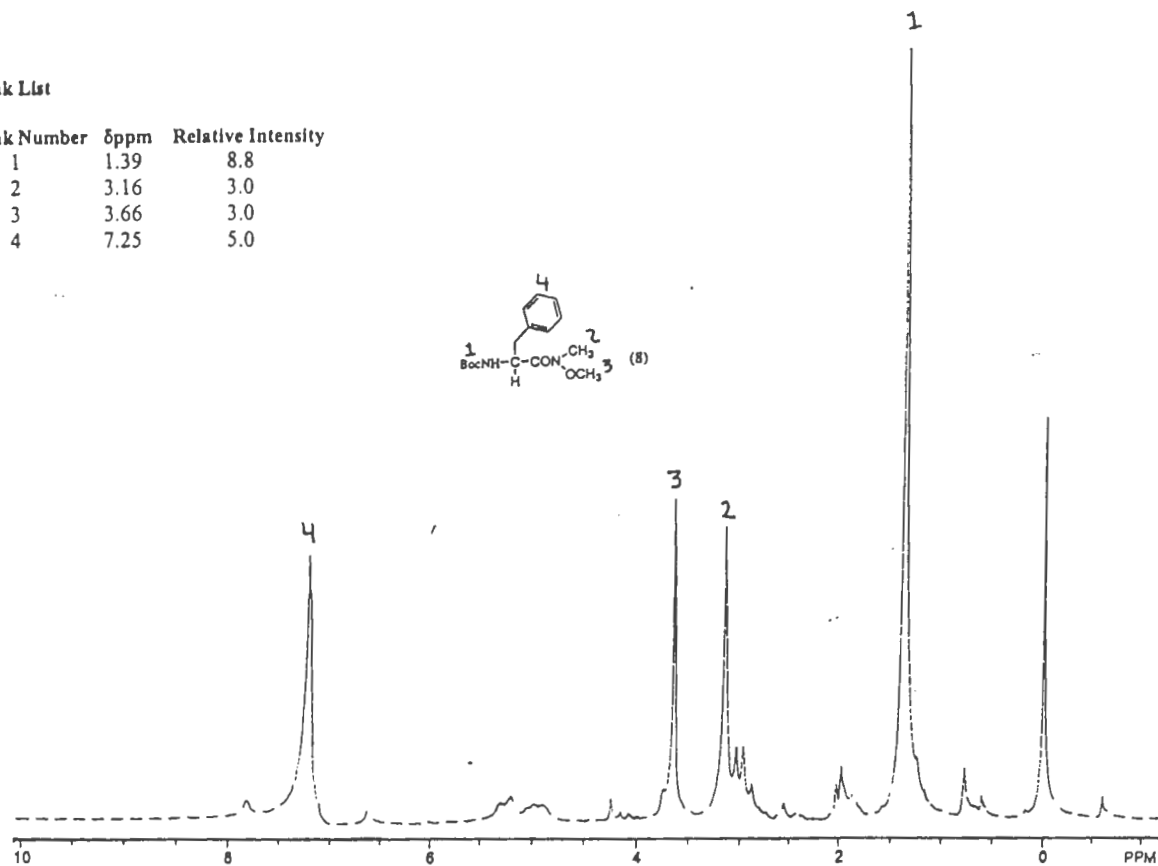
Figure 3.2 ^{1}HNMR spectrum of Boc-phenylalanine-N-methoxy-N-methylamine 8 (90 MHz, CDCl$_3$)

Peak List

Peak Number	δppm	Relative Intensity
1	1.40	9.05
2	7.28	5.0
3	9.05	0.92
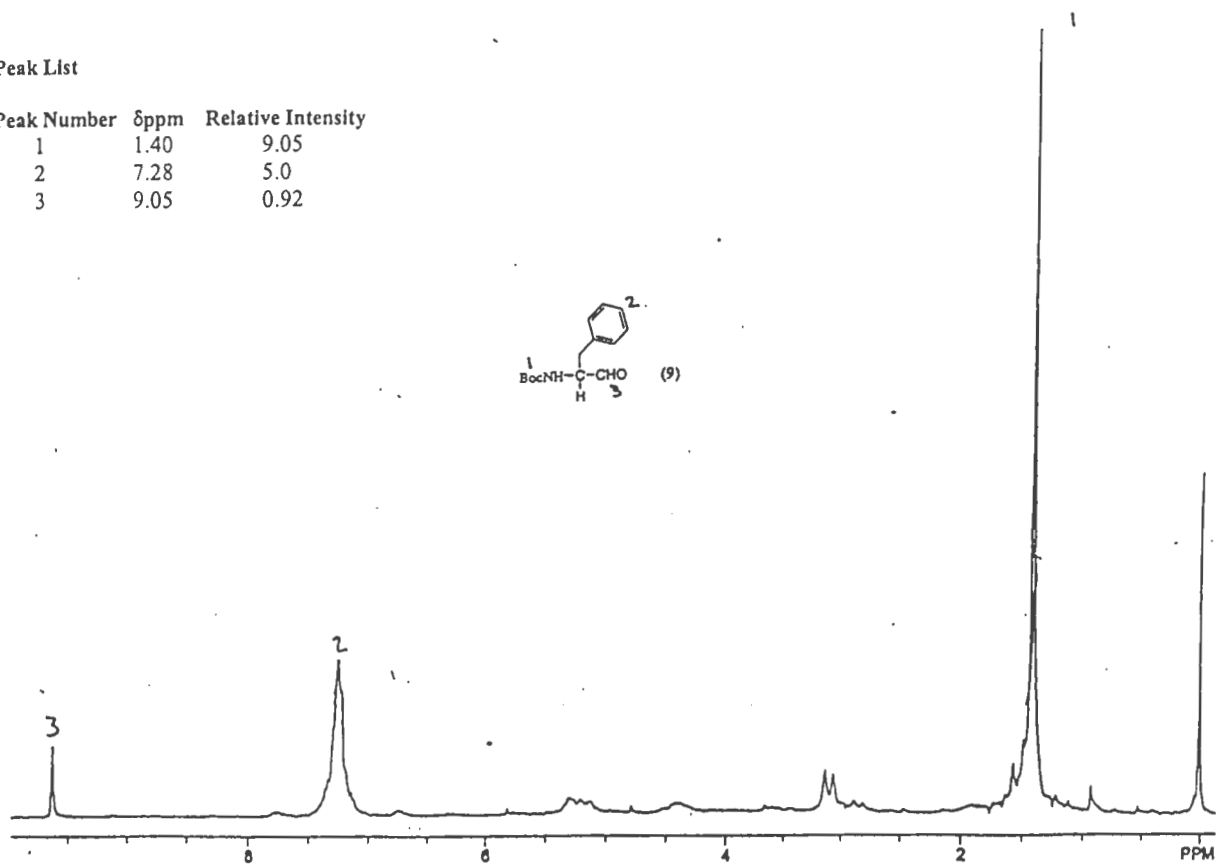
Figure 3.3 ^{1}HNMR spectrum of Boc-phenylalaninal 9 (90 MHz, CDCl$_3$)

Peak List

Peak Number	δppm	Relative Intensity
1	1.40	8.70
2	3.90	2.90
3	7.28	5.0
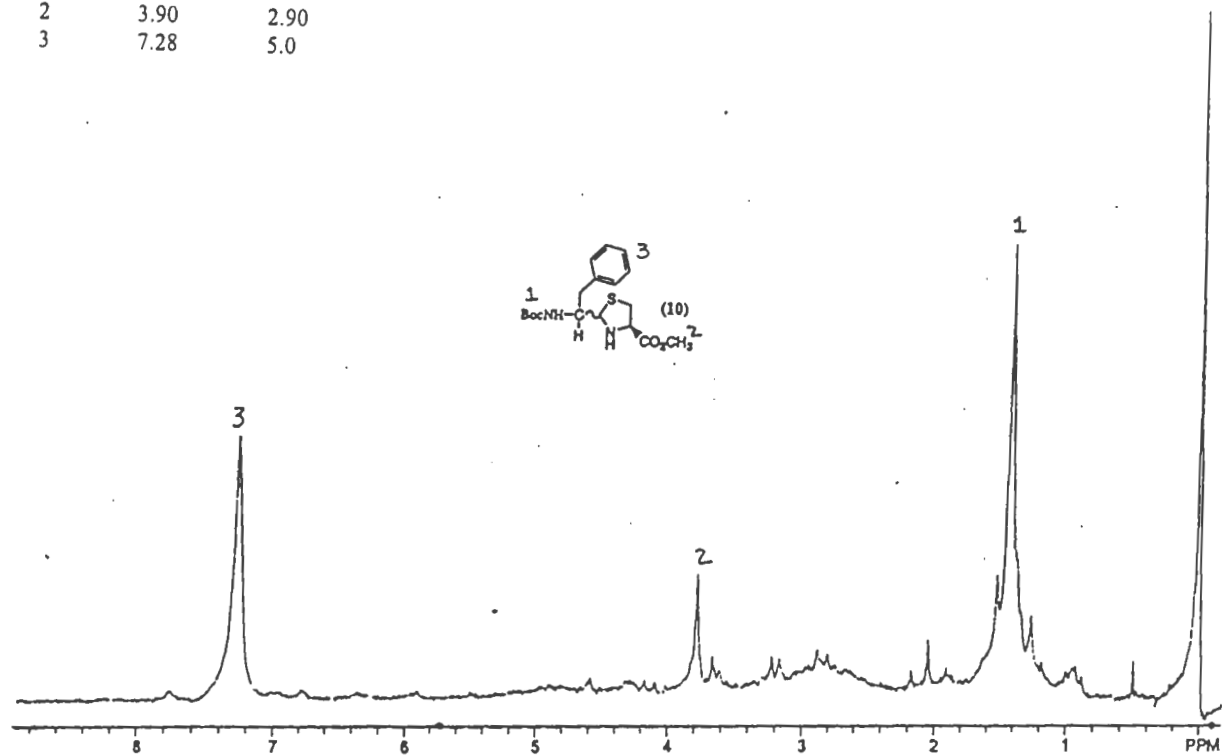
Figure 3.4 ^{1}HNMR spectrum of Methyl 2-(1`-Boc-phenylethyl) thiazolidine-4-carboxylate 10 (90 MHz, CDCl$_3$)

Peak List

Peak Number	δppm	Relative Intensity
1	1.40	8.70
2	3.90	2.90
3	7.28	5.0
4	8.10	0.90
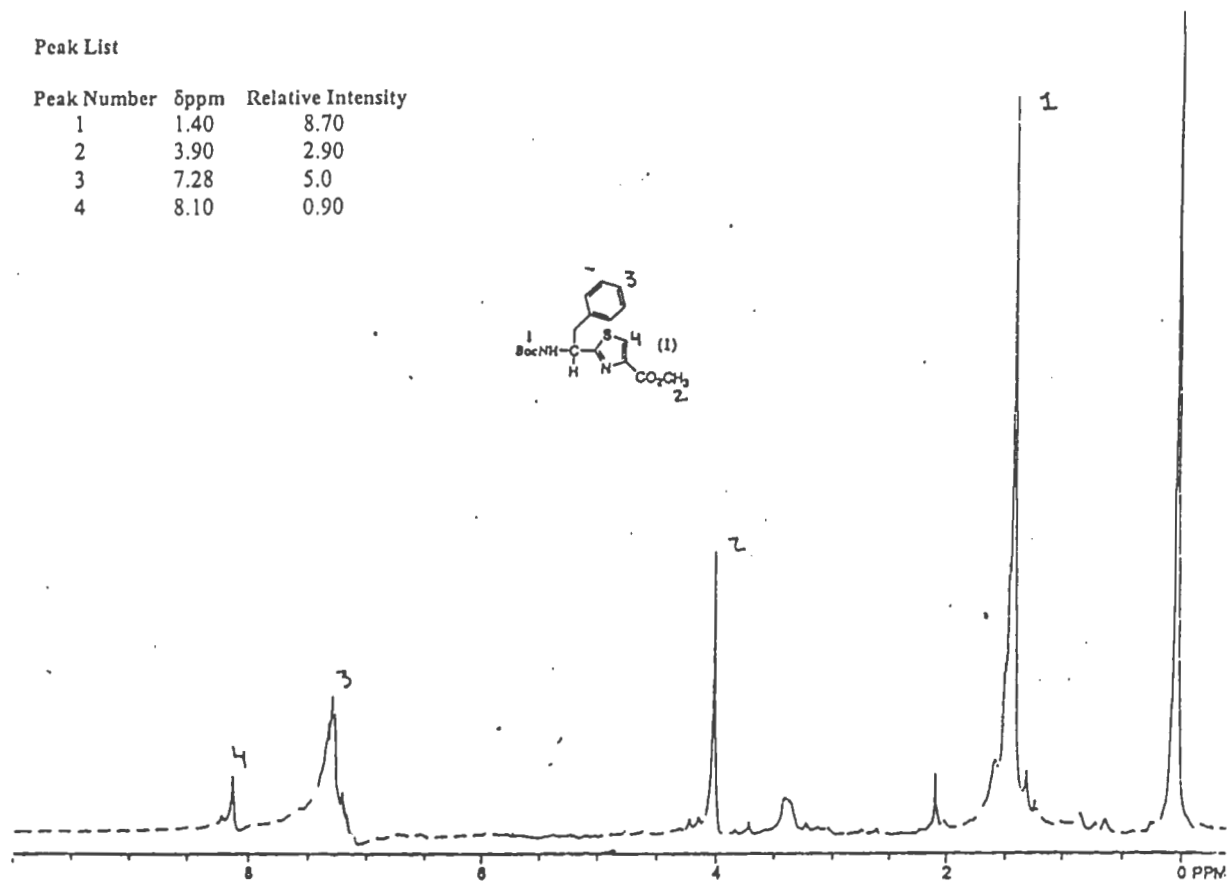
Figure 3.5 ^{1}HNMR spectrum of Methyl 2-(1'-Boc-phenylethyl) thiazole-4-carboxylate 1 (90 MHz, CDCl$_3$)

Literature Cited

(1) Lewis, J. R., Muscarine, Oxazole, Imidazole, Thiazole, and Peptide Alkaloids, and Other Miscellaneous Alkaloids, *Natural Products Report*, 13 (5), 435, (1996).

(2) Selva, E., Beretta, G., Montanini, N., Saddler, G. S., Gastaldo, L., Ferrari, P., Lotenzetti, R., Landini, P., Ripamonti, F., Goldstein, B. P., Berti, M., Montanaro, L. and Denaro, M., Antibiotic GE2270A. A novel inhibitor of bacterial protein synthesis. I- Isolation and characterization, *The Journal of Antibiotics*, 44, 693, (1991).

(3) Luesch, H., Yoshida, W. Y., Moore, R. E., Pau, V. J., Mooberry, S. L., Isolation and Structure of the cytotoxin Lyngbyabellin B and absolute configuration of Lyngbyapeptin A from the marine cyanobacterium *Lyngbya majuscula.*, *Journal of Natural Products*, 63, 611, (2000).

(4) Oka, H., Yoshinari, T., Kawamura, K., Satoh, F., Funaishi, K., Okura, A., A new topoisomerase- II inhibitor, BE 10988, produced by a streptomycete. I. Taxonomy, fermentation, isolation and characterization. *The Journal of Antibiotics*, 44, 486, (1991).

(5) Rashid, M. A., Gustafson, K. R., Boswell, J. L., Boyd, M. R., Haligramides A and B, two new cytotoxic hexapeptides from the marine sponge *Haliclona nigra*. *Journal of Natural Products*, 63, 956, (2000).

(6) Ratti, E., Lauinger, C., and Ressler, J., Configuration of the asparaginyl and aspartyl residues of bacitracin., *Journal of Organic Chemistry*, 33, 1309, (1986).

(7) Rashid, M., Gustafson, K., Cardellina, J., and Boyd, M., Patellamide F, A new cytotoxic cyclic peptide from the colonial ascidian *Lissoclinum patella.*, *Journal of Natural Products*, 58, 594, (1995).

(8) Vizan, J. L., Chico, C. H., Delcastillo, I., Moreno, F., The peptide antibiotic microcin B17 induces double strand cleavage of DNA mediated by *E. coli* DNA gyrase. *EMBO Journal*, 10, 467, (1991).

(9) Roy, R. S., Gehring, A. M., Milne, J. C., Belshaw, P. J., and Walsh, C. T., Thiazole and oxazole peptides: biosynthesis and molecular machinery, *Natural Product Report*, 16, 249, (1999).

(10) Von Dohren, H. and Kleinkauf, H. 'Enzymology of Peptide Synthetases' in *Biotechnology of Antibiotics*, Marcell Dekker Inc., New York, 1997, p 217.

(11) Roy, R. S., Gehring, A. M., Milne, J. C., Belshaw, P. J., and Walsh, C. T., Thiazole and oxazole peptides: Biosynthesis and Molecular Machinery, *Natural Products Report*, 16, 249, (1999).

(12) Yorgery, P., Davagnino, J., and Kotler, R., The maturation pathway of microcin B17, a peptide inhibitor of DNA gyrase, *Molecular Microbiology*, 9, 897, (1993).

(13) Davaginino, J., Herrero, M., Furlong, D., Moreno, F., and Kotler, R., The DNA replication inhibitor microcin B17 is a forty three amino acid protein containing sixty percent glycine, *Proteins*: *Structure, Function and Genetics*, 1, 230, (1986).

(14) Garrido, M. C., Herrero, M., Kotler, R. and Moreno, F., The export of the DNA replication inhibitor Microcin B17 provides immunity for the host cell, *EMBO Journal*, 7, 1853, (1988).

(15) Herrero, M., and Moreno, F., Microcin B17 blocks DNA replication and induces the SOS system in *Escherichia coli*, *Journal.of General Microbiology*, 132, 393, (1986).

(16) Vizan, J. L., Chico, C. H., Delcastillo, I., Moreno, F., The peptide antibiotic microcin B17 induces double strand cleavage of DNA mediated by *E. coli* DNA gyrase, *EMBO. Jounal*, 10, 467, (1991).

(17) Cozzarelli, N. R., DNA gyrase and the supercoiling of DNA, *Science*, 207, 953, (1980).

(18) Gellert, M., DNA topoisomerase, *Annual. Review of. Biochemistry*, 50, 879, (1981).

(19) Yamagishi, J., Yoshida, H., Yamayoshi, M., and Nakamura, S., Nalidixic acid-

resistant mutations of gyr B gene of *Escherichia coli*, *Molecular and. General. Genetics*, 204, 367, (1986).

(20) Sugino, A., Higgins, N. P., Brown, P. O., Peebles, C. L., and Cozzarelli, N. R., Energy coupling in DNA gyrase and the mechanism of action of novobiocin, *Proceedings of. The National. Academy of. Science, USA*, 74, 4767, (1978).

(21) Roy, R. S., Gehring, A. M., Milne, J. C., Belshaw, P. J., and Walsh, C. T., Thiazole and oxazole peptides: Biosynthesis and Molecular Machinery, *Natural Product. Report*, 16, 249, (1999).

(22) Storm, D. R., Mechanism of bacitracin action: a specific lipid-peptide membrane, *Annual NY Academy of Science*, 235, 387, (1974).

(23) Absalen, M. J., Wu, W., Kozarich, J. W., and Stubbe, J., Sequence-specific double strand breaks using hairpin oligonucleotides, *Biochemistry*, 34, 2076, (1995).

(24) Gordon, E. M., Barrett, R. W., Dower, W. J., Fodor, P. A., and Gallop, M. A., Applications of combinatorial technologies to drug discovery. 2. combinatorial organic synthesis, library screening strategies and future directions, *Journal of Medicinal Chemistry*, 37, 1251, (1994).

(25) McBride, J. D., Freeman, H. N., Leatherbarrow, R. J., Identification of chemotrypsin inhibitors from a second-generation template assisted combinatorial peptide library., *Journal of Peptide Science*, 6, 446, (2000).

(26) Chan, P. M., Nestler, H. P., Miller, W. T., Investigating the substrate specificity of the HER2/NEU tyrosine kinase using peptide libraries., *Cancer Letters*, 160, 159, (2000).

(27) Li, C., Martin, L. M., A robust method for determining DNA binding constants using capillary zone electrophoresis, *Analytical Biochemistry*, 263, 72, (1998).

(28) Li, C., *Design, Synthesis And Analysis of Peptides*, (1997).

(29) Hu, B., *Synthesis and Bioactivity of Peptidomimetics*, (1999).

(30) Kondejewski, L. H., Farmer, S. W., Wishart, D. S., Hancock, R. E., Hodges, R. S., Gramicidin S is active against both gram-positive and gram-negative bacteria., *International Journal of Peptide and Protein Research*, 47, 460, (1996).

(31) Guo, D., Mant, C., Taneja, A., Parker, J. M. and Hodges, R. S., Predicition of peptide retention times in reversed-phase high performance liquid chromatography, *Journal of Chromatography*, 359, 499, (1986).

(32) Li, C., Martin, L. M., A robust method for determining DNA binding constants using capillary zone electrophoresis, *Analytical Biochemistry*, 263, 72, (1998).

(33) Futaki, S., Suzuki, T., Ohashi, W., Arginine-rich peptides. An abundant source of membrane permeable peptides having potential as carriers for intracellular protein delivery, *Journal of Biological Chemistry*, 276, 5836, (2001).

(34) Neu, H. C. The Crisis in Antibiotic Resistance, *Science*, 257, 1064, (1992).

(35) Schaberg, D. R., Rubens, C. E., Alford, R. H., Evolution of antimicrobial resistance and nosocomial infections., *American Journal of Medicine,* 70, 445, (1981).

(36) Tossi, A., Sandri, L. and Giangaspero, A., Amphipathic, α-Helical Antimicrobial Peptides., *Biopolymers*, 55, 4, (2000).

(37) Christensen, B., Fink, J., Merrifield R. B., Mauzerall, D., Channel-forming properties of cecropins and related model compounds incorporated into planar lipid membranes., *Proceedings of The National Academy of Science*, USA, 85, 5072, (1988).

(38) Ludtke, S. J.; He, K.; Huang, H. W., Antimicrobial peptide pores in membranes detected by neutron in-plane scattering., *Biochemistry*, 34, 16764, (1995).

(39) Matsuzaki, K., Murase, O., Fujii, N., Miyajima, K., Translocation of a channel-forming antimicrobial peptide, magainin 2, across lipid bilayer by forming a pore.,

Biochemistry, 34, 6521, (1995).

(40) Hultmark, D., Steiner, H., Rasmuson, T., Boman, H. G., Insect immunity, Purification and properties of three inducible bactericidal proteins from the hemolymph of immunized pupae of *Hyalophora cecropia*, *European Journal of Biochemistry*, 106, 7, (1980).

(41) Steiner, H., Hultmark, D., Engstrom, A., Bennich, H., Boman, H. G., Sequence and specificity of two antibacterial proteins involved in insect immunity., *Nature*, 292, 246, (1981).

(42) Dempsey, C. The actions of mellitin on membranes, *Biochemistry and Biophysics Acta*, 1031, 143, (1990).

(43) Cole, A., Weis, P., Diamond, G., Isolation and characterization of pleurocidin, an antimicrobial peptide in the skin secretions of winter flounder, *Journal of Biological Chemistry*, 272, 12008, (1997).

(44) Lazarovici, P., Pimor, N and Loew, L. M. Purification and pore-forming activity of two hydrophobic polypeptides from the secretion of the red sea Moses sole (*Pardachirus marmoratus*), *Journal of Biological Chemistry*, 261, 16704, (1986).

(45) Bechinger, B. Structure and Functions of Channel-Forming Peptides: Magainins, Cecropins, Mellitin and Alamethacin., *Journal of Membrane Biology*, 156, 197, (1997).

(46) Stewart, J. M. and Young, J. D., *Solid Phase Peptide Synthesis*, Second Edition, (1983).

(47) Merrifield, R. B., Vizioli, L. D., and Boman, H. G., Synthesis of the Antibacterial Peptide Cecropin A(1-33)., *Biochemistry*, 21, 5020, (1982).

(48) Matsuzaki, K., Sughita, K., Harada, M., Fujii, N., Miyajima, K., Modulation of magainin 2-lipid bilayer interactions by peptide charge, *Biochemistry*, 36, 2104, (1997).

(49) Boman, H. G., Wade, D., Boman, I. A., Wahlin, B., Merrifield, R. B., Antibacterial and antimalarial properties of peptides that are cecropin-mellitin hybrids., *FEBS Letters*, 259, 1, 103, (1989).

(50) Cavallarin, L., Andreu, D. San secundo, B., Cecropin A-derived peptides are potent inhibitors of fungal plant pathogens., *Mol Plant Microbe Interact*, 11, 218, (1999).

(51) Subbalakshmi, C., Nagaraj, R., Sitaram, N., Biological activities of C-terminal 15 residue synthetic fragment of mellitin: design of an analog with improved antibacterial activity., *FEBS Letters*, 448, 62, (1999).

(52) Scott, M. G., Yan, H., Hancock, E. W., Biological properties of structurally related alpha-helical cationic antimicrobial peptides., *Infection and Immunity*, 67, 2005, (1999).

(53) Jia, X., Patrzykat, A., Devlin, R. H., Ackerman, P. A., Antimicrobial Peptides Protect coho Salmon from *Vibrio anguillarum* Infections., *Applied and Environmental Microbiology*, 66, 1928, (2000).

(54) Schiffer, M. and Edmundson, A. B., Use of helical wheels to represent the structures of proteins and to identify segments with helical potential, *Biophysical Journal.*, 7, 121, (1967).

(55) Kyte, J. and Doolittle, R. F., A simple method for displaying the hydropathic character of a protein., *Journal of Molecular Biology.*, 157, 105, (1982).

(56) W., Kenner, G. W., Sheppard R. C., and Stehr, C. E., The synthesis of (-)-sandaracopimaradiene from androstane derivatives, *Journal of Chemical society.*, 2143, (1963).

(57) Boden, D. J., Pattenden, G., and Ye, T., The synthesis of optically active thiazoline and thiazole derived peptides from *N*-protected α- amino acid, *Synthesis Letters*, 417, (1995).

(58) Hamada, Y., Shibata, M., Suguira, T., Kato, S., and Shiori, T., New Methods and Reagents in Organic Synthesis. 67. A General Synthesis of Derivatives of Optically Pure 2-(1-Aminoalkyl) thiazole-4-carboxylic acids, *Journal of Organic Chemistry.*, 52, (1987).

(59) Fehrentz, J. A., and Castro, B., An efficient Synthesis of Optically Active α-(*t*-butoxycarbonylamino) aldehydes from α-amino acids, *Synthesis*, 676, (1983).

(60) Sibi, M. P., Chemistry of *N*-Methoxy-*N*-Mehthylamides. Application in Synthesis. A review, *Organic Preparations and Procedures Int.*, 25, (1), 15, (1993).

(61) Wang, J. C., and Liu, L. F., *In Molecular Genetics*, Editor:. JH Taylor, 65-88, (1979).

(62) Kornberg, A. and Baker, T. A., *DNA Replication,* (1992).

(63) Brown, P. O., and Cozarrelli, N. R., A sign Inversion Mechanism for Enzymatic Supercoiling of DNA, *Science*, 206, 1081, (1979).

(64) Sugino, A., and Cozarelli, N. R., The Intrinsic ATPase of Dna gyrase, *Journal of Biological Chemistry*, 225, 6299-62306, (1980).

(65) Gellert, M., DNA Topoisomerase, *Annual Review of Biochemistry*, 50, 879, (1981).

(66) Cozzarelli, N. R., DNA Gyrase And The Supercoiling of DNA, *Science*, 207, 953, 960, (1980).

(67) Gellert, M., and Mizuuchi, K., O'Dea, M. H., and Nash, H. A., Novobiocin and Coumermycin Inhibit DNA Supercoiling Catalyzed by DNA Gyrase, *Proceedings of The National Academy of Science*, 73, 3872, (1976).

(68) Hsiang, Y., Hertzberg, R., Hecht, S., and Liu, L. F., Camptothecin Induced Protein-Linked DNA breaks Via Mammalian DNA Topoisomerase I, *Journal of Biological Chemistry*, 260, 14873, (1985).

APPENDIX Topo I, II Inhibition Of A Tetrapeptide Library

ABSTRACT

DNA topoisomerases are a class of enzymes that catalyze interconversions between topological isomers of DNA double helices. DNA topoisomerases are broadly classified into type I and type II. DNA topoisomerases are implicated in a large number of intracellular processes and inhibition of DNA topoisomerases is a target of anticancer drugs. DNA gyrase is a prokaryotic type II topoisomerase and drugs that inhibit DNA gyrase can be used as antibacterial drugs.

In this section, we describe our methods to assay a library of tetrapeptides for topoisomerase I and topoisomerase II inhibition. In a topoisomerase inhibition assay; the active enzyme will relax supercoiled DNA, inhibition prevents relaxation.

Increasing the inhibitor concentration should eventually completely inhibit DNA relaxation. The products are analyzed using agarose gel electrophoresis. Relaxed DNA has a bigger radius than its supercoiled counterpart, thus would migrate slower than supercoiled DNA in an agarose gel. The amount of relaxed DNA is quantitated by scanning the gel for the intensity of fluorescence of the relaxed and supercoiled DNA. Most of the tetrapeptides inhibited both topoisomerase I and II at the concentrations tested although the peptides were tested in different concentrations, the degree of inhibition of either topoisomerase I or II did not linearly correlate with the concentrations of the peptides.

4.1 INTRODUCTION

DNA topoisomerases are a class of enzymes that catalyze interconversions between topological isomers of DNA double helices[61]. DNA topoisomerases are implicated in a large number of intracellular processes. DNA topoisomerases relax supercoiled DNA strands. Replication is the best known process that generate positive supercoils during semiconservative replication of DNA [62]. Transcription is a second example of a cellularprocess that generates supercoils. DNA supercoiling has strong effects on DNA structure and its interactions with other molecules. It directly impedes processes like m-RNA synthesis and interferes with polymerase processivity[63]. DNA topoisomerases are broadly classified into two mechanistic types; DNA topoisomerase type I and DNA topoisomerase type II. Type I topoisomerases break and reseal only one DNA strand while type II DNA topoisomerases catalyze double strand breakage and rejoining in an ATP driven reaction[64]. DNA topoisomerase I and II change DNA linking numbers in units of 1 and 2 respectively[65].

Inhibition of DNA topoisomerases is increasingly becoming a target for anticancer and antibacterial drugs. In the presence of a topoisomerase poison, the enzyme loses its ability to relax supercoiled DNA. A prokaryotic type II topoisomerase, DNA gyrase, is unique to prokaryotes[66]. DNA gyrase is an attractive target for selective antibacterial agents, such as fluoroquinolone antibiotics[67]. Camptothecin, a clinically used anticancer drug inhibits human topoisomerase I[68]. In this section, we describe our methods to assay inhibition of DNA

114

topoisomerases I and II by sixteen compounds from a tetrapeptide library. In a topoisomerase inhibition assay, the active enzyme will relax supercoiled DNA, inhibition prevents relaxation.

Increasing the inhibitor concentration should eventually completely inhibit DNA relaxation. The products are analyzed using agarose gel electrophoresis. Relaxed DNA has a bigger radius than its supercoiled counterpart, thus would migrate slower than supercoiled DNA in an agarose gel. The amount of relaxed DNA is quantitated by scanning the gel for the intensity of fluorescence of the relaxed and supercoiled DNA.

4.2 EXPERIMENTAL

Apparatus

E-C Midicell EC 350 electrophoretic gel system, with buffer container, two silver electrodes and a power supply, were purchased from E-C Apparatus Corp. (New York). Pippetters, 50 μl, 200 μl and 1000 μl were purchased from Gilson (France). The heating block with a constant temperature controller was obtained from VWR Scientific Company. A Kodak digital camera; (DC 120 Zoom), 254 nm light table (Fotodyne Incorporated) and Kodak Digital Science 1D software was recorded, visualized and used to analyze bands. Distilled water was obtained from Milli-Q Plus PF system (Millipore).

Chemicals

Tris-HCl, Tris-base, boric acid and dithiothreitol (DTT) were purchased from Fluka Chemie AG (Switzerland). Supercoiled DNA pBR322 (1 mg/ml) and Topoisomerase I (200 units, wheat germ) were purchased from Promega (WI, USA). Tetrapeptides were synthesized via the solid-phase synthesis. Agarose Low EEO was purchased from Fisher Scientific (New Jersey). Sodium chloride and ethylenediaminetetraacetic acid (EDTA) were from Sigma Chem. CO. (St. Louis, MO, USA). Magnesium chloride and glycerin (certified A. C. S.)were obtained from Fisher Scientific (New Jersey). Ethidium bromide (95 %) was purchased from Aldrich Chem. CO. (Milwakee, WI).

PROCEDURES

Buffers:

1x TBE Gel Buffer:

Tris Base   10.9 g, 89 mmoles.

Boric Acid 5.5 g, 90 mmoles.

EDTA   0.73 g, 25 mmoles.

Distilled Water to 1 Liter, pH = 8.4.

10 x Reaction Buffer for Topo I:

Tris Base   1.97 g, 16 mmoles.

Tris HCl   5.3 g, 33 mmoles.

EDTA   0.029 g, 0.09 mmoles.

Dithiothreitol 0.15 g, 0.97 mmoles.

Add distilled water to 100 ml, pH = 7.8.

DNA plasmid dilution buffer:

Tris Base 0.067g., 0.5 mmoles.

Tris HCl   0.69 g.,   4 mmoles.

EDTA   0.29 g.,   1 mmoles.

Add distilled water to 100 ml, adjust pH to 7.4.

Staining Solution:

200 µl Ethidium Bromide (1 mg / ml)

200 ml TBE buffer.

Gel Preparation:

1 % Agarose gels were prepared by heating 1 g. of agarose in 100 ml TBE buffer

for 2 min., pouring the solution into gel plates and allowing the gel to cool down at room

temperature.

Topo I Assay:

The smallest effective concentration of topo I, which fully relaxed the supercoiled plasmid pBR322 was first determined, and then utilized in the topo I inhibition assay. The gel results for this determination are shown in figure 4.2.1, and the plot of enzymatic activity was linear up to 1.5 units (Figure 4.2.2). 20 units of enzyme caused a new product to form which had lower mobility than relaxed pBR 322. The smallest effective concentration of topo I required to unwind > 80 % of 0.05 μg of plasmid in 30 min. at 37°C was 1 units. A unit is defined by the manufacturer as the amount of enzyme required to convert 1 μg of pGM®-9Zf(-) Vector DNA from supercoiled form to relaxed form in 30 min. at 37°C.

Relaxation Assay:

In a clean autoclaved microcentrifuge tubes, 3 μl 10 x reaction buffer, 5 μl pBR (0.01 μg / μl), 2 μl topo I in several concentrations (such that total activity 20, 5.7, 1.54, 0.86, 0.19 Units, dilutions of the enzyme were made in 50 % glycerol, 50 % 10 x reaction buffer) were mixed (10 μl total), vortexed and incubated at 37°C for 30 min. The reaction was stopped by adding 2 μl 30 % bromophenol dye and 10 μl was loaded into the wells of the gel. The gels were run at 75 Volts, 15 milliamps. at room temperature for 2 hours in 1200 ml TBE buffer. The gel was stained with ethidium bromide for 1 hour at room temperature. The bands were visualized by fluorescence on a UV light box, photographed with a digital camera and analyzed using Kodak software.

Topo I Inhibition by Tetrapeptides:

Tetrapeptide solutions were prepared in several dilutions using 90 % 1 x reaction buffer, 10 % glycerol. In a clean micro-centrifuge tube, 1 μl of 10 x reaction

buffer, 2 μl of peptide solution and 2 μl of topo I (1 U/μl) were mixed, vortexed and incubated at 37°C for 10 min. 5 μl of pBR 322 DNA, (0.01 μg / μl) was added, the tubes vortexed and incubated at 37°C for 30 min. The reaction was stopped by adding 2 μl of 30 % bromophenol dye to each tube and 10 μl of the mixture was loaded into the wells of the gel. The gels were run at 75 Volts, 15 milliamps. at room temperature for 2 hours in 1200 ml TBE buffer. The gel was stained with ethidium bromide for 1 hour at room temperature. The gel data for the inhibition assay is shown in figure 4.3.

Topo II Assay:

Topo II was purchased from USB Corp., (OH, USA). The smallest effective concentration to fully relax 0.02 μg supercoiled pBR322 was determined and used in topo II inhibition assays. The smallest concentration of topo II to fully relax supercoiled pBR322 was 1 unit. A unit is defined by the manufacturer as the amount of enzyme that fully relaxes 0.3 μg of negatively supercoiled pBR322 plasmid DNA in 15 minutes at 30°C under standard assay conditions. The gel results are shown in figure 4.4.

Relaxation Assay:

Topo II reaction buffer was supplied by USB Corp. as 10 x concentrate (100 mM Tris, pH 7.9, 500 mM NaCl, 500 mM KCl, 50 mM $MgCl_2$, 1 mM EDTA, 0.15 mg/ml BSA, 10 mM ATP). Topo II dilution buffer (10 mM sodium phosphate, pH 7.1, 50 mM NaCl, 0.2 mM DTT, 0.1 mM EDTA, 0.5 mg/ml BSA, 10 % glycerol). In a clean autoclaved centrifuge tube, 14 μl of distilled water, 2 μl of 10 x reaction buffer, 2 μl of DNA (0.01 μg/μl), 2 μl of topo II (10, 5, 1, 0.1 units diluted in topo

II dilution buffer). The reaction was incubated at 30°C for 15 minutes. The reaction was stopped by adding 4 μl of dye solution (20 % bromophenol blue, 1 % SDS).

The wells in the gel were each loaded with 20 μl and the gels were run at 75 Volts, 15 milliamps. for 2 hours in 1200 TBE at room temperature. The gels were stained for 1 hour with ethidium bromide at room temperature. The bands were visualized by fluorescence on a UV light box, photographed with a digital camera and analyzed using Kodak software.

Topo II Inhibition by Tetrapeptides:

In micro-centrifuge tubes, 12 μl of distilled water, 2 μl of 10 x reaction buffer, 2 μl of tetrapeptide solutions (serial dilutions in distilled water), 2 μl of topo II (1 unit) were mixed, vortexed and incubated at 30°C for 10 minutes. Supercoiled plasmid pBR322 (2 μl, 0.01 μg/μl) was then added and the reaction mixture was incubated at 30°C for 15 minutes. The reaction was stopped by adding 4 μl of dye solution(20 % bromophenol blue, 1 % SDS).

Each well in the gel was loaded with 20 μl of the reaction mixture and the gels were run at 75 Volts, 15 milliamps. for 2 hours in 1200 TBE at room temperature. The gels were stained for 1 hour with ethidium bromide at room temperature. The bands were visualized by fluorescence on a UV light box, photographed with a digital camera and analyzed using Kodak software.

The gel data for topo II inhibition by tetrapeptides are shown in figure 4.5, figure 4.6, figure 4.7 and figure 4.8.

120

# 1	RSSS-NH$_2$	# 9	SSSR- NH$_2$
# 2	RLSS- NH$_2$	# 10	SLSR- NH$_2$
# 3	RDSS- NH$_2$	# 11	SDSR- NH$_2$
# 4	RHSS- NH$_2$	# 12	SHSR- NH$_2$
# 5	RSSH- NH$_2$	# 13	SSHR- NH$_2$
# 6	RLSH- NH$_2$	# 14	SLHR- NH$_2$
# 7	RDSH- NH$_2$	# 15	SDHR- NH$_2$
# 8	RHSH- NH$_2$	# 16	SHHR- NH$_2$

D-3-(4-thiazolyl)alanine (D)   L-arginine (R)   L-3-(3-benzothienyl)alanine (S)

L-histidine (H)   L-3-(4-thiazolyl)alanine (L)
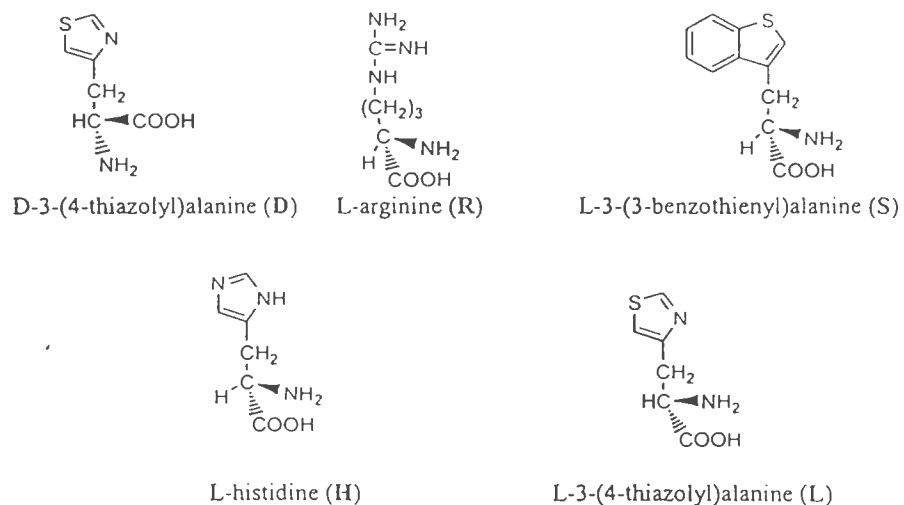
Figure 4.1 The sequences and building blocks of tetrapeptide library.

121
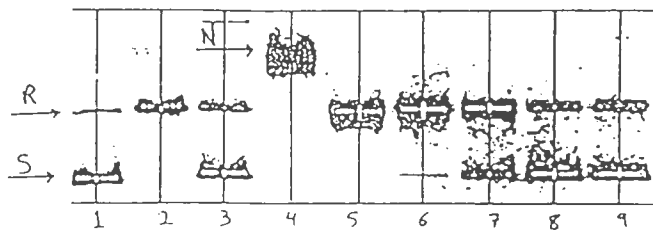
Lane	Sample
1	Control, 0.05 μg pBR 322
2	0.05 μg pBR 322 + 20 units old topo I
3	0.05 μg pBR 322 + 0.1 units old topo I
4	0.05 μg pBR 322 + 20 units topo I
5	0.05 μg pBR 322 + 5.7 units topo I-100%
6	0.05 μg pBR 322 + 1.54 units topo I-100%
7	0.05 μg pBR 322 + 0.86 units topo I
8	0.05 μg pBR 322 + 0.19 units topo I
9	0.05 μg pBR 322 + 0.09 units topo I

Figure 4.2.1 Determination of the smallest effective concentration of topo I, which can

fully relax 0.05 μg of the supercoiled plasmid pBR 322 in 30 min. at 37°C using 1 %

agarose gel electrophoresis.

N = Nicked plasmid pBR 322

R = Relaxed plasmid pBR 322

S = Supercoiled plasmid pBR 322

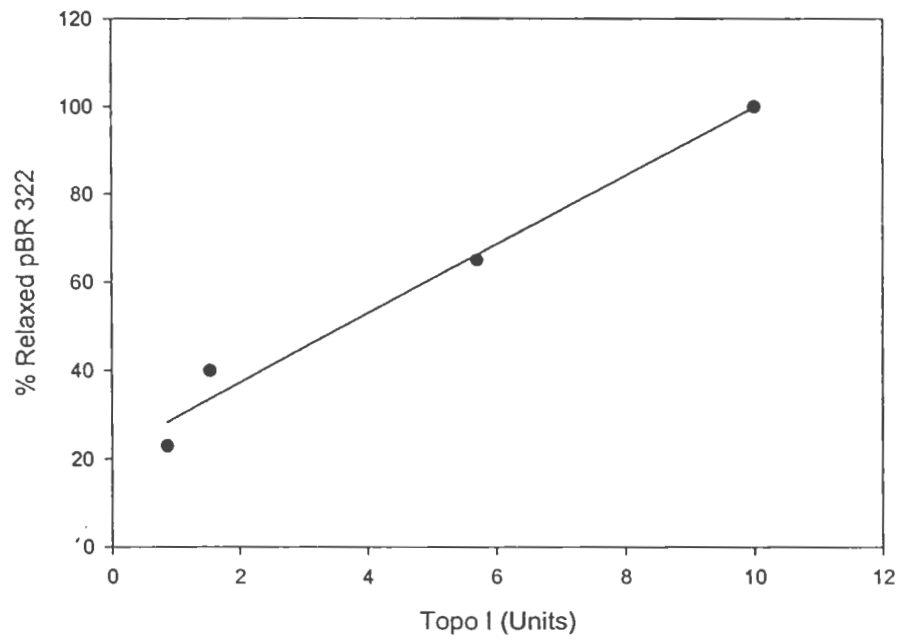Topo I Enzyme concentration (Units) and % relaxed pBR 322.

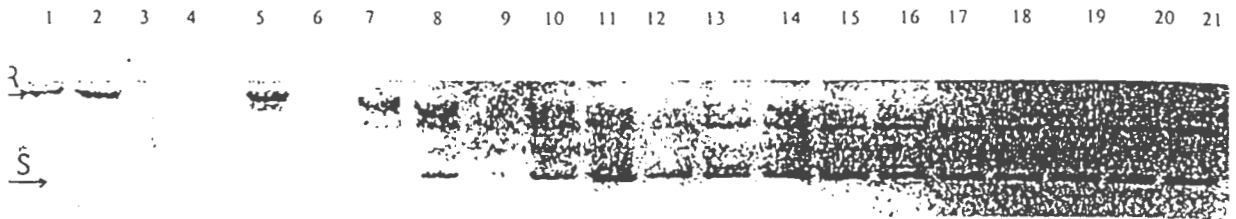Figure 4.2.2 Plot of Topo I concentration and % relaxed pBR 322

Figure 4.3 Gel data on topo I inhibition by tetrapeptides (1-16).

Lane	Inhibition	Sample
1	-	0.05 μg pBR 322+2 units topo I
2	-	0.05 μg pBR 322+2 units topo I.
3	ND	0.05 μg pBR 322+2 units topo I+pep # 1 (0.02 Au/μl).
4	ND	0.05 μg pBR 322+2 units topo I+pep # 2 (0.02 Au/μl).
5	0	0.05 μg pBR 322+2 units topo I+pep # 3 (0.02 Au/μl).
6	ND	0.05 μg pBR 322+2 units topo I+pep # 4 (0.02 Au/μl).
7	+	0.05 μg pBR 322+2 units topo I+pep # 5 (0.02 Au/μl).
8	+	0.05 μg pBR 322+2 units topo I+pep # 6 (0.02 Au/μl).
9	ND	0.05 μg pBR 322+2 units topo I+pep # 7 (0.02 Au/μl).
10	+	0.05 μg pBR 322+2 units topo I+pep # 8 (0.02 Au/μl).
11	+	0.05 μg pBR 322+2 units topo I+pep # 9 (0.02 Au/μl).
12	+	0.05 μg pBR 322+2 units topo I+pep # 10 (0.02 Au/μl).
13	+	0.05 μg pBR 322+2 units topo I+pep # 11 (0.02 Au/μl).
14	+	0.05 μg pBR 322+2 units topo I+pep # 12 (0.02 Au/μl).
15	++	0.05 μg pBR 322+2 units topo I+pep # 13 (0.02 Au/μl).
16	++	0.05 μg pBR 322+2 units topo I+pep # 14 (0.02 Au/μl).
17	++	0.05 μg pBR 322+2 units topo I+pep # 15 (0.02 Au/μl).
18	++	0.05 μg pBR 322+2 units topo I+pep # 16 (0.02 Au/μl).
19	-	Control, 0.05 μg pBR 322.
20	-	Control, 0.05 μg pBR 322.
21	-	Control, 0.05 μg pBR 322.

ND= not determined.

R = Relaxed plasmid pBR 322

S = Supercoiled plasmid pBR 322
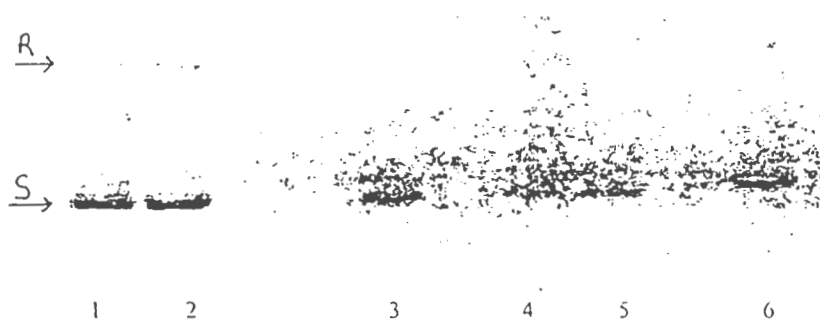
Figure 4.4 Determination of the smallest effective concentration of topo II, which can

fully relax 0.02 μg of the supercoiled plasmid pBR322, using 1 % agarose gel electrophoresis.

Lane	Sample
1	0.02 μg plasmid pBR 322.
2	0.02 μg plasmid pBR 322.
3	0.02 μg plasmid pBR 322+topo II (10 units).
4	0.02 μg plasmid pBR 322+topo II (5 units).
5	0.02 μg plasmid pBR 322+topo II (1unit).
6	0.02 μg plasmid pBR 322+topo II (0.1units).

R = Relaxed plasmid pBR 322

S = Supercoiled plasmid pBR 322

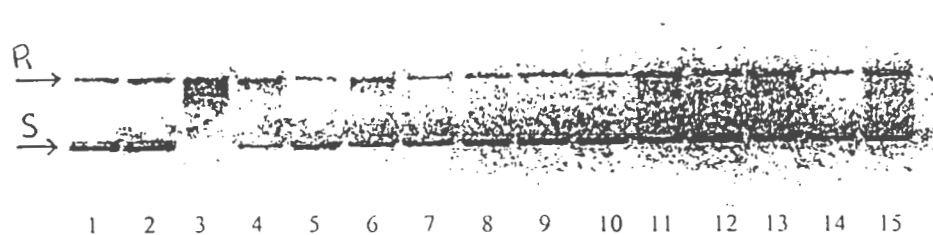| Lane	Sample	Ratio of Supercoiled DNA/ (Supercoiled DNA+Relaxed DNA).
1	0.02 μg supercoiled pBR 322.	70.59 %
2	0.02 μg supercoiled pBR 322	66.5 %
3	0.02 μg supercoiled pBR 322+ topo II (1 unit).	0 %
4	0.02 μg supercoiled pBR 322+ topo II (1 unit)+ pep # 1(0.01 Au/μl).	44 %
5	0.02 μg supercoiled pBR 322+ topo II (1 unit)+ pep # 1(0.004 Au/μl).	77.3 %
6	0.02 μg supercoiled pBR 322+ topo II (1 unit)+ pep # 1(0.002 Au/μl).	51.7 %
7	0.02 μg supercoiled pBR 322+ topo II (1 unit)+ pep # 2(0.01 Au/μl).	70.02 %
8	0.02 μg supercoiled pBR 322+ topo II (1 unit)+ pep # 2(0.004 Au/μl).	72.4 %
9	0.02 μg supercoiled pBR 322÷ topo II (1 unit)+ pep # 2(0.002 Au/μl).	75.1 %
10	0.02 μg supercoiled pBR 322+ topo II (1 unit)+ pep # 3(0.01 Au/μl).	74.07 %
11	0.02 μg supercoiled pBR 322+ topo II (1 unit)+ pep # 3(0.004 Au/μl).	60.5 %
12	0.02 μg supercoiled pBR 322+ topo II (1 unit)+ pep # 3(0.002 Au/μl).	74.2 %
13	0.02 μg supercoiled pBR 322+ topo II (1 unit)+ pep # 4(0.01 Au/μl).	52 %
14	0.02 μg supercoiled pBR 322+ topo II (1 unit)+ pep # 4(0.004 Au/μl).	82 %
15	0.02 μg supercoiled pBR 322+ topo II (1 unit)+ pep # 4(0.002 Au/μl).	65.5 %

Figure 4.5 Inhibition of topo II by tetrapeptides (1-4).

R = Relaxed plasmid pBR 322

S = Supercoiled plasmid pBR 322

Lane	Sample	Ratio of Supercoiled DNA/ (Supercoiled DNA+Relaxed DNA).
1	0.02 μg supercoiled pBR 322.	70.59 %
2	0.02 μg supercoiled pBR 322.	66.5 %
3	0.02 μg supercoiled pBR 322+ topo II (1 unit).	0 %
4	0.02 μg supercoiled pBR 322+ topo II (1 unit)+ pep # 5(0.01 Au/μl).	44 %
5	0.02 μg supercoiled pBR 322+ topo II (1 unit)+ pep # 5(0.004 Au/μl).	77.3 %
6	0.02 μg supercoiled pBR 322+ topo II (1 unit)+ pep # 5(0.002 Au/μl).	51.7 %
7	0.02 μg supercoiled pBR 322+ topo II (1 unit)+ pep # 6(0.01 Au/μl).	70.02 %
8	0.02 μg supercoiled pBR 322+ topo II (1 unit)+ pep # 6(0.004 Au/μl).	72.4 %
9	0.02 μg supercoiled pBR 322+ topo II (1 unit)+ pep # 6(0.002 Au/μl).	75.1 %
10	0.02 μg supercoiled pBR 322+ topo II (1 unit)+ pep # 7(0.01 Au/μl).	74.07 %
11	0.02 μg supercoiled pBR 322+ topo II (1 unit)+ pep # 7(0.004 Au/μl).	60.5 %
12	0.02 μg supercoiled pBR 322+ topo II (1 unit)+ pep # 7(0.002 Au/μl).	74.2 %
13	0.02 μg supercoiled pBR 322+ topo II (1 unit)+ pep # 8(0.01 Au/μl).	52 %
14	0.02 μg supercoiled pBR 322+ topo II (1 unit)+ pep # 8(0.004 Au/μl).	82 %
15	0.02 μg supercoiled pBR 322+ topo II (1 unit)+ pep # 8(0.002 Au/μl).	65.5 %

Figure 4.6 Inhibition of topo II by tetrapeptides (5-8).

R = Relaxed plasmid pBR 322
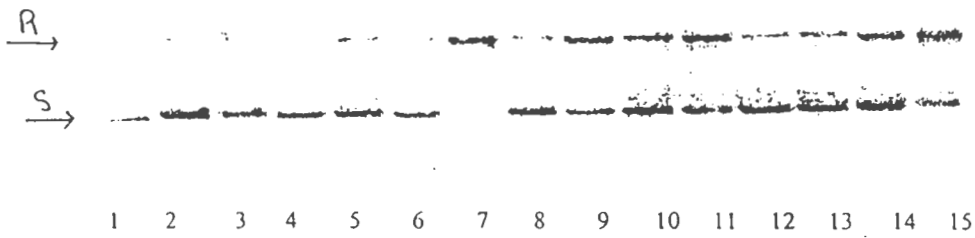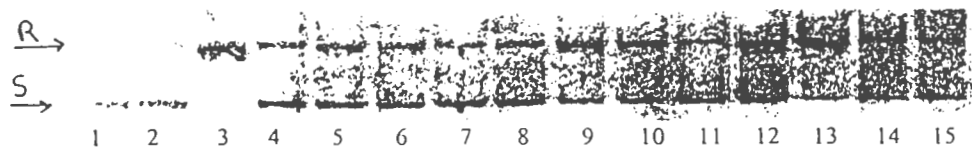
S = Supercoiled plasmid pBR 322

R →

S →

1 2 3 4 5 6 7 8 9 10 11 12 13 14 15

Lane	Sample	Ratio of Supercoiled DNA/ (Supercoiled DNA+Relaxed DNA).
1	0.02 μg supercoiled pBR 322.	82.85 %
2	0.02 μg supercoiled pBR 322.	82.68 %
3	0.02 μg supercoiled pBR 322+ topo II (1 unit)+ pep #9(0.01 Au/μl).	84.77 %
4	0.02 μg supercoiled pBR 322+ topo II (1 unit)+ pep #9(0.004 Au/μl).	81.13 %
5	0.02 μg supercoiled pBR 322+ topo II (1 unit)+ pep #9(0.002 Au/μl).	66.89 %
6	0.02 μg supercoiled pBR 322+ topo II (1 unit)+ pep #10 (0.01 Au/μl).	66.9 %
7	0.02 μg supercoiled pBR 322+ topo II (1 unit)+ pep #10 (0.004 Au/μl).	0 %
8	0.02 μg supercoiled pBR 322+ topo II (1 unit)+ pep #10 (0.002 Au/μl).	69.96 %
9	0.02 μg supercoiled pBR 322+ topo II (1 unit)+ pep #11 (0.01 Au/μl).	41.92 %
10 ´	0.02 μg supercoiled pBR 322+ topo II (1 unit)+ pep #11 (0.004 Au/μl).	61.16 %
11	0.02 μg supercoiled pBR 322+ topo II (1 unit)+ pep #11(0.002 Au/μl).	36.32 %
12	0.02 μg supercoiled pBR 322+ topo II (1 unit)+ pep # 12 (0.01 Au/μl).	75.06 %
13	0.02 μg supercoiled pBR 322+ topo II (1 unit)+ pep #12 (0.004 Au/μl).	75.7 %
14	0.02 μg supercoiled pBR 322+ topo II (1 unit)+ pep #12 (0.002Au/μl).	49.57 %
15	0.02 μg supercoiled pBR 322+ topo II (1 unit).	25.15 %

Figure 4.7 Inhibition of topo II by tetrapeptides (9-12).

R = Relaxed plasmid pBR 322

S = Supercoiled plasmid pBR 322

Lane	Sample	Ratio of Supercoiled DNA/ (Supercoiled DNA+Relaxed DNA).
1	0.02 μg supercoiled pBR 322.	82.6 %
2	0.02 μg supercoiled pBR 322.	80.1 %
3	0.02 μg supercoiled pBR 322+ topo II (1 unit).	0 %
4	0.02 μg supercoiled pBR 322+ topo II (1 unit)+ pep #13 (0.01 Au/μl).	74.397 %
5	0.02 μg supercoiled pBR 322+ topo II (1 unit)+ pep #13 (0.004 Au/μl).	66.79 %
6	0.02 μg supercoiled pBR 322+ topo II (1 unit)+ pep #13 (0.002 Au/μl).	68.58 %
7	0.02 μg supercoiled pBR 322+ topo II (1 unit)+ pep #14 (0.01 Au/μl).	76.81 %
8	0.02 μg supercoiled pBR 322+ topo II (1 unit)+ pep #14 (0.004 Au/μl).	77.17 %
9	0.02 μg supercoiled pBR 322+ topo II (1 unit)+ pep #14 (0.002 Au/μl).	43.77 %
10	0.02 μg supercoiled pBR 322+ topo II (1 unit)+ pep #15 (0.01 Au/μl).	60.63 %
11	0.02 μg supercoiled pBR 322+ topo II (1 unit)+ pep #15 (0.004 Au/μl).	79.9 %
12 '	0.02 μg supercoiled pBR 322+ topo II (1 unit)+ pep #15(0.002 Au/μl).	46.39 %
13	0.02 μg supercoiled pBR 322+ topo II (1 unit)+ pep # 16 (0.01 Au/μl).	25.71 %
14	0.02 μg supercoiled pBR 322+ topo II (1 unit)+ pep #16 (0.004 Au/μl).	44.9 %
15	0.02 μg supercoiled pBR 322+ topo II (1 unit)+ pep #16 (0.002Au/μl).	61.7 %

Figure 4.8 Inhibition of topo II by tetratpeptides (13-16)

R = Relaxed plasmid pBR 322

S = Supercoiled plasmid pBR 322

4.3 RESULTS AND DISCUSSION

The smallest effective concentration of topoisomerase I, which fully relaxed the supercoiled plasmid pBR322 was determined and then utilized in the topo I inhibition assay. Figure 4.2.1 shows the concentration dependant relaxation of pBR 322 by topoisomerase I.. The smallest effective concentration of topoisomerase I required to unwind > 80 % of 0.05 μg of plasmid in 30 min. at 37°C was 1 units.Topoisomerase I inhibition assays by the tetrapeptide library compounds were based on the differential migration of supercoiled versus the relaxed forms of plasmid pBR 322 on a 1 % agarose gel under 75 volts, 15 milliamps at room temperature for 2 hours. Figure 4.3 shows the result of this assay. Preliminary screening indicated that compounds in the tetrapeptide library inhibited topoisomerase I at micromolar concentrations.

The smallest effective concentration of topoisomerase II, which fully relaxed the supercoiled plasmid pBR322 was determined and then utilized in the topo II inhibition assay. Figure 4.4 shows the concentration dependant relaxation of pBR 322 by topoisomerase II.

The ratio of supercoiled DNA concentration to the sum total of supercoiled and relaxed DNA concentrations was used to determine the degree of inhibition of topoisomerase II. The compounds were tested in serial concentrations.

Figure 4.5 shows the inhibition of topoisomerase II by compounds **RSSS-NH$_2$**, **RLSS-NH$_2$**, **RDSS-NH$_2$** and **RHSS-NH$_2$**. Both **RLSS-NH$_2$** and **RDSS-NH$_2$** did not show inhibition of topoisomerase II in any of the concentration tested. Both **RSSS-NH$_2$** and **RHSS-NH$_2$** inhibited topoisomerase II at the concentrations tested

130

although the degree of inhibition did not linearly correlate with the concentrations used. Figure 4.6 shows the inhibition of topo II by compounds **RSSH-NH$_2$**, **RLSH-NH$_2$, RDSH-NH$_2$**, and **RHSH-NH$_2$**. Peptides **RLSH-NH$_2$** and **RDSH-NH$_2$** did not inhibit topoisomerase II at the concentrations used in the assay while **RSSH-NH$_2$** and **RHSH-NH$_2$** inhibited topoisomerase II but not in a concentration-dependant manner.

Figures 4.7 and 4.8 show the inhibition of topoisomerase II by **SSSR-NH$_2$, SLSR-NH$_2$, SDSR-NH$_2$, SHSR-NH$_2$, SSHR-NH$_2$, SLHR-NH$_2$, SDHR-NH$_2$** and **SHHR-NH$_2$**. The concentrations tested did inhibit topoisomerase II activity although the degree of inhibition did not linearly correlate with peptide concentrations. This might be due to that the concentrations used were higher than the linear concentration range.

Bibliography

Absalen, M. J., Wu, W., Kozarich, J. W., and Stubbe, J., Sequence-specific double strand breaks using hairpin oligonucleotides, *Biochemistry*, 34, 2076, (1995).

Bechinger, B. Structure and Functions of Channel-Forming Peptides: Magainins, Cecropins, Mellitin and Alamethacin., *Journal of Membrane Biology*, 156, 197, (1997).

Boden, D. J., Pattenden, G., and Ye, T., The synthesis of optically active thiazoline and thiazole derived peptides from *N*-protected α- amino acid, *Synthesis Letters*, 417, (1995).

Boman, H. G., Wade, D., Boman, I. A., Wahlin, B., Merrifield, R. B., Antibacterial and antimalarial properties of peptides that are cecropin-mellitin hybrids., *FEBS Letters*, 259, 1, 103, (1989).

Brown, P. O., and Cozarrelli, N. R., A sign Inversion Mechanism for Enzymatic Supercoiling of DNA, *Science*, 206, 1081, (1979).

Cavallarin, L., Andreu, D. San secundo, B., Cecropin A-derived peptides are potent inhibitors of fungal plant pathogens., *Mol Plant Microbe Interact*, 11, 218, (1999).

Chan, P. M., Nestler, H. P., Miller, W. T., Investigating the substrate specificity of the HER2/NEU tyrosine kinase using peptide libraries., *Cancer Letters*, 160, 159, (2000).

Christensen, B., Fink, J., Merrifield R. B., Mauzerall, D., Channel-forming properties of cecropins and related model compounds incorporated into planar lipid membranes., *Proceedings of The National Academy of Science*, USA, 85, 5072, (1988).

Cole, A., Weis, P., Diamond, G., Isolation and characterization of pleurocidin, an antimicrobial peptide in the skin secretions of winter flounder, *Journal of Biological Chemistry*, 272, 12008, (1997).

Cozzarelli, N. R., DNA gyrase and the supercoiling of DNA, *Science*, 207, 953, (1980).

Davaginino, J., Herrero, M., Furlong, D., Moreno, F., and Kotler, R., The DNA replication inhibitor microcin B17 is a forty three amino acid protein containing sixty percent glycine, *Proteins: Structure, Function and Genetics*, 1, 230, (1986).

Dempsey, C. The actions of mellitin on membranes, *Biochemistry and Biophysics Acta*, 1031, 143, (1990).

Fehrentz, J. A., and Castro, B., An efficient Synthesis of Optically Active α-(*t*-butoxycarbonylamino) aldehydes from α-amino acids, *Synthesis*, 676, (1983).

Futaki, S., Suzuki, T., Ohashi, W., Arginine-rich peptides. An abundant source of membrane permeable peptides having potential as carriers for intracellular protein delivery, *Journal of Biological Chemistry*, 276, 5836, (2001).

Garrido, M. C., Herrero, M., Kotler, R. and Moreno, F., The export of the DNA replication inhibitor Microcin B17 provides immunity for the host cell, *EMBO Journal*, 7, 1853, (1988).

Gellert, M., DNA Topoisomerase, *Annual Review of Biochemistry*, 50, 879, (1981).

Gellert, M., and Mizuuchi, K., O`Dea, M. H., and Nash, H. A., Novobiocin and Coumermycin Inhibit DNA Supercoiling Catalyzed by DNA Gyrase, *Proceedings of The National Academy of Science*, 73, 3872, (1976).

Gordon, E. M., Barrett, R. W., Dower, W. J., Fodor, P. A., and Gallop, M. A., Applications of combinatorial technologies to drug discovery. 2. combinatorial organic synthesis, library screening strategies and future directions, *Journal of Medicinal Chemistry*, 37, 1251, (1994).

Guo, D., Mant, C., Taneja, A., Parker, J. M. and Hodges, R. S., Predicition of peptide retention times in reversed-phase high performance liquid chromatography, *Journal of Chromatography*, 359, 499, (1986).

Hamada, Y., Shibata, M., Suguira, T., Kato, S., and Shiori, T., New Methods and Reagents in Organic Synthesis. 67. A General Synthesis of Derivatives of Optically Pure 2-(1-Aminoalkyl) thiazole-4-carboxylic acids, *Journal of Organic Chemistry.*, 52, (1987).

Herrero, M., and Moreno, F., Microcin B17 blocks DNA replication and induces the SOS system in *Escherichia coli*, *Journal.of General Microbiology*, 132, 393, (1986).

Hsiang, Y., Hertzberg, R., Hecht, S., and Liu, L. F., Camptothecin Induced Protein-Linked DNA breaks Via Mammalian DNA Topoisomerase I, *Journal of Biological Chemistry*, 260, 14873, (1985).

Hu, B., *Synthesis and Bioactivity of Peptidomimetics*, (1999).

Hultmark, D., Steiner, H., Rasmuson, T., Boman, H. G., Insect immunity, Purification and properties of three inducible bactericidal proteins from the hemolymph of immunized pupae of *Hyalophora cecropia*, *European Journal of Biochemistry*, 106, 7, (1980).

Jia, X., Patrzykat, A., Devlin, R. H., Ackerman, P. A., Antimicrobial Peptides Protect coho Salmon from *Vibrio anguillarum* Infections., *Applied and Environmental Microbiology*, 66, 1928, (2000).

Kyte, J. and Doolittle, R. F., A simple method for displaying the hydropathic character of a protein., *Journal of Molecular Biology.*, 157, 105, (1982).

Lazarovici, P., Pimor, N and Loew, L. M. Purification and pore-forming activity of two hydrophobic polypeptides from the secretion of the red sea Moses sole (*Pardachirus marmoratus*), *Journal of Biological Chemistry*, 261, 16704, (1986).

Lewis, J. R., Muscarine, Oxazole, Imidazole, Thiazole, and Peptide Alkaloids, and Other Miscellaneous Alkaloids, *Natural Products Report*, 13 (5), 435, (1996).

Li, C., *Design, Synthesis And Analysis of Peptides*, (1997).

Li, C., Martin, L. M., A robust method for determining DNA binding constants

using capillary zone electrophoresis, *Analytical Biochemistry*, 263, 72, (1998).

Luesch, H., Yoshida, W. Y., Moore, R. E., Pau, V. J., Mooberry, S. L., Isolation and Structure of the cytotoxin Lyngbyabellin B and absolute configuration of Lyngbyapeptin A from the marine cyanobacterium *Lyngbya majuscula.*, *Journal of Natural Products*, 63, 611, (2000).

Ludtke, S. J.; He, K.; Huang, H. W., Antimicrobial peptide pores in membranes detected by neutron in-plane scattering., *Biochemistry*, 34, 16764, (1995).

Kondejewski, L. H., Farmer, S. W., Wishart, D. S., Hancock, R. E., Hodges, R. S., Gramicidin S is active against both gram-positive and gram-negative bacteria., *International Journal of Peptide and Protein Research*, 47, 460, (1996).

Kornberg, A. and Baker, T. A., *DNA Replication,* (1992).

Matsuzaki, K., Murase, O., Fujii, N., Miyajima, K., Translocation of a channel-forming antimicrobial peptide, magainin 2, across lipid bilayer by forming a pore., *Biochemistry*, 34, 6521, (1995).

Matsuzaki, K., Sughita, K., Harada, M., Fujii, N., Miyajima, K., Modulation of magainin 2-lipid bilayer interactions by peptide charge, *Biochemistry*, 36, 2104, (1997).

McBride, J. D., Freeman, H. N., Leatherbarrow, R. J., Identification of chemotrypsin inhibitors from a second-generation template assisted combinatorial peptide library., *Journal of Peptide Science*, 6, 446, (2000).

Merrifield, R. B., Vizioli, L. D., and Boman, H. G., Synthesis of the Antibacterial Peptide Cecropin A(1-33)., *Biochemistry*, 21, 5020, (1982).

Neu, H. C. The Crisis in Antibiotic Resistance, *Science*, 257, 1064, (1992).

Oka, H., Yoshinari, T., Kawamura, K., Satoh, F., Funaishi, K., Okura, A., A new topoisomerase- II inhibitor, BE 10988, produced by a streptomycete. I. Taxonomy,

fermentation, isolation and characterization. *The Journal of Antibiotics*, 44, 486, (1991).

Rashid, M. A., Gustafson, K. R., Boswell, J. L., Boyd, M. R., Haligramides A and B, two new cytotoxic hexapeptides from the marine sponge *Haliclona nigra. Journal of Natural Products*, 63, 956, (2000).

Rashid, M., Gustafson, K., Cardellina, J., and Boyd, M., Patellamide F, A new cytotoxic cyclic peptide from the colonial ascidian *Lissoclinum patella., Journal of Natural Products*, 58, 594, (1995).

Ratti, E., Lauinger, C., and Ressler, J., Configuration of the asparaginyl and aspartyl residues of bacitracin., *Journal of Organic Chemistry*, 33, 1309, (1986).

Roy, R. S., Gehring, A. M., Milne, J. C., Belshaw, P. J., and Walsh, C. T., Thiazole and oxazole peptides: biosynthesis and molecular machinery, *Natural Product Report*, 16, 249, (1999).

Schaberg, D. R., Rubens, C. E., Alford, R. H., Evolution of antimicrobial resistance and nosocomial infections., *American Journal of Medicine,* 70, 445, (1981).

Scott, M. G., Yan, H., Hancock, E. W., Biological properties of structurally related alpha-helical cationic antimicrobial peptides., *Infection and Immunity*, 67, 2005, (1999).

Selva, E., Beretta, G., Montanini, N., Saddler, G. S., Gastaldo, L., Ferrari, P., Lotenzetti, R., Landini, P., Ripamonti, F., Goldstein, B. P., Berti, M., Montanaro, L. and Denaro, M., Antibiotic GE2270A. A novel inhibitor of bacterial protein synthesis. I- Isolation and characterization, *The Journal of Antibiotics*, 44, 693, (1991).

Sibi, M. P., Chemistry of *N*-Methoxy-*N*-Mehthylamides. Application in Synthesis. A review, *Organic Preparations and Procedures Int.*, 25, (1), 15, (1993).

Steiner, H., Hultmark, D., Engstrom, A., Bennich, H., Boman, H. G., Sequence and specificity of two antibacterial proteins involved in insect immunity., *Nature*, 292, 246, (1981).

Stewart, J. M. and Young, J. D., *Solid Phase Peptide Synthesis*, Second Edition, (1983).

Storm, D. R., Mechanism of bacitracin action: a specific lipid-peptide membrane, *Annual NY Academy of Science*, 235, 387, (1974).

Subbalakshmi, C., Nagaraj, R., Sitaram, N., Biological activities of C-terminal 15 residue synthetic fragment of mellitin: design of an analog with improved antibacterial activity., *FEBS Letters*, 448, 62, (1999).

Sugino, A., and Cozarelli, N. R., The Intrinsic ATPase of Dna gyrase, *Journal of Biological Chemistry*, 225, 6299-62306, (1980).

Sugino, A., Higgins, N. P., Brown, P. O., Peebles, C. L., and Cozzarelli, N. R., Energy coupling in DNA gyrase and the mechanism of action of novobiocin, *Proceedings of. The National. Academy of. Science*, USA, 74, 4767, (1978).

Tossi, A., Sandri, L. and Giangaspero, A., Amphipathic, α-Helical Antimicrobial Peptides., *Biopolymers*, 55, 4, (2000).

Vizan, J. L., Chico, C. H., Delcastillo, I., Moreno, F., The peptide antibiotic microcin B17 induces double strand cleavage of DNA mediated by *E. coli* DNA gyrase. *EMBO Journal*, 10, 467, (1991).

Von Dohren, H. and Kleinkauf, H. 'Enzymology of Peptide Synthetases' in *Biotechnology of Antibiotics*, Marcell Dekker Inc., New York, 1997, p 217.

Wang, J. C., and Liu, L. F., *In Molecular Genetics*, Editor:. JH Taylor, 65-88, (1979).

Yamagishi, J., Yoshida, H., Yamayoshi, M., and Nakamura, S., Nalidixic acid-resistant mutations of gyr B gene of *Escherichia coli*, *Molecular and. General. Genetics*, 204, 367, (1986).

Yorgery, P., Davagnino, J., and Kotler, R., The maturation pathway of microcin B17, a peptide inhibitor of DNA gyrase, *Molecular Microbiology*, 9, 897, (1993).